A Thesis for the Degree of Doctor of Philosophy in Pharmacology

Structure Determination of Secondary Metabolites from Korean Sponges

February 2018

by
Jung-Kyun Woo

Natural Products Science Major, College of Pharmacy
Doctoral Course in the Graduate School
Seoul National University

Abstract

Structure Determination of Secondary Metabolites from Korean Sponges

Jung-Kyun Woo
Natural Products Science Major
College of Pharmacy
Doctoral Course in the Graduate School
Seoul National University

Secondary metabolites from marine organisms, such as phytoplankton, algae, tunicates, echinoderms, molluscs, cnidarians, marine bacteria, sponges, have been studied progressively with development of analysis instruments for decades. As a result, the number of marine natural products has exponentially increased during the last two decades. Tens of thousands of marine natural products have been discovered until now and it was caused by huge endeavors of scientists. Diverse major fields of studies, such as organic chemistry, ecology, biology, pharmacology, have all been involved in marine natural products and it creates synerge effects each other. Secondary metabolites from marine organisms structurally differ from terrestrial ones and it relates to be a rich source of potent substances. Moreover, these would give a motivation to organic chemists synthesizing organic compounds. A number of bioactivity tests, for instances, anti-microbial, -inflammatory, -viral, -cancer, were adapted to

lots of marine natural products and it also motivates scientists to develop potential drugs. Approximately 75 percent of structurally unique compounds from marine organisms originated from marine invertebrates, belonging to the phyla Porifera and Coelenterate. Because of its worldwide distribution in the ocean, it is easy to approach collection, and various structural classes for secondary metabolites. Among these marine invertebrates, sponges were considered as preferred sources for marine natural products. This work has been studied for secondary metabolites of Korean marine sponges to discover new structural and bioactive interests. The research purposed to enhance the utility of marine natural products in the industry and essential technologies needed to produce natural product-based drug discovery. During the course of search for bioactive natural products from Korean marine sponges, I researched by using Korean marine sponges *Clathria gombawuiensis*, *Dictyonella* sp., *Phorbas* sp., and *Smenospongia* sp. Each extracts exhibited significant inhibitory activities against either K562 human leukemia cell line or brine shrimp lethality. Secondary metabolites from these sponges have been isolated by using various analyses instruments and chromatographic methods. Finally, 16 new compounds and 11 known compounds have been successfully isolated and structurally elucidated using combined spectroscopic and chemical analyses. These compounds have been derived from various biogenetic origins and have belonged to various structural classes: sesterterpene, saponin, steroid, and diterpene. All compounds have been examined under various bioactivities: cyotoxicity, antimicrobial activity, and inhibitory activities of isocitrate lyase (ICL), Sortase A (SrtA), and Na^+/K^+-ATPase. Several compounds displayed moderate cytotoxic, anti-microbial, and/or enzyme-inhibitory activities.

1. Sesterterpenes, a Saponin, and Steroids from the Sponge *Clathria gombawuiensis*

The new sesterterpenes, including gombaspiroketals A-C, phorone B, and ansellone C (**1**-**5**), gombaside A as a sponin (**6**), and steroids (**7**-**12**) together with a known steroid were isolated from the Sponge *Clathria gombawuiensis* collected from Korean waters. On the basis of the results of combined spectroscopic analyses, the structures of these compounds were determined to be highly rearranged sesterterpene spiroketal methoxyacetals (**1** and **2**) and a corresponding hemiacetal (**3**). The relative and absolute configurations were assigned by NOESY analysis and ECD calculations, respectively. These compounds exhibited moderate cytotoxicities and antibacterial activities. the structures of phorone B (**4**) and ansellone C (**5**) were determined to be the sesterterpenes of the phorone and ansellone classes, respectively, whereas the saponin gombaside A (**6**) was a nortriterpene sodium *O*-sulfonato-glucuronide of the rare 4,4,14-trimethylpregnane class. The absolute configuration of the glucuronate of **6** was assigned by an application of the phenylglycine methyl ester (PGME) method. The new compounds exhibited moderate cytotoxicity against A549 and K562 cell lines, and compound **6** showed antibacterial activity. The cytotoxicity of **4** may be related to the presence of a free phenolic −OH group, as the corresponding O-methoxy derivative of **4** is inactive. Six new polyoxygenated steroids (**7**-**12**) along with clathriol (**13**) were isolated from the Korean marine sponge *Clathria*

gombawuiensis as well. Based upon the results of combined spectroscopic analyses, the structures of gombasterols A-F (**7**-**12**) were elucidated to be those of highly oxygenated steroids possessing a 3β,4α,6α,7β-tetrahydroxy or equivalent (7β-sodium *O*-sulfonato for **9**) substitution pattern and a C-15 keto group as common structural motifs. The relative and absolute configurations of these steroids, including the rare 14β configuration of **7**-**10**, were determined by a combination of NOESY, *J*-based analyses, the 2-methoxy-2-(trifluoromethyl)phenylacetic acid (MTPA) method, and X-ray crystallographic analysis. The absolute configuration of **11** was also assigned by these methods. These compounds moderately enhanced 2-deoxy-2-[(7-nitro-2,1,3-benzoxadiazol-4-yl)amino]-D-glucose (2-NBDG) uptake in differentiated 3T3-L1 adipocytes and phosphorylation of AMP-activated protein kinase (AMPK) and acetyl-CoA carboxylase (ACC) in differentiated mouse C2C12 skeletal myoblasts.

2. Steroids from the Sponge *Dictyonella* sp.

One new dictyoneolone (**14**), a new secosteroid was isolated along with two known ergosterol peroxide (**15** and **16**) from a *Dictyonella* sp. sponge collected from Gageo-do, Korea. Based upon the results of combined spectroscopic analyses, the structure of this compound was determined to possess a highly unusual B/C fused ring. The configurations of **14** were determined by a combination of proton-proton couplings and

NOESY analyses. Dictyoneolone exhibited weak cytotoxicity against the K562 and A549 cancer cell lines.

3. Diterpenes and Sesterterpenes from the Sponge *Phorbas* sp.

Three new diterpenes (**17** – **19**), which reminds of gagunin and linear diterpene bearing cyclohexane moiety, were isolated together with 5 known compounds (**20** – **24**) from the sponge *Phorbas* sp. All of these new compounds have common points that it is originated from diterterpene skeleton. These are constructed as diverse type and number of rings. For instances, **17** and **24** are made by successively linked cyclic-penta, hexa, hepta moieties. Phorbaketals are rearranged sesterterpene as spiroketal in B/C ring. The structures of these new compounds (**17 - 19**), were determined by combined spectroscopic analyses.

4. Scalarane Sesterterpenes from the Sponge *Smenospongia* sp.

3 known scalaranes were isolated from the sponge *Smenospongia* sp. collected from Gageo-do, Korea. Based on the results of combined spectroscopic and chemical analyses, the known scalarane sesterterpenes differ from each other in hydroxyl or acetyl groups. These were already known absolute configuration.

Key words: Korean sponges, natural products, structure determination.
Student number: 2014-30571

List of Contents

List of Tables

List of Figures

I. Introduction

The discovery of marine natural products is nearing the 50 year lapsed since its origin in the 1960s with pioneering studies by Paul Scheuer. Their early studies to understand the general and organic chemistry of marine organisms, it has grown and evolved to be highly multidisciplinary, integrating methods development in organic structure analysis, toxicology, medicinal and synthetic chemistry, pharmacology, biosynthesis and genomics. This field is growing a combinational and social significance at in the early days, and several marine-inspired or -derived drugs are now on the market or in various stages of clinical trial. Furthermore, more than 120 marine natural products are articles of commerce for their utility as reference standards and pharmacological probes of cell biology.

Marine organisms are extensively recognized having diverse classes of natural products. For decades, chemists, ecologists, biologists, have done research to discover what secondary metabolites in each classified marine organism.[1-3] They are not only having marine natural products (MNPs) but those have significant bioactivities as producing potential drugs. With advances in technology, the number of new marine structures reported goes up steeply until now.

More than 22,000 of marine natural products have been found from

marine organisms at least. In addition to these publications there are approximately another 10,000 publications which include synthesis, reviews, and biological activity studies on the subject of marine natural products. Several of the compounds have shown that demonstrate significant activities in anti-viral, antitumor, anti-inflammatory, analgesia, immunomodulation, and allergy assays.[4, 5]

There are FDA-approved marine-derived drugs including one additional drug registered in the EU. Cytarabine (Ara-C) and vidarabine (Ara-A), the first FDA-approved marine-derived drugs, originally isolated from the Caribbean sponge *Tethya crypta*.[1] Cytarabine was approved by the FDA in 1969 as an anticancer drug, while vidarabine was approved in 1976 as an antiviral agent. Next trabectedin, isolated from the marine tunicate *Ecteinascidia turbinata*, the first marine anti-cancer agent to take approval by the EU for the treatment of soft tissue sarcoma and relapsing ovarian cancer. Ziconotide (Prialt™) gained FDA approval in 2004 for the management of severe chronic pain. It was synthetic peptide which isolated from the venom of the cone snail *Conus magus*.[1] Besides, diverse structural classes of drug candidate are in clinical or preclinical trials (Figure 1).

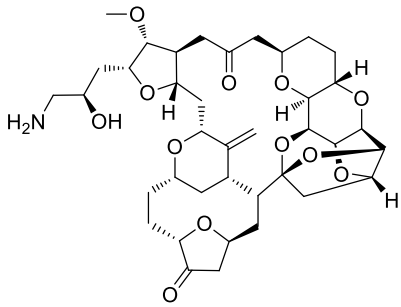

Eribulin (Halaven^{TM}) : antitumor
(Sponge *Lissodendoryx* sp.)

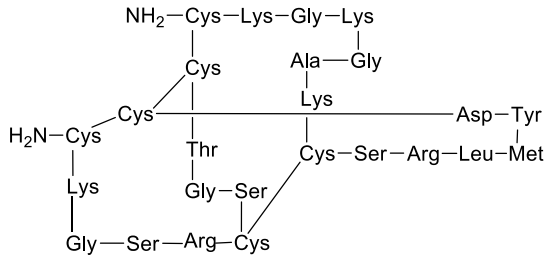

Ziconotide (Prialt^{TM}) : analgesic
(Cone snail *Conus magus*)

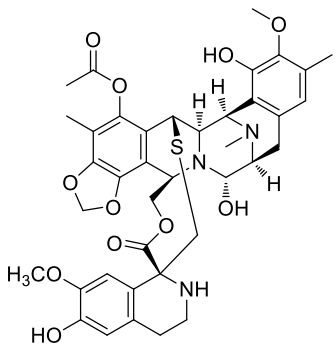

Trabectedin : antitumor
(Ascidian *Ecteinascidia turbinata*)

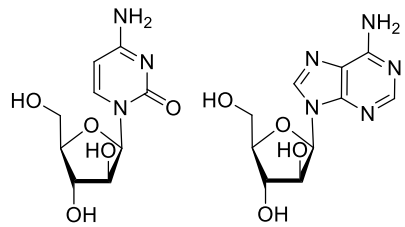

Ara-C (Cytarabine^{TM}), Ara-A (Vidarabine^{TM}) :
antiviral, antitumor (Sponge *Cryptotethya crypta*)

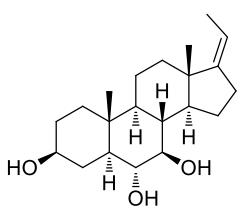

IPL-576092 : antiinflammatory
(Sponge *Petrosia contignata*)

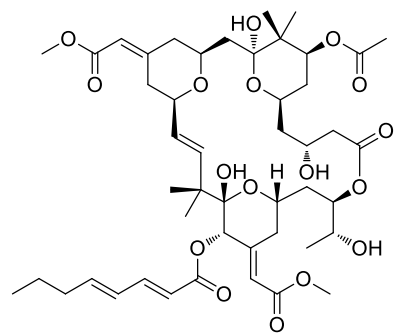

Bryostatin 1 : antitumor
(Bryozoan *Bugula neritina*)

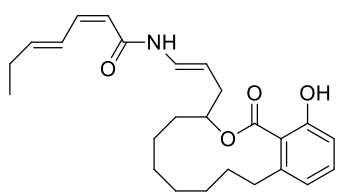

Dolastatin 10 : antitumor
(Sea hare *Dolabella auricularia*)

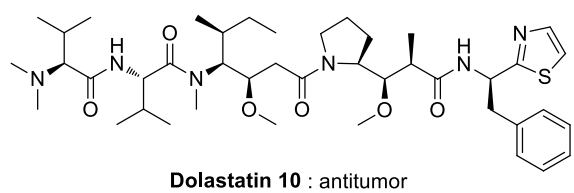

Dolastatin 10 : antitumor
(Sea hare *Dolabella auricularia*)

Figure 1. Examples of marine natural products in clinical and preclinical trials

Since structurally unique compounds had been mostly isolated from marine invertebrates including the phyla Porifera and Coelenterate (ca. 75%). Among these, the major bioactive compounds were from Porifera and Coelenterate, accounting for 56.9% of the total bioactive compounds.[6]

Sponges (phylum Porifera) are one of the most diverse marine organisms, more than thousands species and inhabit all over the world. These are found throughout tropical and polar regions, ranging from tidal zone to depths exceeding 8,800 m.[6] Because of wide distribution of sponges in the world, these are mostly used to isolate interesting metabolites. Sponge-derived compounds possess a wide range of chemical classes (e.g., terpenoids, alkaloids, peptides, and polyketides) (Figure 2) and biotechnologically relevant properties (e. g., anticancer, antibacterial, antifungal, antiviral, and antiprotozoal).[7-9]

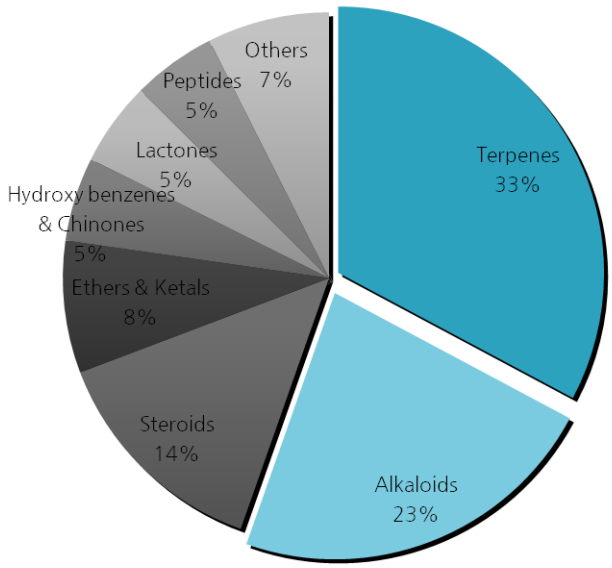

Figure 2. Chemical classes of new compounds isolated from marine sponges

Marine sponges have been recognized as a drug box regarding great potential. Several compounds proved to have antibacterial, antiviral, antifungal, antimalarial, antitumor, immunosuppressive, and cardiovascular activity. Even though pharmacophores in many compounds by which they interfere with human pathogenesis have not been clearly identified untill now. However, sponges produce a different type of carbon skeletons, which have been found to be the main component interfering with human pathogenesis at different sites. The fact that different diseases have the capability to react at different sites in the body can increase the chances to produce targeted medicines.

Among those are ready to develop using in pharmaceutical agents. Drug candidates in clinical or preclinical tests are including psammaplysin H (antimalarial, *Aplysinella strongylata*), discodermolide (immune suppressive; *Discodermia dissoluta*), spongistatin 1 (anticancer; *Spongia* sp.), manzamine A (antimalaria, tuberculosis, HIV; *Acanthostrongylophora* sp.), monanchocidin (anticancer; *Monanchora pulchra*), smenospongine (anticancer, antiangiogenic; *Smenospongia* sp.), renieramycin M (anticancer; *Reniera* sp.) (Figure 3).[10] Invertebrates have been collected from various locations of Korean sea. Choosing a target organism is crucial by observation of chemical analysis and bioassays of the crude extracts. Four specimens had been chosen based on evaluation of chemical investigation.

Focus on the metabolites from Korean marine sponges, there are lots of bioactive secondary metabolites even though those are not developed as a drug yet: cytotoxic diterpenoids pseudodimers from *Phorbas gukhulensis*, bioactive sesterterpenoids from *Monanchora* sp., anti-inflammatory iondinated acetylenic acids from *Suberites mammailaris*, cytotoxic furanosesterterpene tetronic acids from *Sarcotragus* sp.[11] For example, especially gombamide A from the sponge *Clathria gombawuiensis* and phorbaketal from *Phorbas* sp. were synthesized by other chemistry groups recently. This may give them good chances to be a potential drug.

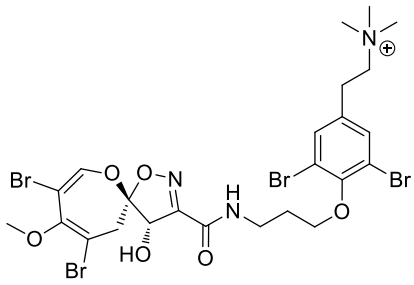

Psammaplysin H : antimalaria
(*Aplysinella strongylata*)

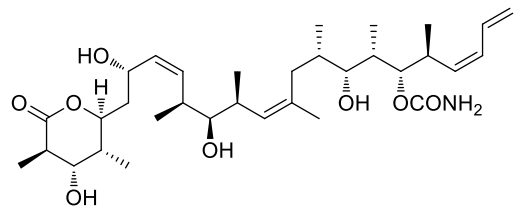

Discodermolide : immunosuppressive
(*Discodermia dissoluta*)

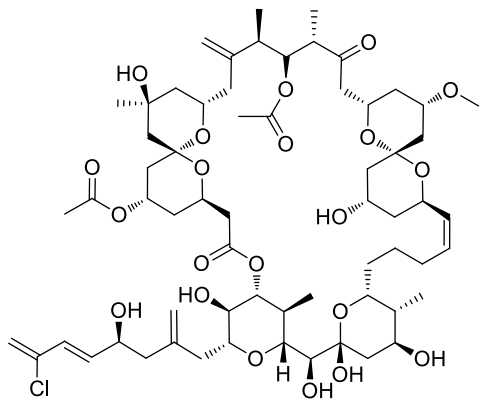

Spongistatin 1 : antitumor
(*Spongia* sp.)

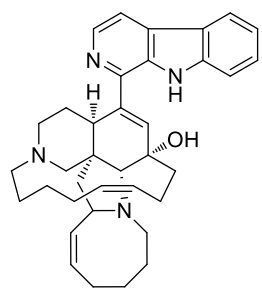

Manzamine A : antimalaria, tuberculosis, HIV
(*Acanthostrongylophora* sp.)

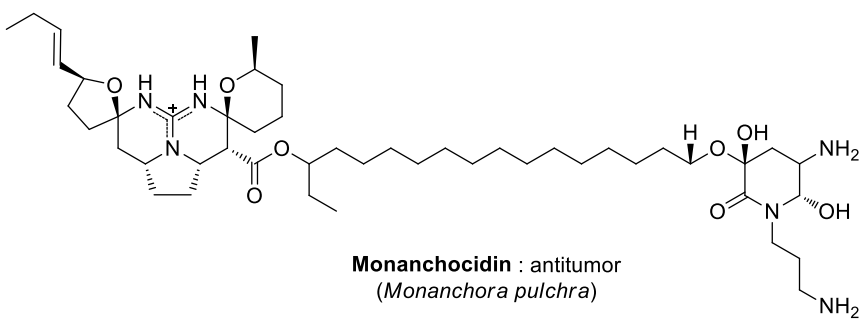

Monanchocidin : antitumor
(*Monanchora pulchra*)

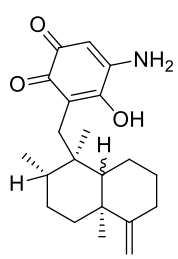

Smenospongine : antitumor, antiangiogenic
(*Smenospongia* sp.)

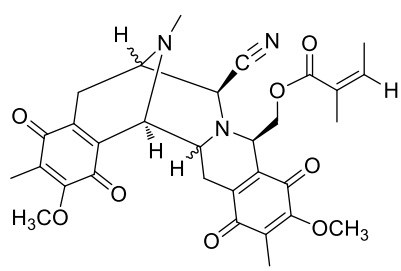

Renieramycin M : antitumor
(*Reniera* sp.)

Figure 3. Examples of potential drug leads derived from marine sponges

During the searching for bioactive secondary metabolites from Korean marine sponges, I dealt with the Korean intrinsic sponges *Clathria gombawuiensis*, *Dictyonella* sp., *Phorbas* sp. and *Smenospongia* sp. The crude extract of which exhibited significant inhibitory activity against either brine shrimp lethality or K562 human leukemia cell line. Secondary metabolites have been isolated from these selected organisms, utilizing various laboratory techniques and chromatographic methods. Finally, 16 novel compounds and 11 known compounds have been structurally determined using combined spectroscopic and chemical analyses. These compounds have been derived from various biogenetic origins and have belonged to various structural classes: sesterterpene sulfates and fatty acid taurines, sesquiterpene quinones, nitrogen containing macrolides, and manzamine alkaloids. All isolates have been examined under various bioactivities: cyotoxicity, antimicrobial activity, and inhibitory activities of isocitrate lyase (ICL), sortase A (SrtA), and Na^+/K^+-ATPase. Several compounds displayed significant cytotoxic, antimirobial, and/or enzyme-inhibitory activities.

II. Studies on the Metabolites from Marine Sponges

1. Sesterterpenes, a Saponin, and Steroids from the Sponge *Clathria gombawuiensis*

The new sesterterpenes, including gombaspiroketals A-C, phorone B, and ansellone C (**1**-**5**), gombaside A as a sponin (**6**), and steroids (**7**-**12**) together with a known steroid were isolated from the Sponge *Clathria gombawuiensis* collected from Korean waters. On the basis of the results of combined spectroscopic analyses, the structures of these compounds were determined to be highly rearranged sesterterpene spiroketal methoxyacetals (**1** and **2**) and a corresponding hemiacetal (**3**). The relative and absolute configurations were assigned by NOESY analysis and ECD calculations, respectively. These compounds exhibited moderate cytotoxicities and antibacterial activities. the structures of phorone B (**4**) and ansellone C (**5**) were determined to be the sesterterpenes of the phorone and ansellone classes, respectively, whereas the saponin gombaside A (**6**) was a nortriterpene sodium *O*-sulfonato-glucuronide of the rare 4,4,14-trimethylpregnane class. The absolute configuration of the glucuronate of 6 was assigned by an application of the phenylglycine methyl ester (PGME) method. The new compounds exhibited moderate cytotoxicity against A549 and K562 cell lines, and compound **6** showed antibacterial activity. The cytotoxicity of **4** may be related to the presence of a free phenolic −OH

group, as the corresponding O-methoxy derivative of **4** is inactive. Six new polyoxygenated steroids (**7**-**12**) along with clathriol (**13**) were isolated from the Korean marine sponge *Clathria gombawuiensis* as well. Based upon the results of combined spectroscopic analyses, the structures of gombasterols A-F (**7**-**12**) were elucidated to be those of highly oxygenated steroids possessing a 3β,4α,6α,7β-tetrahydroxy or equivalent (7β-sodium *O*-sulfonato for **9**) substitution pattern and a C-15 keto group as common structural motifs. The relative and absolute configurations of these steroids, including the rare 14β configuration of **7**-**10**, were determined by a combination of NOESY, *J*-based analyses, the 2-methoxy-2-(trifluoromethyl)phenylacetic acid (MTPA) method, and X-ray crystallographic analysis. The absolute configuration of **11** was also assigned by these methods. These compounds moderately enhanced 2-deoxy-2-[(7-nitro-2,1,3-benzoxadiazol-4-yl)amino]-D-glucose (2-NBDG) uptake in differentiated 3T3-L1 adipocytes and phosphorylation of AMP-activated protein kinase (AMPK) and acetyl-CoA carboxylase (ACC) in differentiated mouse C2C12 skeletal myoblasts.

1-1. Introduction

Frequent encounters and structural diversity of sesterterpenes are the most distinctive features that distinguish sponge metabolites from those of terrestrial and other marine organisms.[11] Several compounds, including

halisulfates, scalaranes, and suvanines, possess notable carbon skeletons, and exhibit significant antimicrobial, cytotoxic, and/or enzyme inhibitory activities.[11-14]

Marine sponges of the genus *Clathria* (order Poecilosclerida, family Microcionidae)[11] are widely distributed at the shallow waters of tropical and temperate regions but far more abundant at the coast of Southern Hemisphere.[12] Since the beginning of its chemical investigation in late 1970's,[13] these animals have produced novel metabolites of a very diverse structural classes such as alkaloids, carotenoids, lipids, nucleosides, peptides, steroids, sugars, and terpenoids.[14,15] Among these, the most frequently encountering groups might be the alkaloids[6] represented by the cyclic guanidines araiosamines,[16f] batzelladines,[16d] and crambescidins.[15] Also noticeable are the cyclic peptides[17] including the microcionamides.[17b] Another interesting examples of *Clathria*-derived metabolites might be the highly oxygenated steroids possessing cis C/D ring juncture.[18] Several of these compounds exhibited potent and diverse bioactivities such as antiinflammatory, antimalarial, antimicrobial, antiviral, and cytotoxic activities as well as the inhibition of cell division of fertilized starfish eggs.[14,15,16d,17a,17b]

During the course of my search for bioactive compounds from Korean water sponges, I recently reported gombamide A, a modified cyclic thiopeptide from the organic extract of *Clathria gombawuiensis*.[15] In addition, the ^{1}H NMR and bioactivity test results showed the presence of

terpenoids in the moderately polar chromatographic fraction of the same extract. Based on spectroscopic analyses, I report here the structure determination of gombaspiroketals A-C (**1**-**3**), which are sesterterpenes of a new skeletal class. These compounds exhibited moderate cytotoxicities and antibacterial activities as well as weak inhibition of Na^+/K^+-ATPase and isocitrate lyase (ICL).

I reported gombamide A, a modified cyclic thiopeptide from the sponge *Clathria gombawuiensis*.[19] More recently, I also reported gombaspiroketals A-C, sesterterpenes of a new skeletal class from the less polar chromatographic fractions of the same extract.[20] However, the NMR data of these fractions revealed the presence of additional terpene metabolites as minor constituents. Here, I report the structures of two new sesterterpenes phorone B (**4**), ansellone C (**5**), and a new nortriterpene saponin gombaside A (**6**). Compounds **4** and **5** belong to the recently reported phorone[21] and ansellone classes,[22] respectively, while **6** was a sodium sulfatidyl glucuronate of the rare 4,4,14-trimethylpregnane class. The sugar residue of this compound is an unprecedented one whose absolute configurations were determined first time by PGME method. These compounds were moderately active against K562 and A549 cell-lines. Additionally, compound **6** showed moderate antibacterial activities.

Marine sponges are widely recognized to be the very prolific sources of structurally unique steroids that possess a diverse array of unusual carbon frameworks and functionalities.[11,44] The distinctive

structural features of sponge-derived steroids have led to significant interest in their biosynthetic pathways. It is possible to cleave the bonds of the steroidal tetracyclic rings and to generate secosteroids. In addition, various metabolites, such as sugars, can be attached to a variety of sites on the steroids.[45-47] Among these steroids, a particularly remarkable deviation from the common frameworks would be the occurrence of a 14β configuration at the C/D ring juncture. Since the isolation of contignasterol, the first example of this framework, from Petrosia contignata,[48] this configuration has been intermittently found in steroids from *Clathria lissosclera*,[49] *Haliclona* sp.,[50] *Ircinia* sp.,[51] *Xestospongia bergquista*,[52] and an unidentified specimen of the family Phloeodictyidae (Oceanapiidae).[53] More recently, this configuration has also been found in a number of steroidal glycosides from Pandaros acanthifolium.[54] Although the 14β steroids such as cardenolides are found from a number of plants,[55] the occurrence of these biosynthetically distinct compounds from only sponges among marine organisms significantly emphasizes the structural diversity of sponge-derived steroids.

^{1}H NMR analysis and cytotoxicity determination of the moderately polar chromatographic fractions revealed the presence of another group of metabolites, inspiring my extensive investigation. Here, I report the structure determination of the six new polyoxygenated steroids gombasterols A-F (**7**-**12**) along with the previously reported clathriol (**13**) using a combination of spectroscopic analyses. These polyoxygenated

steroids possess 3β,4α,6α,7β-tetrahydroxy (or 7β-sodium *O*-sulfonato for **9**) and C-15 keto groups as common structural motifs, which are reminiscent of contignasterol.[48] The relative and absolute configurations of these compounds were assigned by diverse spectroscopic methods such as NOESY analysis, *J*-based analysis, the MTPA method, and X-ray crystallographic analysis. The rare 14β configuration, which resulted in a cis C/D ring juncture was found in several compounds. These polyhydroxy steroids from sponges support a structural relation with those of the contignasterol class. The absolute configuration of clathriol (**13**) had not been reported previously, but was assigned in this work.[49] These compounds moderately enhanced 2-deoxy-2-[(7-nitro-2,1,3-benzoxadiazol-4-yl)amino]-D-glucose (2-NBDG) uptake in differentiated 3T3-L1 adipocytes and phosphorylation of AMP-activated protein kinase (AMPK) and acetyl-CoA carboxylase (ACC) in the differentiated mouse C2C12 skeletal myoblasts.

1-2. Results and discussion

The molecular formula of gombaspiroketal A (**1**) was deduced to be $C_{26}H_{38}O_5$ from HRFABMS analysis. The sesterterpene nature of this compound was apparent from its ^{13}C NMR data, in which signals of twenty-five carbons and a methoxy carbon at δ_C 56.6 were clearly observed. A conspicuous signal was that of a carbonyl carbon at δ_C 200.7, which was interpreted as a conjugated ketone by the absorption band at 1675 cm^{-1} and

the absorption maximum at 228 nm in the IR and UV spectra, respectively. Additionally, six olefinic carbons (3 x C and 3 x CH) at δ_C 144-126 and four oxygen-bearing carbons (1 x C, 2 x CH and 1 x CH_2) at δ_C 100-63 were observed (Table 1). Among the latter carbons, the downfield shifts and multiplicities of two carbons at δ_C 99.3 (C) and 98.2 (CH) were indicative of a ketal and an acetal, respectively, which suggests the highly oxygenated nature of this compound. The remaining fourteen carbons were also categorized by their multiplicities (2 x C, 1 x CH, 7 x CH_2, and 4 x CH_3). These ^{13}C NMR data, in conjunction with the eight degrees of unsaturation in the molecular formula, revealed that **1** was a tetracyclic compound.

Given this information, the structure of compound **1** was determined through a combination of 2-D NMR analyses (Figure 1). Proton COSY and HSQC data revealed the presence of three spin systems. Among these, a methylene and three methine protons, including the olefinic proton at δ_H 6.80, showed several carbon-proton long range correlations with the carbonyl and a quaternary olefinic carbon at δ_C 200.7 and 139.4, respectively, in the HMBC data. Additionally, correlations between the vinyl methyl protons at δ_H 1.81 and carbonyl and olefinic carbons were observed, indicating a 2-methylcyclohexenone moiety (C-1~C-7). This partial structure was extended to include an oxygenated vinyl group (C-8~C-10) by the HMBC correlations between the H-6, H-7 and oxymethylene protons at δ_H 4.06 (2 H, s) and the trisubstituted double bonded carbons at δ_C 143.7

and 126.2. Further extension of this moiety to include a ketal and a methylene was also established by several HMBC correlations between the H-10 olefinic proton at δ_H 5.59 and carbons at δ_C 99.3 (C-11) and 46.0 (C-12).

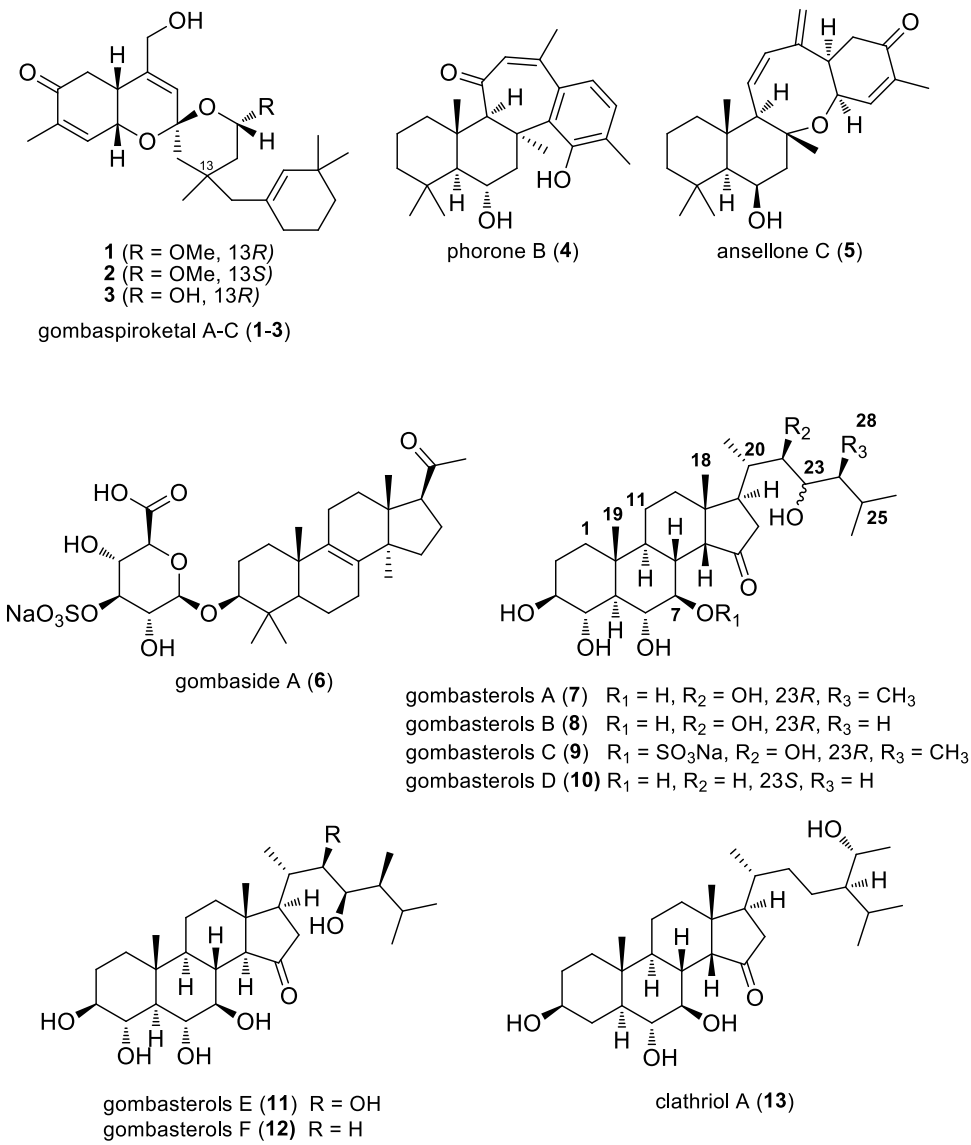

Figure 4. Chemical structures of isolated compounds **1-13**.

Meanwhile, the COSY data also revealed the presence of a linear trimethylene motif (C-21~C-23) whose connection with a geminal dimethyl group was established by several HMBC correlations between the protons and carbons in these groups (Figure 5). Additional HMBC correlations of H-21 and H-22 with the olefinic carbons at δ_C 133.0 and 138.2 indicated a dimethylcyclohexene moiety (C-18~C-25), which was extended to include a methylene group by correlations with the protons at δ_H 1.83 (2 H, s). The connection between this cyclohexene and the earlier established ketone-containing moiety was also indicated by the HMBC data, in which key correlations were observed between an isolated methyl proton at δ_H 1.16 (3 H, s, H-14) with the C-12, C-15 and a quaternary carbon at δ_C 35.2 (C-13).

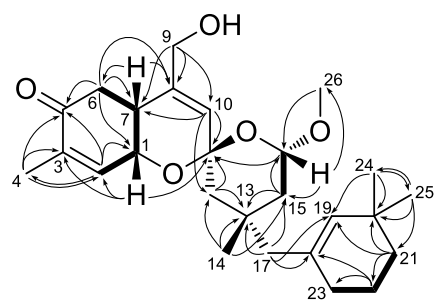

Figure 5. Key correlations of COSY (bold line) and HMBC (arrow) experiments for compound **1**.

The remaining proton spin system defined by the COSY analysis was an isolated system consisting of an acetal proton at δ_H 4.92 (1 H, dd, *J* =

10.0, 2.1 Hz) and methylene protons at 1.56 (1 H, dd, *J* = 13.2, 2.1 Hz) and 1.30 (1 H, dd, *J* = 13.2, 10.0 Hz). The connection of this moiety at the C-13 quaternary carbon was deduced from the HMBC correlation of the C-15 methylene carbon at δ_C 43.3 with the H-14. The presence of a methoxy group at the C-16 acetal center was also shown by mutual HMBC correlations between these groups. Similarly, the linkage between the C-16 acetal and C-11 ketal, which created a tetrahydropyran, was demonstrated by the correlation at H-16/C-11 (Figure 6).

The molecular formula of **1** had one remaining degree of unsaturation which resulted from an oxycyclic moiety involving C-1, C-9, and C-11. With several HMBC correlations for these oxygenated centers, a 3-D model study confirmed a linkage between C-1 and C-11, thus defining a dihydropyran moiety, and the rigid vinyl methylene at C-11 was attached to a hydroxyl group. Thus, the planar structure of gombaspiroketal A (**1**) was determined to be a tetracyclic sesterterpene of a new skeletal class. A literature study revealed that the bicyclic ketal moiety of **1** had a resemblance to phorbaketals and alotaketals from the sponges *Phorbas* sp., *Monanchora* sp., and *Hamigera* sp.[16-18] However, to the best of my knowledge, the highly rearranged carbon skeleton of the C-13~C-25 portion of this compound is unprecedented.

Gombaspiroketal A (**1**) possesses five asymmetric carbon centers: C-1, C-7, C-11, C-13, and C-16. The relative configurations at these centers were determined by proton-proton coupling constants and NOESY analysis

(Figure 6). The small vicinal coupling constant (J = 3.5 Hz) and strong NOESY cross-peaks at H-1/H-6a (δ_H 2.57), H-1/H-7, H-6a/H-7, and H-6b (δ_H 2.39)/H-9 revealed a *syn* orientation for H-1 and H-7 and a *cis* A/B ring junction. Similarly, a strong cross peak at H-14/H-16, supported by those at H-12a (δ_H 1.53)/H-14, H-14/H-15a (δ_H 1.56), and H-15b (δ_H 1.30)/H-17, revealed a 1,3-diaxial orientation of these protons on the C-ring. Finally, based on a series of cross-peaks at H-1/H-16, H-1/H-26, and H-10/H-12b (δ_H 1.49), the spiroketal was found to have the C-12 and 11-16 ether oxygen at α- and β- orientation to the B ring, respectively. Thus, the relative configurations were assigned as 1*R**, 7*R**, 11*R**, 13*S**, and 16*S** for **1**.

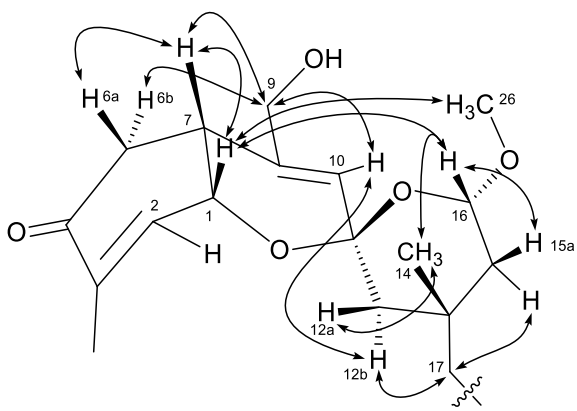

Figure 6. Key correlations of NOESY (arrow) experiment for compound **1**.

The absolute configuration of **1** was determined by comparing its CD spectrum and the ECD spectra of two possible enantiomers, which were calculated using time-dependent density-functional theory (TD-DFT) at the B3LYP/def2-TZVPP//B3LYP/def-SV(P) level for all atoms. As shown in Figure 3, the ECD spectra of (1*R*, 7*R*, 11*R*, 13*S*, 16*S*)-**1** was in accordance

with the experimental CD spectra of **1**. The ECD spectra and the CD spectra of **1** displayed diagnostic negative and positive cotton effects at around 245 and 340 nm, respectively. In addition, this interpretation agreed with the absolute configurations of the cyclohexenone and dihydropyran moieties obtained by X-ray diffraction analysis of ansellone A from the sponge *Phorbas* sp.[19] As a result, gombaspiroketal A (**1**) was determined to be a sesterterpene spiroketal-methoxyacetal with a novel skeletal structure.

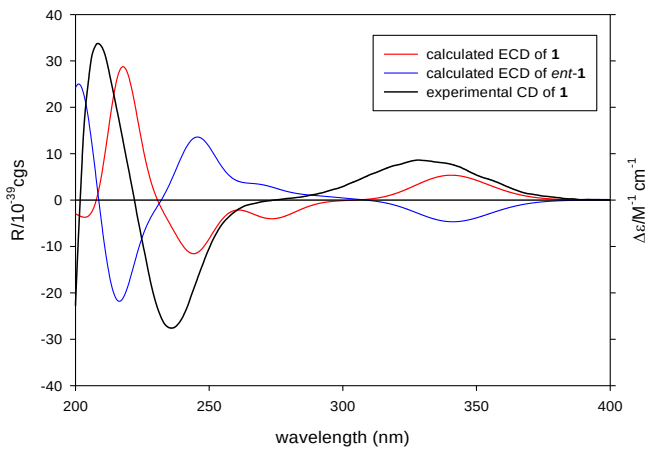

Figure 7. Experimental CD spectra of **1** (black), calculated ECD spectra of **1** (red), and *ent*-**1** (blue).

The molecular formula of gombaspiroketal B (**2**) was deduced to be $C_{26}H_{38}O_5$, which is identical to that of **1**, by HRFABMS analysis. The ^{13}C and ^{1}H NMR data of this compound were also similar to those of **1**. Detailed examination of these NMR data revealed that the signals of the protons and carbons at C-12, C-14, and C-15, which are adjacent to the C-13 asymmetric

center, had shifted significantly, while the other asymmetric centers shifted negligibly (Table 1). As the combined 2-D NMR analyses of **2** showed similar proton-proton and carbon-proton correlations as **1**, these NMR spectroscopic changes as well as the opposite sign of the specific rotation indicated that the opposite configuration at C-13 compared to **1**. Furthermore, the CD curves of **2** showed variations from **1** and **3**. This interpretation was supported by the NOESY data, as cross-peaks were found at H-14/H-12b (δ_H 1.28), H-14/H-15b (δ_H 1.12), H-17/H-15a (δ_H 1.80), H-17/H-16, and H-17/H-12a (δ_H 1.82). The reversed C-13 configuration based on NOE data also coincided with the downfield shift of the C-14 methyl carbon at δ_C 31.2, which had an equatorial orientation on the C ring.[16] Thus, the structure of gombaspiroketal B (**2**) was determined to be the 13*R* diastereomer of **1**.

Gombaspiroketal C (**3**) was isolated as an amorphous solid and was found to have a molecular formula of $C_{25}H_{36}O_5$ by HRFABMS analysis. The ^{1}H and ^{13}C NMR data of this compound were very similar to those of **1**; however, the signals for the C-26 methoxy group were not present, and the signals of the neighboring C-16 acetal center had substantially shifted. Thus, the 16-methoxy acetal was replaced by the corresponding hemiacetal, which was confirmed by combined 2-D NMR analyses. Therefore, gombaspiroketal C (**3**) was determined to be a hemiacetal derivative of **1**.

The most noticeable difference in this skeleton compared to cyclic sesterterpenes from common biosynthetic pathways is the migration of the dimethylcyclohexenyl methylene moiety (C-17~C-25) from C-16 to C-13. This 1,3-migration may induce the attachment of an oxygen at C-16 to accommodate carbocation that may also result in the formation of a spiroketal moiety at C-11. To the best of my knowledge, this type of 1,3-migration is unprecedented among sponge sesterterpenes.

Sesterterpenes derived from marine sponges exhibit diverse and potent bioactivities. From my experiments, compounds **1-3** showed cytotoxicities in the K562 and A549 cell-lines that were comparable to those of doxorubicin (Table 2). Compounds **1** and **3** also displayed moderate antibacterial activities while their diastereomer **2** was virtually inactive. The same trend was also observed for inhibition of the enzymes Na^+/K^+-ATPase and isocitrate lyase (ICL), which can be attributed to the 3-dimensional structure of spiroketal.

Table 1. Results of bioactivity tests **1**-**3**.

	A549	K562	MIC (μg/mL)						Na^+/K^+	ATPase	ICL
	LC_{50} (μM)		Gram(+) Bacteria			Gram(-) Bacteria				IC_{50} (μM)	
compound			A	B	C	D	E	F			
1	1.45	0.77	25.0	6.25	12.5	12.5	6.25	>100		10.9	57.4
2	2.02	1.87	>100	ND	ND	ND	50.0	ND		77.9	>100
3	0.85	4.65	25.0	6.25	25.0	25.0	12.5	>100		18.7	66.3
Doxorubicin	0.79	0.70									
Ampicillin			0.39	0.39	0.39	0.78	0.39	3.12			
Ouabain										3.37	
3-NP[a]											2.54

A : *Staphylococcus aureus* (ATCC 6538p), B : *Bacillus subtilis* (ATCC 6633), C : *Kocuria rhizophila* (NBRC 12708), D : *Salmonella enterica* (ATCC 14028), E : *Proteus hauseri* (NBRC 3851), F : *Escherichia coli* (ATCC 35270).
[a]: 3–nitropropionic acid.
ND : not determined

The molecular formula of **4** was deduced to be $C_{25}H_{34}O_3$ by HRFABMS analysis. The terpene nature of this compound was inferred by the ^{13}C and ^{1}H NMR data in which signals of six upfield methyl carbons and their singlet methyl protons were conspicuously observed (Table 3). The ^{13}C NMR data also showed signals of a carbonyl carbon at δ_C 203.2 and eight aromatic and/or olefinic ones at δ_C 152.6-126.3. Aided by an absorption maximum at 235 (log ε 4.01) nm in the UV spectrum and an absorption band at 1687 cm^{-1} in the IR data, the carbonyl group was thought to be conjugated with a double bond. The remaining ten carbons were divided into 3 x C, 3 x CH, and 4 x CH_2 by their types of proton attachments. Aided with the nine degree of unsaturation inherent in the mass analysis, overall these interpretations indicated that **4** must be a tetracyclic compound, further supporting its terpene nature.

The planar structure of **4** was determined by a combination of 2-D NMR experiments including the HMBC which provided crucial evidences by the correlations of the methyl protons with neighboring carbons (Figure 8). First, all of the protons and their attached carbons were adequately matched by HSQC data. Long-range correlations of two singlet methyl protons at δ_H 0.99 and 0.93 with neighboring carbons including the quaternary one at δ_C 35.1 in HMBC data revealed the characteristic isopropyl head of the terpene compound. The ^{1}H COSY data revealed a linear spin system of three methylenes, adjacent to the isopropyl group, with one (δ_C 42.6, δ_H 1.95 and 0.69) at the terminus. The HMBC correlations of an isolated methyl proton (δ_H 1.33) with this terminal methylene carbon, a methine carbon (δ_C 59.9) and a quaternary carbon (δ_C 38.6) secured a six-membered ring (C-1~C-5 and C-10) attached with three methyl groups (C-20, C-21, and C-23).

The ^{1}H COSY data also revealed a linear spin system consisting of the H-5 methine (δ_H 0.80), an oxymethine (δ_H 4.14) and a methylene (δ_H 3.48 and 2.33). The HMBC correlations of the methylene carbon (δ_C 42.8), a methine carbon (δ_C 69.9) and a quaternary one (δ_C 40.0) with an isolated methyl proton (δ_H 1.31) placed these groups at the neighboring positions. With an additional correlation of the methine carbon with the H-23 methyl proton, these 2-D NMR data allowed the construction of another six-membered ring (C-5~C-10) attached by two methyl groups (C-22 and C-23).

In the meanwhile, the chemical shifts of two downfield protons (δ_H 7.31 and 7.06) as well as the diagnostic coupling constant (J = 8.0 Hz) between these indicated to be the *ortho*-coupled aromatic ones. The HMBC correlations of these protons and a benzylic methyl proton (δ_H 2.23) with neighboring carbons defined a 1-methyl-2-hydroxy-3,4-dialkyl benzene moiety and adequately assigned all of its carbons (C-14~C-19 and C-25). The direct attachment of this moiety at C-8 of the bicyclic system was also deduced by the HMBC correlation at H-22/C-19 (Figure 8).

The remaining NMR signals in **4** were those of a carbonyl carbon (δ_C 203.2) and a tri-substituted double bond (δ_C 132.3, δ_H 6.15; δ_C 151.4) matching the pre-described conjugated ketone functionality attached by a vinyl methyl group (δ_C 29.3, δ_H 2.32). The attachment of this moiety at C-9 of the bicyclic system was allowed by the HMBC correlations at H-9/C-11 (ketone) and H-12 (olefin)/C-9. Similarly, its connection at C-14 of the benzene moiety was accomplished by the HMBC correlation at H-12/C-14 (Figure 8). Thus, the planar structure of compound **4** was defined to be a tetracyclic sesterterpene with two hydroxy and a conjugated ketone functionalities. A literature survey revealed that the carbon framework of this compound is remarkably unusual with the recently reported phorone A from the sponge *Phorbas* sp. as the only previous example.[26]

Compound **4** possessed five asymmetric carbon centers at C-5, C-6, C-8, C-9, and C-10 located in ring B. The relative configurations at these

centers were assigned by NOESY analysis (Figure 9). The mutual cross-peaks among H-6, H-21, and H-23 oriented these protons at the same face of the ring system. Contrarily, the cross-peaks at H-3α (δ_H 1.10)/H-5 and H-5/H-20 oriented the H-5 methine at the opposite face of the ring system that was further extended by the cross-peaks at H-5/H-9 and H-9/H-22. Thus, the overall relative configurations were assigned to be 5*S**, 6*S**, 8*S**, 9*R**, and 10*S**.

Compound **4** possessed a secondary hydroxy group at C-6 of ring B that made an ideal target for the assignment of the absolute configurations based on Mosher's analysis. The reactions were carried out for both **4** and its 18-*O*-methylated derivative of **4**, prepared to prevent the interference of an additional MTPA esterification at the acidic 18-phenolic group. However, attempts under various conditions failed to produce the desired MTPA-adducts from neither compound that contradicted the case of phorone A.[26]

Re-examination of the ^{1}H NMR data revealed that the vicinal proton-proton coupling constants (J = 8.0, 4.9, 3.1 and 7.2, 3.8, 3.8 Hz for **4** and derivative, respectively) of the H-6 oxymethine proton deviated significantly from the expected values of an equatorially oriented ring proton in a chair-type cyclohexane system. A DFT calculation model study showed that, due to the severe spatial crowding with the nearby 18-OH group, the ring B of these compounds was distorted to a half-chair. This conformational change oriented the 6-OH spatially near to C-20 and C-22

methyl groups (3.21 and 2.39 Å, respectively for derivative) that might prevent an esterification between the massive MTPA acid chloride and sterically hindered hydroxy group. Contrarily, the ring B of phorone A, free from the steric hindrance induced by the phenolic group, might have chair form. Accordingly the equatorially oriented 6-OH could be esterified with MTPA. Thus, the structure of compound **4**, designated to be phorone B, was determined to be a new sesterterpene of a rare skeletal class.

The molecular formula of compound **5** was established to be $C_{25}H_{36}O_3$ by HRFABMS analysis. Although the presence of ^{1}H and ^{13}C signals of several methyl groups and a carbonyl carbon indicated the same sesterterpene ketone nature of this compound as **4**, a detailed comparison of the NMR data revealed the significant differences including the disappearance of a phenol moiety in **5**, which prompted us to analyze the whole spectroscopic data extensively.

Starting from the assignment of terminal isopropyl head of a terpene chain at C-4, C-20, and C-21, the combination of ^{1}H COSY and HMBC experiments defined the same [6,6]-bicyclic system substituted with four methyl groups at C-20~C-23 as **4**. However, the remarkable downfield shift of the C-8 quaternary carbon (δ_C 80.1) indicated the attachment of an additional oxygenated functionality in **5**. A combination of the ^{1}H COSY and HMBC data also revealed not only the presence of a conjugated diene but also its direct attachment at C-9 of the bicyclic system. The key HMBC

correlations for this interpretation were those at H-9/C-11, H-11/C-10, H-11/C-13, H-12/C-13, H-24/C-12, and H-24/C-13 (Figure 8). Thus, the presence of an exo-methylene containing diene was defined for **5**.

The ^{1}H COSY data of **5** revealed the presence of a long spin system linearly consisting of protons of a methylene (H-15, δ_H 2.79 and 2.38), a methine (H-14, δ_H 3.42), an oxymethine (H-19, δ_H 4.69) and terminating by an olefinic methine (H-18, δ_H 6.47) that was confirmed by the HMBC correlations between these protons and neighboring carbons; H-14/C-15, H-14/C-19, H-15/C-19, and H-19/C-17. Similarly a methyl proton (H-25, δ_H 1.72) was placed at the allylic position to the C-18 olefin by the HMBC correlations at H-18/C-25, H-25/C-17, and H-25/C-18. In addition, correlations of a carbonyl carbon (C-16, δ_C 202.3) with these protons closed down the ^{1}H COSY and HMBC based system to construct a α-methyl-cyclohexenone moiety corresponding the *o*-methylphenol of **4** (Figure 8).

The linkage of the newly defined cyclohexenone moiety to the other portion of the molecule was also accomplished by HMBC and NMR chemical shift analyses. That is, the linkage between the C-13 and C-14 was evidenced by the key correlations at H-12/C-14, H-14/C-13, and H-24/C-14, in good accordance with the chemical shift of H-14 (δ_H 3.42). Similarly, the presence of an ether bridge between C-8 and C-19 was evidenced by the downfield shift of these carbons and the HMBC correlation at H-19/C-8. Thus, the planar structure of compound **5** was determined to be a tetracyclic

sesterterpene containing an eight-membered oxocane moiety. A literature survey revealed that the carbon skeleton of **5** was highly unusual with the recently found ansellone B from the sponge *Phorbas* sp. as the only previous example.[27] The major structural difference occurred in the oxocane ring C in which the 9-OAc group of ansellone B was replaced by a double bond in **5** that was supported by the comparison of the NMR data of **5** obtained in C_6D_6 with those of ansellone B in literature (Table 3).

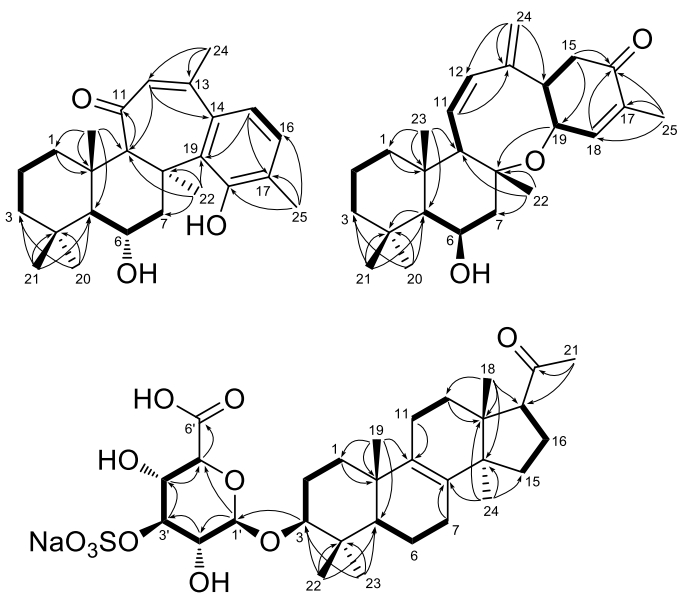

Figure 8. Key correlations of COSY (bold line) and HMBC (arrow) experiments for compounds **4**-**6**.

Compound **5**, designated to be ansellone C, possessed asymmetric carbon centers at C-5, C-6, C-8, C-9, C-10, C-14, and C-19 whose relative configurations were assigned by NOESY analysis (Figure 9). The cross-

peaks of H-23 with both of H-21 and H-22 oriented these methyl groups at the same face of the bicyclic system. Contrarily, the H-5, H-6, H-9, H-20 were oriented at the opposite face of the bicycle by a series of cross-peaks involving these; H-3α (δ_H 1.19)/H-5, H-5/H-7α (δ_H 2.11), H-5/H-9, H-5/H-20, H-6/H-20, and H-7α/H–9. Thus, the relative configurations at the bicyclic system of **5** were assigned to be 5*S**, 6*R**, 8*R**, 9*R**, and 10*S**, opposite from ansellone B at C-6.

The additional asymmetric centers at C-14 and C-19 at C/D ring juncture were also assigned by the NOESY correlations between the H-14 and H-19 methine protons and those at ring B. That is, the cross-peaks were found at H-9/H-14, H-7α/H-18, H-7α/H-19, and H-14/H-19. Thus, the *cis* C/D ring juncture and 14*R** and 19*R** configurations were assigned for **5**. Despite the presence of a secondary hydroxy group at C-6, several attempts to determine its absolute configurations by Mosher's method were unsuccessful since no MTPA-adducts were provided despite of attempts under various conditions. A DFT calculation model showed that the axially oriented 6-OH group was spatially proximal with the neighboring H-21, H-22, and H-23 methyl groups forming 1,3-diaxial orientation preventing the approach of the bulky MTPA-chloride.[31] Thus, the structure of ansellone C (**5**) was determined to be a tetracyclic sesterterpene of a rare structural class.

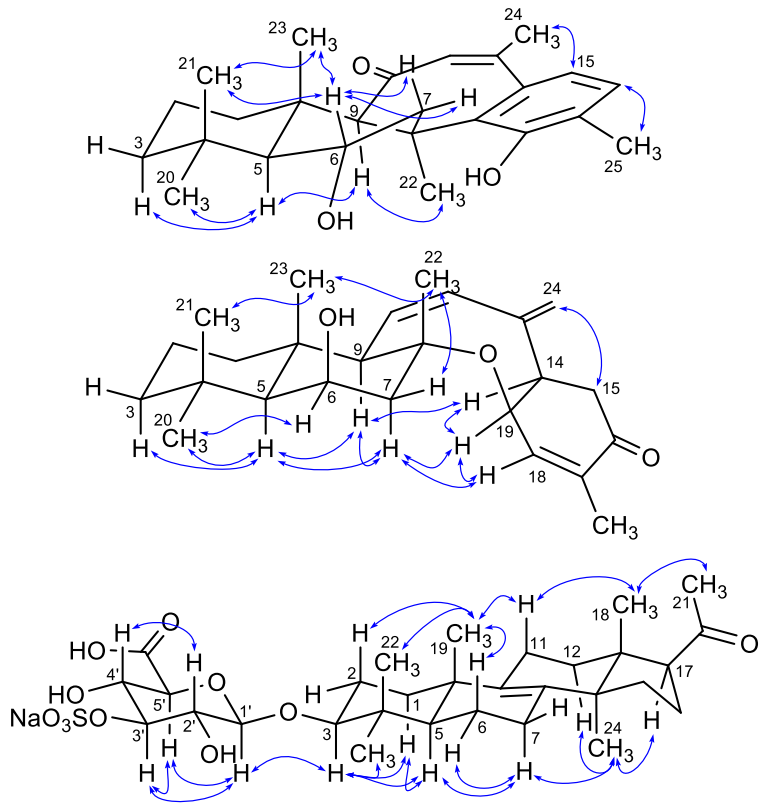

Figure 9. Selected NOESY correlations (blue arrow) for compounds **4**-**6**.

Structure comparison of phorone B (**4**) and ansellone C (**5**) with recently reported sponge-derived sesterterpenes revealed biogenetic relations among these. In particular, phorones, ansellones, phorbasones, and isophorbasone A might be derived from a common tricyclic precursor while phorbaketals and gombaspiroketals might be deviated in early stages of biosynthetic pathway.[16,25-27,32,33] However, this postulation needs to be verified by experimental data.

The molecular formula of compound **6** was established to be $C_{30}H_{45}O_{11}SNa$ by HRFABMS analysis. The NMR data of this compound were reminiscent of those from **4** and **5** by the presence of signals of six upfield

methyl groups (δ_C 31.5-16.8, δ_H 2.11-0.61) and a carbonyl carbon (δ_C 213.1) suggesting a polyprenyl-derived origin. However, the significant differences including the presence of several oxymethines (δ_C 106.4-72.2, δ_H 4.42-3.44) and an additional carbonyl carbon (δ_C 176.3) suggested this to belong to a different structural class such as a saponin. Furthermore, the presence of an oxidative sulfur functionality, inherent in the mass and IR (1380 cm^{-1}) data, prompted us to analyze spectroscopic data extensively (Table 2).

Starting from the founding of isopropyl head of a terpene compound (C-4, C-22, and C-23), a combination of ^{1}H COSY and HMBC data readily defined a trimethylcyclohexane moiety as ring A, similar to **4** and **5**. The characteristic shifts of both carbon and proton at C-3 (δ_C 90.6, δ_H 3.20) revealed the presence of an oxygenated substituent which was described later. In the meanwhile, the ^{1}H COSY data showed a linear proton spin system consisting of the H-5 methine and two methylenes. The chemical shifts of the terminal methylene protons (δ_H 2.10 and 2.09) suggested the attachment of a double bond at this methylene. The long-range correlations of these protons placed a quaternary carbon (δ_C 134.9) at the adjacent C-8 while a similar correlation with the H-19 methyl protons assigned another carbon (δ_C 136.3) at the C-9. Thus, the ring B (C-5~C-10), a cyclohexene moiety with a tetra-substituted double bond, was adequately constructed.

The remaining portion of **6** was also determined by combined 2-D NMR experiments. A linear attachment of two methylenes (C-11 and C-12) at C-8 olefin was secured by both ^{1}H COSY and HMBC data. The extension of these methylenes to construct ring C as a cyclohexane (C-8, C-9, C-11~C-14) substituted with two methyl groups (C-18 and C-24) was accomplished by the HMBC correlations of the methyl protons with the ring carbons. Similarly, the extension of this ring to have a cyclopentane as ring D was made by the ^{1}H COSY data, followed by the HMBC correlations; H-16/C-14, H-17/C-13, H-17/C-18, H-18/C-17, and H-24/C-15. Finally, the attachment of an acetyl group at C-17 of ring D was also made by the HMBC correlations of a singlet methyl proton (δ_H 2.11, H-21) with the C-17 and a carbonyl carbon (δ_C 213.1, C-20). Thus, the main framework of compound **6** was defined to be a norlanostane nortriterpene of 4,4,14-trimethylpregnane class.

The configurations at the asymmetric centers in the main framework were determined by the NOESY data (Figure 9). The conspicuous cross-peaks of the H-18, H-19, and H-22 methyl protons with those at the 1,3-diaxial positions assigned all of these at the same face of the pregnane ring plane. An additional cross-peak at H-18/H-21 also indicated a β-orientation of the C-20 acetyl group to the ring D. In contrast, the mutual cross-peaks of H-1α (δ_H 1.24), H-3, and H-5 with an additional one at H-3/H-23 placed these at the opposite face of the ring plane and a *trans* A/B

ring juncture. Similarly, those at H-6α (δ_H 1.53)/H-7α (δ_H 2.09), H-7α/H-24, and H-12α (δ_H 1.77)/H-24 assigned a *trans* C/D ring juncture. The α-orientation of H-17 was also confirmed by the cross-peak at H-17/H-24. Thus, the whole relative configurations of the asymmetric centers at the norlanostane moiety were adequately assigned.

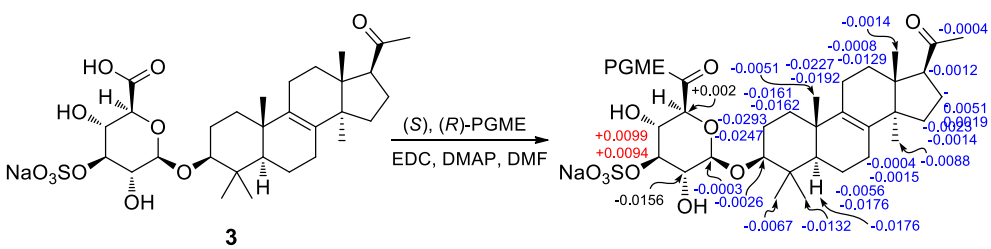

Figure 10. Δδ (*S*-*R*) values (in ppm) obtained from the (*S*)- and (*R*)-PGME amide derivatives of **3**.

The mass and NMR data of **6** revealed the presence of an additional six carbon unit. Both of the ^{13}C and ^{1}H NMR data (δ_C 176.3, 106.4-72.2, δ_H 4.42-3.44), in conjunction with the partial formula of $C_6H_9O_{10}SNa$ from the high-resolution mass and the strong absorption band at 1380 cm^{-1} from the IR data, respectively, suggested this unit to be the sodium salt of a sulfated hexose sugar (Table 4). The ^{1}H COSY data linearly assembled five oxymethine protons while the HMBC data placed the carbonyl carbon at C-6' of the sugar moiety. The pyranose nature of this moiety was also defined by the mutual long-range couplings between the anomeric C-1' and C-5'methine. The sodium sulfate group was placed at C-3' by the downfield

chemical shifts of this methine (δ_C 85.6, δ_H 4.24). The large vicinal couplings (J = 9.5 or 7.8 Hz) between the adjacent ring protons assigned the *axial* orientations for all of these. This interpretation was supported by the NOESY analysis in which the 1,3-diaxial cross-peaks were found at H-1'/H-3', H-1'/H-5', and H-2'/H-4' (Figure 9). Therefore, the sugar moiety was defined to be 3'-sodium sulfatidyl glucuronopyranoside.

The absolute configuration of the glucuronic acid moiety is generally assigned by the acid hydrolysis of compounds followed by the TLC comparison with authentic D-glucuronic acid.[34-36] However, the lack of the pairing L-isomer as the other authentic one severely hindered an unambiguous assignment. Furthermore, the presence of sodium sulfate group in **6** prevented an application of the TLC-based method and required a more reliable one for the glucuronic acid type moieties. This problem was solved by the PGME method in which the presence of a carboxylic acid with a chiral center at its α-position makes this compound an ideal target.[34] The (*S*)- and (*R*)-PGME amides of **6** prepared by the treatment with corresponding PGMEs provided differentiated ^{1}H NMR data (Figure 10). Following the rule of PGME-based assignment, the D-configuration was determined for the glucuronic acid moiety. The β-configuration was also assigned for the anomeric C-1' by both the large $^1J_{CH}$ value (160.2 Hz) and downfield carbon chemical shift (δ_C 106.4). Thus, the structure of nortriterpene saponin **6**, designated to be gombaside A, was determined to

be the 4,4,14-trimethylpregn-$\Delta^{8,9}$-en-18-one-3-*O*-3'-sodium sulfatidyl-β-D-glucuronopyranoside.

Literature survey revealed that, although the compounds possessing the lanostane-derived skeletons are widely distributed in nature, those having the aglycone of **6** were very few and found only from the fungi *Fomes officinalis* and *Ganoderma concinna*.[38-40] Furthermore, the 3'-sodium sulfatidyl glucuronopyranoside unit of this compound is unprecedented to the best of my knowledge, contributing to the structural novelty of **6**.

In my measurement of bioactivity, compounds **4**-**6** were moderately active against K562 and A549 cell-lines (Table 3). In particular, the saponin **6** exhibited potency comparable to those of doxorubicin, with LC_{50} of 2.1, 1.8 μM. The lack of activity of the synthetic 18-methoxy derivative of **4** suggested the role of the phenolic 18-OH group for the cytotoxicity of **4**. Compound **6** was also moderately active against the bacteria *Bacillus subtilis* and *Proteus hauseri*, with LC_{50} 1.6, 3.1 μM, while other compounds were either inactive or untested against the bacterial cell-lines.

Table 2. Results of bioactivity tests **4**-**6**.

	A549	K562	MIC (μg/mL)					
	LC_{50} (μM)		Gram(+) Bacteria			Gram(-) Bacteria		
compound			A	B	C	D	E	F
4	4.7	5.4	>100	ND	ND	ND	>100	ND
5	3.9	4.5	>100	ND	ND	ND	>100	ND
6	2.1	1.8	>100	1.6	>100	>100	3.1	ND
Derivative	>100	>100	ND	ND	ND	ND	ND	ND
Doxorubicin	1.1	1.5						
Ampicillin			0.4	0.4	0.4	0.8	0.4	3.1

A: *Staphylococcus aureus* (ATCC 6538p), B: *Bacillus subtilis* (ATCC 6633), C: *Kocuria rhizophila* (NBRC 12708), D: *Salmonella enterica* (ATCC 14028), E: *Proteus hauseri* (NBRC 3851), F: *Escherichia coli* (ATCC 35270).
ND: not determined

The molecular formula of gombasterol A (**7**) was established to be $C_{28}H_{48}O_7$ by HRFABMS analysis. In the ^{13}C NMR data, signals of a carbonyl (δ_C 223.0) and six oxymethine carbons (δ_C 77.6, 77.3, 76.7, 75.4, 75.2, and 74.7), were conspicuously observed (Table 6). This finding was consistent with the ^{1}H NMR data in which signals of several oxymethine protons were observed in the moderately deshielded region (δ_H 4.41-3.33) (Table 2). The remaining signals in the ^{13}C NMR spectrum were two non-protonated carbons, eight methines, five methylenes, and six methyl carbons in the shielded region.

The COSY results of **7** revealed the presence of a long chain of coupled protons (Figure 11). Starting from the H_2-1 protons, the proton-proton couplings were easily traced to determine a partial structure reaching as far as the H-8 proton with hydroxy groups located at H-3, H-4, H-6, and H-7 based on their characteristic chemical shifts. Similarly, the extension of

proton-proton couplings from H-8 to H_2-12, as well as a branching to H-14, was also accomplished with the COSY data. Then, the characteristic HMBC results of the isolated H_3-19 (δ_H 0.87) with the neighboring C-1, C-5, C-9, and C-10 allowed us to elucidate the bicyclic AB ring moieties. The C ring was similarly constructed base on the long-range correlations of H_3-18 (δ_H 1.20) with C-12, C-13 and C-14 in the HMBC data.

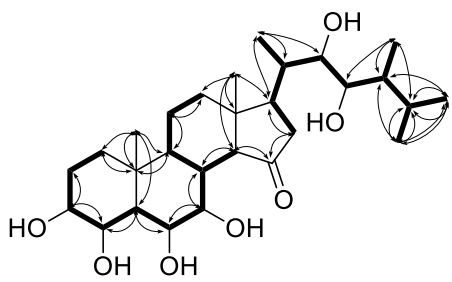

7

Figure 11. Key correlations of COSY (bold line) and HMBC (arrow) experiments for compound **7**.

The COSY data revealed that all remaining protons were also assembled into a single spin system by direct proton-proton couplings (Figure 11). This portion of D ring and side chain was connected to the pre-described C ring based on a 3-bond HMBC correlation at H_3-18/C-17. The HMBC data also revealed another connection based on a correlation between the carbonyl carbon (C-15, δ_C 223.0) and both H-14 and H_2-16, which allowed us to construct the keto-bearing D-ring. Finally, the functionality on the side chain was determined to be the 22,23-dihydroxy-

24-methyl group using a combination of COSY and HMBC data. Thus, the planar structure of gombasterol A (**7**) was determined to be a new steroid bearing the oxygenated functionalities of a keto group at C-15 and six hydroxy groups at C-3, C-4, C-6, C-7, C-22, and C-23.

The relative configurations of the stereogenic centers of the ring portion were assigned on the basis of proton-proton coupling constants and NOESY data. The diagnostic vicinal couplings of key protons on the A and B rings revealed that all of the hydroxy groups were equatorially oriented and the bicyclic ring system was arranged in a chair conformation. The key coupling constants were $J_{2\beta,3}$ = 10.8 Hz, $J_{3,4}$ = 8.7 Hz, $J_{4,5}$ = 10.6 Hz, $J_{5,6}$ = 10.6 Hz, $J_{6,7}$ = 8.8 Hz, and $J_{7,8}$ = 10.7 Hz. This interpretation was confirmed by the NOESY data in which two opposite series of cross-peaks were clearly observed among the ring protons and H_3-19 of the A/B ring juncture (Figure 12). In this interpretation, the H-8 methine proton was also found to be β and axially oriented by its NOESY cross-peaks with H-6 and H_3-19. Additionally, the mutual cross-peaks among H-8, H-14, and H_3-18 allowed us to confidently assign the 14β configuration at the C/D ring juncture.

The relative configurations of the side chain were determined through *J*-based configuration analysis (Figure 13). Aided by the NOESY data, the 2- and 3- bond carbon-proton couplings in the heteronuclear long-range coupling (HETLOC) data revealed sequential *gauche* relationship among the C-21 methyl, C-22 hydroxy, C-23 hydroxy, and C-24 methyl

groups, and allowed the assignment of 20*S**, 22*R**, 23*R**, and 24*S** for the relative configurations. Considering the common 20*S* configuration of steroids, the absolute configuration of this portion was strongly thought to be 20*S*, 22*R*, 23*R*, and 24*S*, and this arrangement was ultimately confirmed by the MTPA method. Interestingly, possibly due to the severe crowding among oxygenated functionalities at the adjacent positions, the MTPA esterifications of **7** with both (*R*)- and (*S*)-MTPA-Cl yielded the 3,7,23-*tris*-MTPA adducts **1S** and **1R**, respectively, as the major products, while the C-4, C-6, and C-22 hydroxy groups were not modified. The Δδ values between the MTPA adducts showed noticeable differentiation around the C-23 stereocenter, confirming the 20*S*, 22*R*, 23*R*, and 24*S* configuration for the side chain (Figure 14). This interpretation was also supported by the X-ray crystallographic analysis of compound **11**, a congener with the same configuration as **7** at the side chain; its structural assignment is discussed later. Thus, the structure of gombasterol A (**7**) was determined to be a new polyoxygenated steroid bearing the 14β configuration.

The molecular formula of gombasterol B (**8**) was established to be $C_{27}H_{46}O_7$ by HRFABMS analysis. The NMR data of this compound were very similar to those of **7** with the lack of a methyl group as the most noticeable difference (Tables 11 and 12). A combination of 2D NMR data readily traced this to the absence of the C-28 methyl group while the remaining portion of molecule was intact in **7**. The configurations of the

ring moieties were also found to be the same as those of **7** based on analyses of proton-proton coupling constants and NOESY data. Based upon the combined results of *J*-based analysis and the Mosher's method, the absolute configurations of the side chain were assigned as 20*S*, 22*R* and 23*R* (Figures 3 and 4). Thus, gombasterol B (**8**) was defined to be the 24-C-demethyl derivative of gombasterol A (**7**).

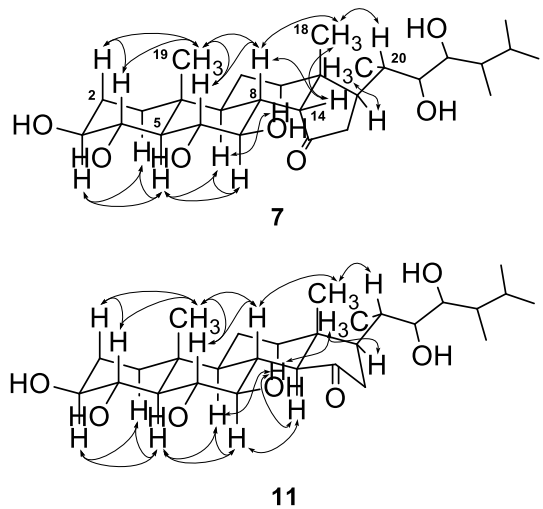

Figure 12. Key correlations of NOESY (arrow) experiments for compounds **7** and **11**.

The molecular formula of gombasterol C (**9**) was deduced to be $C_{28}H_{47}NaO_{10}S$ by HRFABMS analysis. The ^{13}C and ^{1}H NMR data of this compound were very similar to those of **7**. Subsequently, a combined 2D NMR analyses of **9** found the same proton-proton and carbon-proton correlations throughout the entire molecule as **7**. The proton-proton

couplings and NOESY data also showed that these compounds possess identical stereochemistry, including the 14β configuration. Therefore, the structural difference must occur only in the oxygenated functionalities. The difference in the mass data indicated a hydroxy group of **7** had been replaced by a sodium sulfate group in **9**; this was supported by a strong absorption band at 1159 cm^{-1} in the IR data. Re-examination of the ^{13}C and ^{1}H NMR data revealed that carbons and protons at the C-7 methine were noticeably deshielded (δ_C 79.4 and δ_H 5.04, Tables 1 and 2). Thus, gombasterol C (**9**) was defined to be the sodium 7-*O*-sulfonato derivative of gombasterol A (**7**). The only other examples of sponge-derived 14β sterols containing a sodium sulfate group are haliclostannone sulfate[50] and 14β-tamosterone sulfate,[53] both bearing this group at C-2.

The molecular formula of gombasterol D (**10**) was deduced to be $C_{27}H_{46}O_6$ by HRFABMS data. Based upon the results of combined 1D and 2D NMR analyses, this C_{27} steroid was found to possess the same ring portion as **7** and **8**. Therefore the structural difference occurred on its side chain, which bears only a hydroxy group at C-23 (δ_C 70.3 and δ_H 3.69, Tables 6 and 7). The configuration at this isolated center was determined by the Mosher's method. Treatment of **10** with (*R*)- and (*S*)-MTPA-Cl produced the corresponding 3,7,23-tris-MTPA adducts **10S** and **10R**, respectively, as for **7** and **8**. The ring positions for **10** gave similar results to compounds **7** and **8** but the Δδ values for C-23 showed the opposite sign

(Figure 14), thus gombasterol D (**10**) was determined to be a 14β-polyoxygenated steroid with a 23*S* configuration.

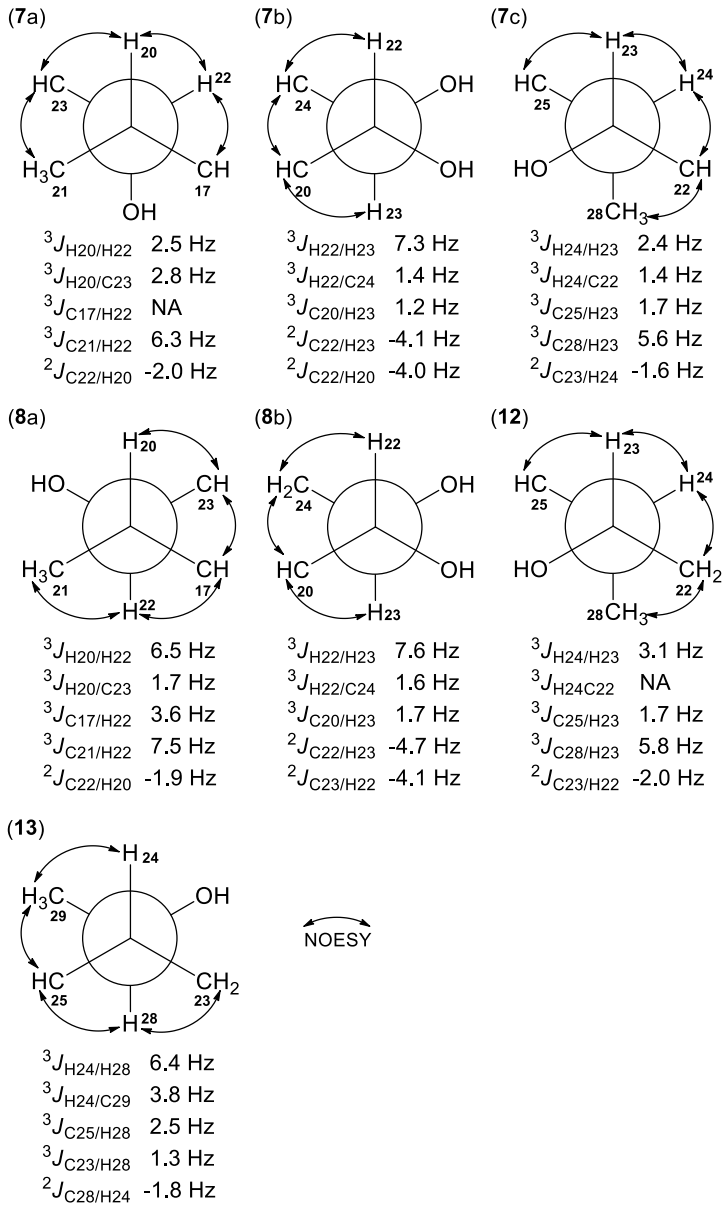

Figure 13. *J*-based configuration analysis of compounds **7**, **8**, **12**, and **13** at (**7**a) C-20 and C-22, (**7**b) C-22 and C-23, (**7**c) C-23 and C-24, (**8**a) C-20 and C-22, (**8**b) C-22 and C-23, (**12**) C-23 and C-24, and (**13**) C-24 and C-28.

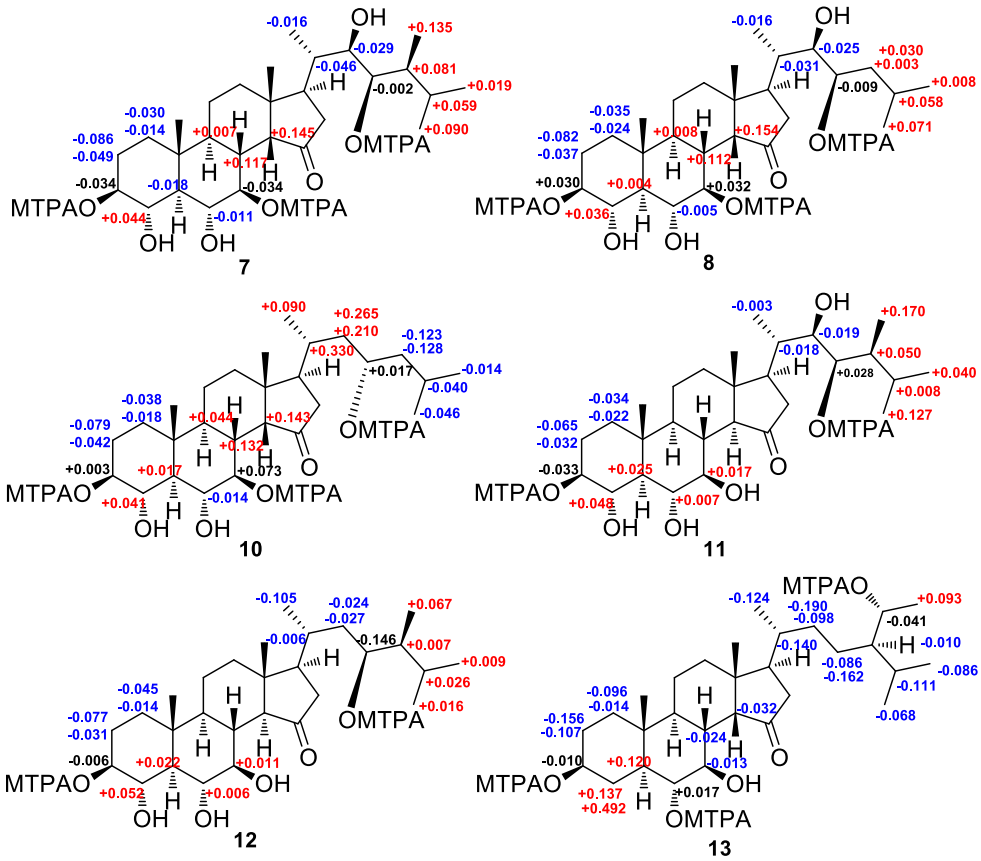

Figure 14. Δδ values (= $\delta_S - \delta_R$; in ppm) obtained for (*S*)- and (*R*)-MTPA esters of compounds **7**, **8**, and **10**-**13**.

Another steroid, gombasterol E (**11**) analyzed for $C_{28}H_{48}O_7$ by HRFABMS analysis. Combined spectroscopic analyses including the 1D and 2D NMR analyses of this compound showed the same proton-proton and proton-carbon correlations as **7**, thus its planar structure was determined to be identical to **7**. However, detailed examination of the ^{13}C and ^{1}H NMR data revealed remarkable shifts at the C-14 methine and neighboring

positions suggesting a configurational difference at this position (Tables 6 and 7). This interpretation was confirmed by the NOESY analysis in which a conspicuous cross-peak was observed at H-8/H-14 (Figure 12). Therefore, **11** must possess the 14α configuration commonly found in most steroids.

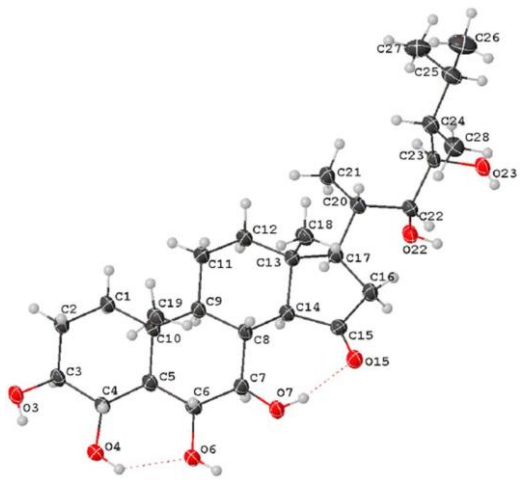

Figure 15. X-ray crystal structure of compound **11**.

The configurations of the side chain were elucidated by the MTPA method. Compounds **11S** and **11R**, the (*S*)-MTPA- and (*R*)-MTPA-adducts of **11**, respectively, were prepared as the major products from the treatment of **11** with (*R*)- and (*S*)-MTPA-Cl, respectively. In contrast to the *tris*-MTPA-esterification at C-3, C-7 and C-23 for **7**, the major products **11S** and **11R** were the *bis*-MTPA-adducts at only the C-3 and C-23. This could be attributed to the *trans* C/D juncture of **11** which brought a severe spatial crowding between the proximal C-7 hydroxy and C-15 keto groups (Figure 2). Nevertheless, the Δδ values between **11S** and **11R** allowed the assignment of the same configurations in **11** as were seen in **7** (Figure 14).

The NMR-based configurational assignments of **11** were further confirmed by X-ray crystallography in which the same absolute configurations were obtained, thus proving the relevance of NMR-based assignments (Figure 15). Overall the structure of gombasterol E (**11**) was unambiguously defined to be the 14-*epi*-derivative of gombasterol A (**7**). This kind of co-occurrence of 14-epimeric steroids from a sponge specimen has only previously been observed in the tamosterone sulfates.[53]

The molecular formula of gombasterol F (**12**) was established to be $C_{28}H_{48}O_6$ by HRFABMS analysis. The NMR data for the ring portion of this compound were very similar to those of **11**, which indicates the same partial structure, including the 14α configuration. Coupled with the lack of an oxygen atom in the mass data, the structural difference between these compounds was traced to the removal of the C-22 hydroxy group of **11** by a combined 2D NMR analyses. The absolute configurations at the side chain were assigned to be 23*S* and 24*S* by NOESY and HETLOC data, and this was confirmed by the MTPA method (Figures 13 and 14). In compound **12**, the dominant *bis*-MTPA-esterification at only C-3 and C-23 hydroxy groups, as found for **11**, supported the argument of steric crowding between the C-7 hydroxy and C-15 ketone group. Thus, the structure of gombasterol F (**12**) was defined to be the 22-dehydroxy derivative of gombasterol E (**11**).

In addition to gombasterols, another steroid (**13**) was isolated and analyzed for $C_{29}H_{50}O_5$ by HRFABMS data. Extensive spectroscopic analyses revealed that this compound was indeed clathriol, a 14β steroid

previously isolated from a New Zealand specimen of the sponge *Clathria lissosclera*.[49] Because the configurations of the side chain portion of this compound was not previously assigned, it was approached by combined *J*-based configuration analysis and Mosher's method as for the gombasterols. As shown in Figure 3, the NOESY and HETLOC data clearly showed *gauche* relationships between both C-23/28-OH and C-25/C-29 (Figure 13), thus 24*R** and 28*R** relative configurations were assigned.

With this assignment in hand, compound **13** was treated with (*R*)- and (*S*)-MTPA-Cl to produce the *tris*-MTPA adducts **13S** and **13R**, respectively. In this case, the MTPA esters in the ring portion were formed at C-3 and C-6, in contrast to at C-3 and C-7 of **7**, **8**, and **10** (Figure 10). This could be attributed to the lack of a C-4α hydroxy group in **13**. Accordingly, the C-6α hydroxy group of **13** may be less spatially crowded than the same group in **7**-**12**, while the C-7β hydroxy group would still be significantly shielded by the C-15 keto group of the D ring. The Δδ values around C-28 showed a distinct pattern indicating the α orientation of the MTPA group. Thus, 24*R* and 28*R* configurations were assigned for clathriol (**13**). This is reminiscent of the identical 24*R* configuration of contignasterol, which has a cyclic hemiacetal at this position.[48]

Sponge-derived 14β steroids and steroidal saponins are reported to exhibit mild but diverse bioactivities such as anti-inflammatory, anti-protozoal, and cytotoxic activities as well as the inhibition of histamine

release.[48b,49,52,54b-c] Despite the modest activity of the chromatographic fraction, none of the individual compounds (**7**-**13**) exhibited noticeable cytotoxicity against K562 or A549 cancer cell-lines (IC_{50} > 10 μM, Supporting Information). These compounds were also inactive against selected strains of pathogenic bacteria and fungi (MIC > 128 μM) and the enzymes isocitrate lyase, Na^+/K^+-ATPase, and sortase A (IC_{50} > 128 μM).

In my further study of bioactivity, anti-diabetic activity of gombasterols were measured for the enhancement of 2-deoxy-2-[(7-nitro-2,1,3-benzoxadiazol-4-yl)amino]-$_D$-glucose (2-NBDG) uptake in differentiated 3T3-L1 adipocytes and the phosphorylation of AMP-activated protein kinase (AMPK) and acetyl-CoA carboxylase (ACC) in differentiated mouse C2C12 skeletal myoblasts. The importance of these tests is, the translocation of glucose transporter type 4 (GLUT4) in muscle and adipose tissues plays an important role for inducible glucose uptake of circulating glucose into muscle and fat cells. There are two physiological pathways which regulate this process, including the AMPK pathway and the insulin signaling pathway.[62a] The activation of the phosphorylation AMPKα (Thr^{172}) could regulate the lipid homeostasis and metabolic control, and this function has been considered as a treatment for type 2 diabetes.[62b] In addition, the previous studies suggested that several downstream targets of AMPK regulated the glucose uptake processes such as decrease of ectopic lipid accumulation by enhancing of the insulin sensitivity, the production

inhibition of hepatic glucose in the liver, and improvement of glucose uptake in the muscle.[62c, d] Recently, the small synthetic and natural products have been reported to improve insulin sensitivity or mimic the action of insulin.[62e] Therefore, the finding of the new drug candidates via AMPK pathway could be used as a promising strategy for the treatment of type 2 diabetes, obesity, and metabolic disorders.

In my measurement, gombasterols showed *in vitro* effect on glucose uptake in 3T3-L1 adipocytes using 2-NBDG as a fluorescent glucose analog. All compounds (**7**–**13**) were evaluated for their potential effects on glucose metabolism and insulin mimetic action at a concentration of 20 μM. Compounds **7**, **8** and **11**–**13** significantly increased 2-NBDG uptake in a concentration-dependent manner. I also observed fluorescent signals after compound treatment under fluorescence microscopy, which confirmed the efficacy of 2-NBDG transportation into the adipocytes (Figure 16). To evaluate the effects of all compounds on the AMPK pathway, an MTT cytotoxicity assay was performed to determine the cytotoxicity of all compounds using the C2C12 myoblasts. The phosphorylated ACC levels were measured by compounds **7**, **8**, and **11**–**13** in comparison to Aicar, which was used as a positive control. Interestingly, the increase in phosphorylation of AMPK induced by **1** was abrogated by pretreatment with compound C, an AMPK inhibitor (Figure 17). All results suggested that these compounds enhanced glucose uptake via the AMPK signaling pathway.

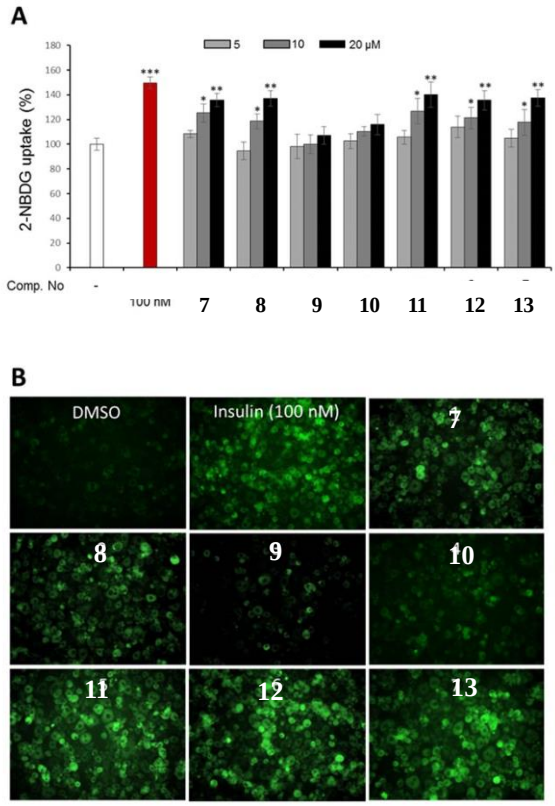

Figure 16. Effects of compounds **7**–**13** on glucose uptake in differentiated 3T3-L1 adipocytes using a fluorescent glucose probe 2-NBDG. (A) The 2-NBDG uptake of compounds **7**–**13** in 3T3-L1 adipocytes was exhibited as fold-increased induction. After 1 hour of incubation, the green fluorescent signals were measured at ex/em = 450/535 nm. Values were expressed as the mean ± SD (*n*=3), * $p < 0.05$ and ** $p < 0.01$, and *** $p< 0.001$ compared to vehicle group. (B) Enhancement of glucose uptake by all compounds (20 μM) or insulin (100 nM) in differentiated 3T3-L1 adipocytes was visualized by fluorescence imaging. The green fluorescent signals in the cells significantly increased, indicating that 2-NBDG was transported into the cells.

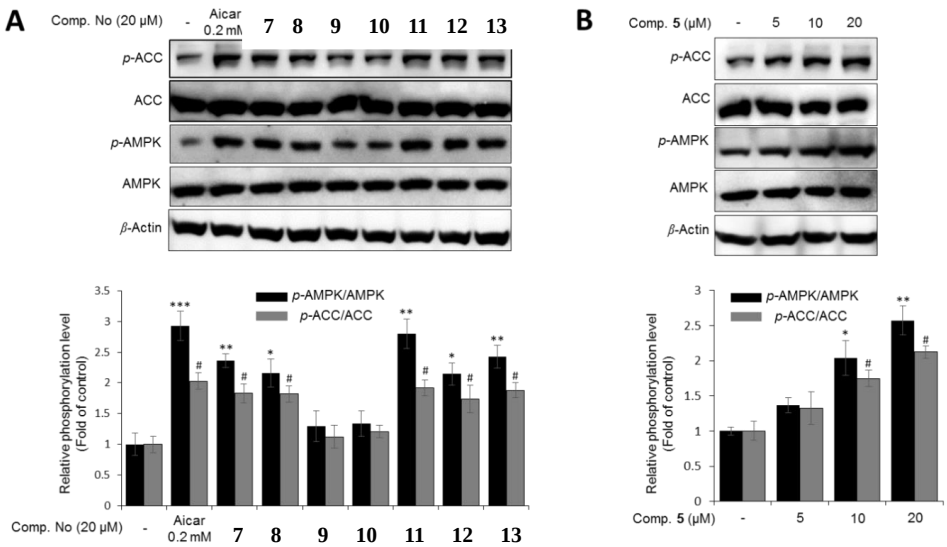

Figure 17. The effects of compounds **7**–**13** on the phosphorylation of AMPK and ACC in the differentiated mouse C2C12 skeletal myoblasts. (A) The cells were incubated with test compounds (20 μM) or an AMPK activator (Aicar, 0.2 mM) for 30 minutes. The levels of *p*AMPK (Thr^{172}) and *p*ACC (Ser^{79}) proteins were evaluated by the western blot method. Each value was expressed as the mean ± SD (*n*=2-4), * $p < 0.05$, and ** $p < 0.01$, *** $p < 0.001$ compared to the vehicle of *p*AMPK; while # $p < 0.05$ compared to the vehicle of *p*ACC. (B) The cells were exposed to compound **5** at various concentrations (5, 10, and 20 μM) for 30 minutes. Western blot analysis was carried out and data were calculated as the mean ± SD (*n*=3), * $p < 0.05$, and ** $p < 0.01$, compared to the control of *p*AMPK; while # $p < 0.05$ compared to the vehicle control of *p*ACC.

In summary, six new polyoxygenated steroids gombasterols A-F (**7**-

12) along with clathriol (**13**) were isolated and structurally elucidated from the Korean sponge *Clathria gombawuiensis*. These steroids possessed 3β,4α,6α,7β–tetrahydroxy (or 7β-sodium *O*-sulfonato for **3**) and C-15 keto groups as common structural motifs. The relative and absolute configurations of these compounds were unambiguously assigned by diverse chemical and spectroscopic methods. The presence of the rare 14β configuration in several compounds (**7**-**12**) significantly contributes to the structural diversity of both sponge-derived steroids and more specifically the metabolites of *C. gombawuiensis*.

1-3. Experimental section

General Experimental Procedures. Optical rotations were measured on a JASCO P-1020 polarimeter using a 1-cm cell. UV and IR spectra were recorded on a Hitachi U-3010 spectrophotometer and JASCO 300E FT-IR spectrometer respectively. NMR spectra were recorded in MeOH-d_4 on Bruker Avance 500 and 600 spectrometers. Proton and carbon NMRs were measured at 500 and 125 MHz (**4**,and **5 8 - 11**) and 600 and 150 MHz (**1-3**, **6, 7, 12**, and **13**), respectively. Mass spectrometric data were obtained at the Korea Basic Science Institute (Daegu, Korea) and were acquired using a JEOL JMS 700 mass spectrometer with *meta*-nitrobenzyl alcohol (NBA) as a matrix for the FABMS. Low-resolution ESIMS data were recorded on an Agilent Technologies 6130 quadrupole mass spectrometer with an Agilent Technologies 1200 series HPLC. HPLC was performed on a SpectraSystem p2000 equipped with a SpectraSystem RI-150 refractive index detector. All solvents were spectroscopic grade or distilled in a glass prior to use.

Animal Material. Specimens of *Clathria gombawuiensis* (Voucher number 06SH-5) were collected by hand using SCUBA equipment off the shore of Gageo-do, Korea, September 9-11, 2006. The detailed morphological features were described in the literature. A voucher specimen

(registry No. spo. 66) is deposited at the Natural History Museum, Hannam University, Daejeon, Korea under the curatorship of Chung J. Sim.

Extraction and Isolation. The freshly collected specimens were immediately frozen and stored at −25 °C until use. The lyophilized specimens were macerated and repeatedly extracted with MeOH (2 L × 3) and CH_2Cl_2 (2 L × 3). The combined extracts (127.2 g) were successively partitioned between *n*–BuOH (36.0 g) and H_2O (84.1 g); the *n*–BuOH fraction was repartitioned between H_2O-MeOH (15:85, 11.64 g) and *n*–hexane (19.74 g). The former layer was separated by C_{18} reversed–phase flash chromatography using a sequential mixture of H_2O and MeOH (six fractions in gradient, H_2O–MeOH, from 50:50 to 0:100), acetone, and finally EtOAc as the eluents.

Based on the results of ^{1}H NMR and cytotoxicity analyses, the fraction that eluted with H_2O–MeOH (10:90; 0.80 g) was separated by semi-preparative reversed-phase HPLC (YMC-ODS column, 10 mm × 250 mm; H_2O–MeOH, 25:75) to yield compounds **1**, **2**, **4**, and **5** which were further purified by HPLC (H_2O–MeOH, 30:70). The H_2O–MeOH (40:60; 0.14 g) fraction was separated by HPLC (H_2O–MeOH, 55:45) to yield compound **3** and **6**. The final isolated amounts of compound **1**-**6** were 5.3, 6.5, 3.5, 5.7, 2.3 and 4.2 mg, respectively. The H_2O–MeOH (20:80; 0.55 g) fraction was separated by semi-preparative reversed-phase HPLC (YMC-

ODS column, 10 mm × 250 mm; 2.0 mL/min, H_2O–MeOH, 30:70) to yield, in order of elution, compounds **9**, **11**, and **12** with retention times (t_R) of 35.5, 46.1, and 66.5 min, respectively. Then each of these compounds was purified by reversed-phase HPLC (YMC-ODS column, 4.6 mm × 25 0 mm; H_2O–MeOH, 40:60). The latter H_2O–MeOH (10:90) fraction was also separated by HPLC (H_2O–MeOH, 20:80; 1.0 mL/min) to afford, in order of elution, compounds **8**, **12**, **7**, and **13** with retention times (t_R) of 22.3, 26.8, 32.3, and 41.0 min, respectively, then purified similarly in analytical HPLC (H_2O–MeOH, 30:70). The amounts isolated were 107.7, 34.9, 6.3, 7.0, 24.1, 12.5, and 15.5 mg, for **7**-**13**, respectively.

Gombaspiroketal A (1): white amorphous solid; $[\alpha]_D^{25}$ +24.2 (*c* 0.45, MeOH); UV (MeOH) λ_{max} (log ε) 205 (4.25), 228 (4.33) nm; IR (ZnSe) ν_{max} 3390, 3075, 2970, 1675, 1521 cm^{-1}; HRFABMS *m*/*z* 431.2799 $[M+H]^+$ (calcd for $C_{26}H_{39}O_5$, 431.2797).

Gombaspiroketal B (2): white amorphous solid; $[\alpha]_D^{25}$ -38.4 (*c* 0.65, MeOH); UV (MeOH) λ_{max} (log ε) 225 (4.45) nm; IR (ZnSe) ν_{max} 3273, 2950, 1670, 1509 cm^{-1}; HRFABMS *m*/*z* 431.2799 $[M+H]^+$ (calcd for $C_{26}H_{39}O_5$, 431.2797).

Gombaspiroketal C (3): white amorphous solid; $[\alpha]_D^{25}$ +20.4 (*c* 0.30, MeOH); UV (MeOH) λ_{max} (log ε) 205 (4.41), 228 (4.30) nm; IR (ZnSe) ν_{max} 3392, 3061, 2963, 1674, 1509, cm^{-1}; HRFABMS *m*/*z* 439.2463

$[M+Na]^+$ (calcd for $C_{25}H_{36}O_5Na$, 439.2460).

Phorone B (**4**): yellow amorphous solid; $[\alpha]_D^{25}$ -50 (*c* 0.40, MeOH); UV (MeOH) λ_{max} (log ε) 211 (4.21), 235(4.01), 313 (3.87) nm; IR (ZnSe) ν_{max} 3354, 2957, 2930, 1687, 1622 cm^{-1}; HRFABMS *m*/*z* 383.2583 $[M+H]^+$ (calcd for $C_{25}H_{35}O_3$, 383.2586).

Ansellone C (**5**): white amorphous solid; $[\alpha]_D^{25}$ -73 (*c* 0.55, MeOH); UV (MeOH) λ_{max} (log ε) 225 (4.02), 309 (3.80) nm; IR (ZnSe) ν_{max} 3365, 2852, 1685, 1545, 1453 cm^{-1}; HRFABMS *m*/*z* 385.2740 $[M+H]^+$ (calcd for $C_{25}H_{37}O_3$, 385.2743).

Gombaside A (**6**): white amorphous solid; $[\alpha]_D^{25}$ -13 (*c* 0.45, MeOH); IR (ZnSe) ν_{max} 3450, 2949, 1740, 1695, 1380 cm^{-1}; HRFABMS *m*/*z* 637.2669 $[M+H]^+$ (calcd for $C_{30}H_{46}O_{11}SNa$, 637.2659).

Gombasterol A (7): white amorphous solid; $[\alpha]_D^{25}$ -5 (*c* 0.2, MeOH); IR (ZnSe) ν_{max} 3649, 2940, 2356, 1726 cm^{-1}; HRFABMS *m*/*z* 519.3303 $[M + Na]^+$ (calcd for $C_{28}H_{48}O_7Na$, 519.3298).

Gombasterol B (8): white amorphous solid; $[\alpha]_D^{25}$ -7 (*c* 0.1, MeOH); IR (ZnSe) ν_{max} 3618, 2961, 2346, 1723 cm^{-1}; HRFABMS *m*/*z* 505.3143 $[M + Na]^+$ (calcd for $C_{27}H_{46}O_7Na$, 505.3141).

Gombasterol C (9): yellow amorphous solid; $[\alpha]_D^{25}$ +18 (*c* 0.3, MeOH); IR (ZnSe) ν_{max} 3696, 2948, 2866, 1728, 1159 cm^{-1}; HRFABMS *m*/*z* 599.2872 $[M + H]^+$ (calcd for $C_{28}H_{48}O_{10}SNa$, 599.2866).

Gombasterol D (10): white amorphous solid; $[\alpha]_D^{25}$ -16 (c 0.3, MeOH); IR (ZnSe) ν_{max} 3622, 2953, 2336, 1731 cm^{-1}; HRFABMS m/z 467.3374 $[M + H]^+$ (calcd for $C_{27}H_{47}O_6$, 467.3373).

Gombasterol E (11): white amorphous solid; mp 154 ℃; $[\alpha]_D^{25}$ -37 (c 0.3, MeOH); IR (ZnSe) ν_{max} 3622, 2970, 2337, 1706 cm^{-1}; HRFABMS m/z 497.3479 $[M + H]^+$ (calcd for $C_{28}H_{49}O_7$, 497.3478).

Gombasterol F (12): white amorphous solid; $[\alpha]_D^{25}$ -13 (c 0.2, MeOH); IR (ZnSe) ν_{max} 3645, 2964, 2325, 1710 cm^{-1}; HRFABMS m/z 481.3530 $[M + H]^+$ (calcd for $C_{28}H_{49}O_6$, 481.3529).

Clathriol (13): yellow amorphous solid; $[\alpha]_D^{25}$ +8 (c 0.2, MeOH); lit. $[\alpha]_D^{25}$ +23 (c 1.4, MeOH)[7]; IR (ZnSe) ν_{max} 3442, 2954, 2881, 1730 cm^{-1}; HRFABMS m/z 501.3563 $[M + Na]^+$ (calcd for $C_{29}H_{50}O_5Na$, 501.3556).

Methylation of Compound 4. To a stirred solution of **4** (0.5 mg) in 0.5 mL of dry pyridine were added CH_3I (80 μL) and DMAP (0.4 mg) under N_2 at room temperature and stirred for 4 h. After the reactions were finished, the solvent was dried by evaporation and separated by HPLC (YMC-ODS column, 4.6 mm × 250 mm; H_2O–MeOH, 20:80) to obtain derivative (0.4 mg). **18-*O*-Methylphorone B** (**derivative**): amorphous white solid; ^1H NMR (MeOH-d_4) δ_H 7.40 (1 H, d, *J* = 8.0 Hz, H-15), 7.15 (1 H, d, *J* = 8.0 Hz, H-16), 6.16 (1 H, s, H-12), 4.08 (1 H, ddd, *J* = 7.2, 3.8, 3.8 Hz, H-6), 3.68 (3 H, s, H-26), 3.48 (1 H, dd, *J* = 16.4, 3.1 Hz, H-7β), 3.45 (1

H, dd, *J* = 16.4, 3.1 Hz, H-7α), 2.84 (1 H, s, H-9), 2.30 (3 H, s, H-24), 2.15 (3 H, s, H-25), 1.84 (1 H, ddd, *J* = 13.1, 3.1, 3.2 Hz, H-1α), 1.66 (1 H, m, H-2β), 1.40 (3 H, s, H-22), 1.35 (1 H, m, H-3α), 1.34 (1 H, m, H-2α), 1.32 (3 H, s, H-23), 1.07 (1 H, ddd, *J* = 13.7, 13.7, 3.4 Hz, H-3β), 0.96 (3 H, s, H-21), 0.90 (3 H, s, H-20), 0.70 (1 H, ddd, *J* = 13.1, 13.1, 3.2 Hz, H-1β), 0.69 (1 H, d, *J* = 8.0 Hz, H-5). LRESIMS *m*/*z* 397.2 $[M+H]^+$ (calcd for $C_{26}H_{37}O_3$, 397.3).

Preparation of (*R*)- and (*S*)-Phenylglycine Methyl Ester (PGME) Amides of 6. To duplicated solutions of compound **6** (0.4 mg each) in 0.5 mL of DMF were added (*S*)- or (*R*)-PGME (0.2 mg), EDC (0.2 mg), and DMAP (0.3 mg), at 42 ^oC and stirred for 18 h. After the reaction was finished, the solvent was removed by evaporation. The residue was partitioned by H_2O and ethyl acetate and the latter layer was separated by HPLC (YMC-ODS column, 4.6 mm × 250 mm; H_2O–MeOH, 27:73) to afford the pure (*S*)- and (*R*)-PGME amide of **6**, respectively.

(S)-PGME Amide of **6:** pale yellow oil; ^1H NMR (MeOH-d_4) δ_H 7.4016-7.3415 (5 H, m, PGME-Ar), 5.5479 (1 H, s, PGME-H-1), 4.5106 (1 H, d, *J* = 7.8 Hz, H´-1), 4.2538 (1 H, dd, *J* = 9.5, 9.5 Hz, H´-3), 3.9102 (1 H, d, *J* = 9.5 Hz, H´-5), 3.7216 (1 H, dd, *J* = 9.5, 9.5 Hz, H´-4), 3.7154 (3 H, s, PGME-OMe), 3.4271 (1 H, dd, *J* = 9.5, 9.5 Hz, H´-2), 3.1988 (1 H, dd, *J* = 11.5, 4.2 Hz, H-3), 2.9858 (1 H, dd, *J* = 8.1, 8.1 Hz, H-17), 2.2472 (1 H, m, H-16α), 2.1997 (1 H, m, H-11α), 2.1469 (1 H, m, H-11β), 2.1131 (3 H, s,

H-21), 2.0833 (1 H, m, H-7β), 2.0717 (1 H, m, H-7α), 2.0390 (1 H, m, H-12α), 1.9019 (1 H, m, H-2β), 1.7868 (1 H, ddd, *J* = 11.6, 11.6, 3.7 Hz, H-12β), 1.7273 (1 H, m, H-1α), 1.7186 (1 H, m, H-6β), 1.7126 (1 H, m, H-15β), 1.7049 (1 H, m, H-16β), 1.6592 (1 H, m, H-2α), 1.5291 (1 H, m, H-6α), 1.3067 (1 H, m, H-15α), 1.2346 (1 H, ddd, *J* = 13.0, 13.0, 2.9 Hz, H-1β), 1.0527 (3 H, s, H-22), 1.0987 (1 H, dd, *J* = 11.5, 4.2 Hz, H-5), 0.9975 (3 H, s, H-24), 0.9925 (3 H, s, H-19), 0.8441 (3 H, s, H-23), 0.6189 (3 H, s, H-18). LRFABMS *m*/*z* 784.2 $[M+H]^+$ (calcd for $C_{39}H_{55}NO_{12}SNa$, 784.3).

(R)-PGME Amide of **6:** pale yellow oil; ^{1}H NMR (MeOH-d_4) δ_H 7.4104-7.3369 (5 H, m, PGME-Ar), 5.5441 (1 H, s, PGME-H-1), 4.5109 (1 H, d, *J* = 7.8 Hz, H´-1), 4.2444 (1 H, dd, *J* = 9.5 9.5 Hz, H´-3), 3.9082 (1 H, d, *J* = 9.5 Hz, H´-5), 3.7239 (3 H, s, PGME-OMe), 3.7117 (1 H, dd, *J* = 9.5, 9.5 Hz, H´-4), 3.4427 (1 H, dd, *J* = 9.5, 9.5 Hz, H´-2), 3.2248 (1 H, dd, *J* = 11.5, 4.2 Hz, H-3), 2.9870 (1 H, dd, *J* = 8.1, 8.1 Hz, H-17), 2.2518 (1 H, m, H-16α), 2.2224 (1 H, m, H-11α), 2.1661 (1 H, m, H-11β), 2.1135 (3 H, s, H-21), 2.0837 (1 H, m, H-7β), 2.0732 (1 H, m, H-7α), 2.0398 (1 H, m, H-12α), 1.9312 (1 H, m, H-2β), 1.7997 (1 H, ddd, *J* = 11.6, 11.6, 3.7 Hz, H-12β), 1.7434 (1 H, m, H-1α), 1.7362 (1 H, m, H-6β), 1.7140 (1 H, m, H-15β), 1.7068 (1 H, m, H-16β), 1.6839 (1 H, m, H-2α), 1.5347 (1 H, m, H-6α), 1.3090 (1 H, m, H-15α), 1.2508 (1 H, ddd, *J* = 13.0, 13.0, 2.9 Hz, H-1β), 1.0594 (3 H, s, H-22), 1.1088 (1 H, dd, *J* = 11.5, 4.2 Hz, H-5), 1.0063 (3 H, s, H-24), 0.9976 (3 H, s, H-19), 0.8574 (3 H, s, H-23), 0.6203 (3 H, s,

H-18). LRFABMS *m*/*z* 784.2 $[M+H]^+$ (calcd for $C_{39}H_{55}NO_{12}SNa$, 784.3).

X-ray Crystal Structure Analysis of Compound 11. White single crystals of compound **11**, which were suitable for X-ray analysis, were obtained by crystallization from CH_2Cl_2-MeOH (9:1). A suitable crystal was selected and placed onto a nylon loop with Paratone-N oil and mounted on a SuperNova, Dual, Cu at zero, AtlasS2 diractometer. The data collection was carried out using Cu Kα radiation and the crystal was kept at 99.9(2) K during data collection. Crystallographic data of **11**: $C_{28}H_{48}O_7$ (M = 496.66); monoclinic crystal (0.219 × 0.106 × 0.028); Space group *P*21; unit cell dimensions a = 14.3972(4) Å, b = 6.5250(2) Å, c = 15.8944(5) Å, β = 110.130(3)°, V = 1401.95(7) $Å^3$; Z = 2; ρcalc = 1.177 g/cm^3; μ = 0.667 mm^{-1}; 27638 reflections measured (7.154° ≤ θ ≤ 152.898°); 5647 unique (*R*int = 0.0495); Final R indexes R1 = 0.0419 (>=2σ(I)) and *w*R2 = 0.1097 (all data); Flack parameter = -0.10(12). Crystallographic data for compound **5** have been deposited in the Cambridge Crystallographic Data Centre (CCDC) with number of 1473565. These data are available, free of charge, from the CCDC via http://www.ccdc.cam.ac.uk/data_request/cif.

Preparation of the (*S*)- and (*R*)-α-Methoxy-α-trifluoromethylphenylacetic chloride (MTPA-Cl) Esterification of Compounds 7, 8 and 10-13. To duplicate solutions of compound **7** (4 mg, 8.1 μmol each) and DMAP (0.5 mg each) in 0.8 mL of anhydrous pyridine

were added (*R*)- or (*S*)-MTPA chloride (8 mg, 0.03 mmol each), which were allowed to stir under N_2 at ambient temperature for 4 h. After the reaction, samples were dried under vacuum and separated by HPLC (YMC-ODS column, 4.6 x 250 mm; H_2O–MeOH, 11:89) to afford the pure (*S*)- and (*R*)-MTPA esters derivatives of **7**, respectively. The (*S*)- and (*R*)-MTPA esters of **8** and **10**-**13** were also prepared by similar manner.

*Tris(S)-MTPA Ester of **7** (**7S**)*: Pale white, amorphous solid; ^{1}H NMR (CD_3OD, 600 MHz) δ_H 7.30-7.70 (15H, m, MTPA-Ar), 6.120 (1H, dd, *J* = 11.7, 9.1 Hz, H-7), 5.462 (1H, dd, *J* = 8.0, 2.8 Hz, H-23), 4.948 (1H, m, H-3), 4.018 (1H, dd, *J* = 11.0, 9.2 Hz, H-4), 3.890 (1H, dd, *J* = 11.0, 9.0 Hz, H-6), 3.814 (1H, dd, *J* = 8.0, 2.1 Hz, H-22), 3.592 (3H, s, MTPA-OMe), 3.465 (3H, s, MTPA-OMe), 3.444 (3H, s, MTPA-OMe), 2.497 (1H, br s, H-16β), 2.430 (1H, dd, *J* = 20.1, 4.2 Hz, H-16α), 2.293 (1H, br s, H-14), 1.913 (1H, m, H-2α), 1.861 (1H, ddd, *J* = 11.0, 6.8, 4.6 Hz, H-8), 1.832 (1H, m, H-17), 1.719 (1H, m, H-20), 1.713 (1H, m, H-1β), 1.709 (1H, m, H-2β), 1.513 (1H, m, H-11α), 1.469 (1H, m, H-24), 1.461 (1H, br d, *J* = 10.7 Hz, H-5), 1.385 (1H, m, H-12α), 1.284 (1H, m, H-12β), 1.271 (1H, m, H-25), 1.262 (1H, m, H-9), 1.251 (1H, m, H-11β), 1.211 (3H, s, H-18), 1.068 (1H, m, H-1α), 1.059 (3H, d, *J* = 6.9 Hz, H-21), 0.996 (3H, d, *J* = 6.7 Hz, H-26), 0.909 (3H, d, *J* = 6.7 Hz, H-28), 0.907 (3H, d, *J* = 6.7 Hz, H-27), 0.871 (3H, s, H-19); LRESIMS *m*/*z* 1145.4 $[M + H]^+$ (calcd for $C_{58}H_{70}F_9O_{13}$, 1145.5).

*Tris(R)-MTPA Ester of **7** (**7R**)*: Pale white, amorphous solid; ^{1}H

NMR (CD_3OD, 600 MHz) δ_H 7.30-7.70 (15H, m, MTPA-Ar), 6.154 (1H, dd, *J* = 10.6, 8.9 Hz, H-7), 5.464 (1H, dd, *J* = 8.0, 1.8 Hz, H-23), 4.982 (1H, m, H-3), 3.974 (1H, dd, *J* = 10.6, 9.0 Hz, H-4), 3.901 (1H, dd, *J* = 10.6, 8.9 Hz, H-6), 3.843 (1H, dd, *J* = 8.0, 2.1 Hz, H-22), 3.609 (3H, s, MTPA-OMe), 3.530 (3H, s, MTPA-OMe), 3.431 (3H, s, MTPA-OMe), 2.496 (1H, br s, H-16β), 2.490 (1H, dd, *J* = 20.0, 4.1 Hz, H-16α), 2.148 (1H, br s, H-14), 1.999 (1H, m, H-2α), 1.848 (1H, m, H-17), 1.744 (1H, m, H-8), 1.765 (1H, m, H-20), 1.758 (1H, m, H-2β), 1.727 (1H, m, H-1β), 1.534 (1H, m, H-11α), 1.454 (1H, br d, *J* = 10.6 Hz, H-5), 1.394 (1H, m, H-12α), 1.388 (1H, m, H-24), 1.295 (1H, m, H-12β), 1.271 (1H, m, H-11β), 1.255 (1H, m, H-9), 1.212 (1H, m, H-25), 1.098 (1H, m, H-1α), 1.092 (3H, s, H-18), 1.075 (3H, d, *J* = 6.9 Hz, H-21), 0.977 (3H, d, *J* = 6.7 Hz, H-26), 0.885 (3H, s, H-19), 0.817 (3H, d, *J* = 6.7 Hz, H-27), 0.774 (3H, d, *J* = 6.7 Hz, H-28); LRESIMS *m*/*z* 1145.4 $[M + H]^+$ (calcd for $C_{58}H_{70}F_9O_{13}$, 1145.5).

*Tris(S)-MTPA Ester of **8** (**8S**)*: Pale white, amorphous solid; ^1H NMR (CD_3OD, 600 MHz) δ_H 7.20-7.70 (15H, m, MTPA-Ar), 6.176 (1H, dd, *J* = 11.1, 9.0 Hz, H-7), 5.349 (1H, ddd, *J* = 10.0, 6.8, 2.8 Hz, H-23), 5.003 (1H, m, H-3), 4.010 (1H, dd, *J* = 11.0, 9.2 Hz, H-4), 3.901 (1H, dd, *J* = 11.0, 9.0 Hz, H-6), 3.651 (1H, dd, *J* = 5.1, 2.5 Hz, H-22), 3.593 (3H, s, MTPA-OMe), 3.530 (3H, s, MTPA-OMe), 3.436 (3H, s, MTPA-OMe), 2.474 (1H, m, H-16α), 2.438 (1H, br s, H-14), 2.468 (1H, m, H-16β), 1.932 (1H, m, H-2α), 1.886 (1H, ddd, *J* = 11.1, 11.1, 4.0 Hz, H-8), 1.813 (1H, m, H-25),

1.809 (1H, m, H-17), 1.710 (1H, m, H-2β), 1.701 (1H, m, H-1β), 1.586 (1H, m, H-24), 1.542 (1H, m, H-20), 1.499 (1H, m, H-11α), 1.489 (1H, m, H-24), 1.461 (1H, br d, *J* = 11.0 Hz, H-5), 1.373 (1H, m, H-12α), 1.264 (1H, m, H-11β), 1.244 (1H, m, H-12β), 1.238 (1H, m, H-9), 1.098 (3H, s, H-18), 1.055 (1H, m, H-1α), 1.026 (3H, d, *J* = 6.4 Hz, H-27), 0.902 (3H, d, *J* = 6.4 Hz, H-26), 0.892 (3H, s, H-19), 0.822 (3H, d, *J* = 6.7 Hz, H-21); LRESIMS *m*/*z* 1131.4 $[M + H]^+$ (calcd for $C_{57}H_{68}F_9O_{13}$, 1131.5).

*Tris(R)-MTPA Ester of **8** (**8R**)*: Pale white, amorphous solid; ^1H NMR (CD_3OD, 600 MHz) δ_H 7.20-7.70 (15H, m, MTPA-Ar), 6.144 (1H, dd, *J* = 11.0, 8.9 Hz, H-7), 5.340 (1H, ddd, *J* = 10.0, 6.8, 2.8 Hz, H-23), 4.973 (1H, m, H-3), 3.974 (1H, dd, *J* = 11.0, 9.2 Hz, H-4), 3.906 (1H, dd, *J* = 11.0, 8.9 Hz, H-6), 3.676 (1H, dd, *J* = 5.0, 2.5 Hz, H-22), 3.593 (3H, s, MTPA-OMe), 3.536 (3H, s, MTPA-OMe), 3.450 (3H, s, MTPA-OMe), 2.445 (1H, m, H-16α), 2.320 (1H, m, H-16β), 2.284 (1H, br s, H-14), 2.014 (1H, m, H-2α), 1.880 (1H, m, H-17), 1.774 (1H, ddd, *J* = 11.0, 11.0, 4.0 Hz, H-8), 1.755 (1H, m, H-25), 1.747 (1H, m, H-2β), 1.725 (1H, m, H-1β), 1.573 (1H, m, H-20), 1.556 (1H, m, H-24), 1.486 (1H, m, H-24), 1.483 (1H, m, H-11α), 1.457 (1H, br d, *J* = 11.0 Hz, H-5), 1.394 (1H, m, H-12α), 1.266 (1H, m, H-12β), 1.234 (1H, m, H-11β), 1.231 (1H, m, H-9), 1.090 (1H, m, H-1α), 1.062 (3H, s, H-18), 0.955 (3H, d, *J* = 6.4 Hz, H-27), 0.894 (3H, d, *J* = 6.4 Hz, H-26), 0.906 (3H, s, H-19), 0.838 (3H, d, *J* = 6.7 Hz, H-21); LRESIMS *m*/*z* 1131.4 $[M + H]^+$ (calcd for $C_{57}H_{68}F_9O_{13}$, 1131.5).

*Tris(S)-MTPA Ester of **10** (**10S**)*: Pale white, amorphous solid; ^{1}H NMR (CD_3OD, 600 MHz) δ_H 7.20-7.80 (15H, m, MTPA-Ar), 6.171 (1H, dd, *J* = 10.4, 8.9 Hz, H-7), 5.228 (1H, m, H-23), 4.951 (1H, m, H-3), 4.025 (1H, dd, *J* = 9.6, 9.4 Hz, H-4), 3.890 (1H, dd, *J* = 10.8, 9.1 Hz, H-6), 3.589 (3H, s, MTPA-OMe), 3.529 (3H, s, MTPA-OMe), 3.474 (3H, s, MTPA-OMe), 2.471 (1H, dd, *J* = 19.5, 10.4 Hz, H-16α), 2.422 (1H, br s, H-14), 2.241 (1H, m, H-16β), 1.921 (1H, m, H-8), 1.910 (1H, m, H-20), 1.882 (1H, m, H-22), 1.915 (1H, m, H-2α), 1.792 (1H, m, H-17), 1.710 (1H, m, H-2β), 1.701 (1H, m, H-1β), 1.551 (1H, m, H-22), 1.821 (1H, m, H-25), 1.539 (1H, m, H-11α), 1.469 (1H, br d, *J* = 10.9 Hz, H-5), 1.385 (1H, m, H-12α), 1.264 (1H, m, H-12β), 1.246 (1H, m, H-9), 1.226 (3H, s, H-18), 1.224 (1H, m, H-11β), 1.202 (1H, m, H-24), 1.179 (1H, m, H-24), 1.063 (1H, m, H-1α), 1.006 (3H, d, *J* = 6.7 Hz, H-21), 0.887 (3H, s, H-19), 0.842 (3H, d, *J* = 6.4 Hz, H-27), 0.812 (3H, d, *J* = 6.4 Hz, H-26); LRESIMS *m*/*z* 1115.4 $[M + H]^+$ (calcd for $C_{57}H_{68}F_9O_{12}$, 1115.5).

*Tris(R)-MTPA Ester of **10** (**10R**)*: Pale white, amorphous solid; ^{1}H NMR (CD_3OD, 600 MHz) δ_H 7.20-7.80 (15H, m, MTPA-Ar), 6.098 (1H, dd, *J* = 10.4, 8.9 Hz, H-7), 5.211 (1H, m, H-23), 4.948 (1H, m, H-3), 3.984 (1H, dd, *J* = 9.6, 9.4 Hz, H-4), 3.904 (1H, dd, *J* = 10.9, 9.0 Hz, H-6), 3.592 (3H, s, MTPA-OMe), 3.491 (3H, s, MTPA-OMe), 3.416 (3H, s, MTPA-OMe), 2.439 (1H, dd, *J* = 19.5, 10.4 Hz, H-16α), 2.279 (1H, br s, H-14), 2.085 (1H, m, H-16β), 1.994 (1H, m, H-2α), 1.861 (1H, m, H-25), 1.789 (1H, m, H-8),

1.752 (1H, m, H-2β), 1.730 (1H, m, H-17), 1.719 (1H, m, H-1β), 1.617 (1H, m, H-22), 1.590 (1H, m, H-20), 1.530 (1H, m, H-11α), 1.452 (1H, br d, *J* = 10.8 Hz, H-5), 1.384 (1H, m, H-12α), 1.341 (1H, m, H-22), 1.325 (1H, m, H-24), 1.307 (1H, m, H-24), 1.258 (1H, m, H-12β), 1.225 (1H, m, H-11β), 1.202 (1H, m, H-9), 1.158 (3H, s, H-18), 1.101 (1H, m, H-1α), 0.916 (3H, d, *J* = 6.7 Hz, H-21), 0.888 (3H, d, *J* = 6.4 Hz, H-27), 0.866 (3H, s, H-19), 0.826 (3H, d, *J* = 6.4 Hz, H-26); LRESIMS *m*/*z* 1115.4 $[M + H]^+$ (calcd for $C_{57}H_{68}F_9O_{12}$, 1115.5).

bis(S)-MTPA Ester of ***11*** *(****11S****)*: Pale white, amorphous solid; ^1H NMR (CD_3OD, 600 MHz) δ_H 7.20-7.70 (10H, m, MTPA-Ar), 5.530 (1H, ddd, *J* = 8.0, 5.6, 1.9 Hz, H-23), 4.920 (1H, m, H-3), 4.008 (1H, dd, *J* = 9.8, 9.8 Hz, H-4), 3.802 (1H, dd, *J* = 10.9, 8.2 Hz, H-6), 3.623 (1H, t, *J* = 8.0 Hz, H-22), 3.612 (3H, s, MTPA-OMe), 3.513 (3H, s, MTPA-OMe), 3.321 (1H, m, H-7), 2.683 (1H, dd, *J* = 19.4, 8.8 Hz, H-16α), 2.207 (1H, d, *J* = 12.8 Hz, H-14), 2.139 (1H, m, H-12α), 1.943 (1H, br d, *J* = 19.4 Hz, H-16β), 1.924 (1H, m, H-2α), 1.762 (1H, m, H-8), 1.731 (1H, m, H-1β), 1.679 (1H, m, H-25), 1.712 (1H, m, H-2β), 1.659 (1H, m, H-17), 1.657 (1H, m, H-20), 1.635 (1H, m, H-11α), 1.489 (1H, m, H-12β), 1.330 (1H, m, H-24), 1.322 (1H, d, *J* = 9.8 Hz, H-5), 1.314 (1H, m, H-11β), 1.138 (1H, m, H-9), 1.092 (1H, m, H-1α), 1.016 (3H, d, *J* = 6.7 Hz, H-26), 1.058 (3H, d, *J* = 6.5 Hz, H-21), 0.943 (3H, d, *J* = 6.7 Hz, H-28), 0.944 (3H, d, *J* = 6.7 Hz, H-27), 0.892 (3H, s, H-18), 0.881 (3H, s, H-19); LRESIMS *m*/*z* 928.4 $[M + H]^+$ (calcd for

$C_{48}H_{63}F_6O_{11}$, 928.4).

*bis(R)-MTPA Ester of **11** (**11R**)*: Pale white, amorphous solid; ^{1}H NMR (CD_3OD, 600 MHz) δ_H 7.20-7.70 (10H, m, MTPA-Ar), 5.502 (1H, ddd, *J* = 8.0, 5.6, 1.9 Hz, H-23), 4.953 (1H, m, H-3), 3.972 (1H, dd, *J* = 9.8, 9.8 Hz, H-4), 3.795 (1H, dd, *J* = 10.9, 8.2 Hz, H-6), 3.702 (3H, s, MTPA-OMe), 3.642 (1H, t, *J* = 8.0 Hz, H-22), 3.612 (3H, s, MTPA-OMe), 3.304 (1H, m, H-7), 2.698 (1H, dd, *J* = 19.4, 8.8 Hz, H-16α), 2.207 (1H, d, *J* = 12.8 Hz, H-14), 2.141 (1H, m, H-12α), 1.989 (1H, m, H-2α), 1.932 (1H, br d, *J* = 19.4 Hz, H-16β), 1.753 (1H, m, H-1β), 1.753 (1H, m, H-8), 1.744 (1H, m, H-2β), 1.675 (1H, m, H-20), 1.671 (1H, m, H-25), 1.656 (1H, m, H-17), 1.634 (1H, m, H-11α), 1.490 (1H, m, H-12β), 1.323 (1H, m, H-11β), 1.297 (1H, d, *J* = 9.8 Hz, H-5), 1.280 (1H, m, H-24), 1.131 (1H, m, H-9), 1.126 (1H, m, H-1α), 1.061 (3H, d, *J* = 6.5 Hz, H-21), 0.979 (3H, d, *J* = 6.7 Hz, H-26), 0.817 (3H, d, *J* = 6.7 Hz, H-27), 0.773 (3H, d, *J* = 6.7 Hz, H-28), 0.903 (3H, s, H-19), 0.858 (3H, s, H-18); LRESIMS *m/z* 913.4 $[M + H]^+$ (calcd for $C_{48}H_{63}F_6O_{11}$, 928.4).

*bis(S)-MTPA Ester of **12** (**12S**)*: Pale white, amorphous solid; ^{1}H NMR (CD_3OD, 600 MHz) δ_H 7.20-7.70 (10H, m, MTPA-Ar), 5.243 (1H, ddd, *J* = 8.0, 5.6, 1.9 Hz, H-23), 4.901 (1H, m, H-3), 4.008 (1H, dd, *J* = 9.8, 9.8 Hz, H-4), 3.790 (1H, dd, *J* = 10.9, 8.2 Hz, H-6), 3.600 (3H, s, MTPA-OMe), 3.509 (3H, s, MTPA-OMe), 3.306 (1H, m, H-7), 2.432 (1H, dd, *J* = 19.4, 8.8 Hz, H-16α), 2.207 (1H, d, *J* = 12.8 Hz, H-14), 2.134 (1H, m, H-

12α), 1.922 (1H, br d, *J* = 19.4 Hz, H-16β), 1.912 (1H, m, H-2α), 1.782 (1H, m, H-25), 1.761 (1H, m, H-8), 1.739 (1H, m, H-1β), 1.719 (1H, m, H-2β), 1.658 (1H, m, H-17), 1.646 (1H, m, H-11α), 1.608 (1H, m, H-22), 1.501 (1H, m, H-20), 1.485 (1H, m, H-12β), 1.387 (1H, m, H-24), 1.364 (1H, m, H-22), 1.311 (1H, m, H-11β), 1.312 (1H, d, *J* = 9.8 Hz, H-5), 1.067 (1H, m, H-1α), 1.023 (1H, m, H-9), 0.968 (3H, d, *J* = 6.7 Hz, H-27), 0.966 (3H, d, *J* = 6.7 Hz, H-28), 0.960 (3H, d, *J* = 6.5 Hz, H-21), 0.928 (3H, d, *J* = 6.7 Hz, H-26), 0.872 (3H, s, H-19), 0.815 (3H, s, H-18); LRESIMS *m*/*z* 913.4 $[M + H]^+$ (calcd for $C_{48}H_{63}F_6O_{10}$, 913.4).

bis(R)-MTPA Ester of ***12*** *(****12R****)*: Pale white, amorphous solid; ^1H NMR (CD_3OD, 600 MHz) δ_H 7.20-7.70 (10H, m, MTPA-Ar), 5.389 (1H, ddd, *J* = 8.1, 5.7, 2.0 Hz, H-23), 4.907 (1H, m, H-3), 3.956 (1H, dd, *J* = 9.8, 9.8 Hz, H-4), 3.784 (1H, dd, *J* = 10.9, 8.2 Hz, H-6), 3.511 (3H, s, MTPA-OMe), 3.504 (3H, s, MTPA-OMe), 3.295 (1H, m, H-7), 2.615 (1H, dd, *J* = 19.4, 8.8 Hz, H-16α), 2.144 (1H, m, H-12α), 2.130 (1H, d, *J* = 12.8 Hz, H-14), 1.989 (1H, m, H-2α), 1.943 (1H, br d, *J* = 19.4 Hz, H-16β), 1.756 (1H, m, H-25), 1.750 (1H, m, H-2β), 1.747 (1H, m, H-1β), 1.741 (1H, m, H-8), 1.670 (1H, m, H-17), 1.654 (1H, m, H-11α), 1.632 (1H, m, H-22), 1.507 (1H, m, H-20), 1.493 (1H, m, H-12β), 1.391 (1H, m, H-22), 1.380 (1H, m, H-24), 1.330 (1H, m, H-11β), 1.290 (1H, d, *J* = 9.8 Hz, H-5), 1.112 (1H, m, H-1α), 1.065 (3H, d, *J* = 6.5 Hz, H-21), 0.975 (1H, m, H-9), 0.952 (3H, d, *J* = 6.7 Hz, H-27), 0.919 (3H, d, *J* = 6.7 Hz, H-26), 0.899 (3H, d, *J* = 6.7 Hz,

H-28), 0.872 (3H, s, H-19), 0.797 (3H, s, H-18); LRESIMS *m*/*z* 913.4 [M + H]$^+$ (calcd for $C_{48}H_{63}F_6O_{10}$, 913.4).

*Tris(S)-MTPA Ester of **13** (**13S**)*: Pale white, amorphous solid; ^{1}H NMR (CD_3OD, 600 MHz) δ_H 7.20-7.70 (15H, m, MTPA-Ar), 5.230 (1H, m, H-28), 4.983 (1H, dd, *J* = 11.4, 9.1 Hz, H-6), 4.889 (1H, m, H-3), 4.558 (1H, dd, *J* = 10.2, 9.7 Hz, H-7), 3.556 (3H, s, MTPA-OMe), 3.490 (3H, s, MTPA-OMe), 3.433 (3H, s, MTPA-OMe), 2.764 (1H, br s, H-14), 2.329 (1H, dd, *J* = 19.8, 10.4 Hz, H-16α), 2.176 (1H, br d, *J* = 19.8 Hz, H-16β), 2.036 (1H, m, H-4α), 1.795 (1H, m, H-4β), 1.766 (1H, m, H-25), 1.760 (1H, m, H-8), 1.751 (1H, m, H-20), 1.744 (1H, m, H-1β), 1.722 (1H, m, H-17), 1.545 (1H, m, H-2α), 1.566 (1H, m, H-5), 1.551 (1H, m, H-11α), 1.545 (1H, m, H-22), 1.478 (1H, m, H-2β), 1.399 (1H, m, H-23), 1.385 (1H, m, H-24), 1.383 (1H, m, H-12α), 1.366 (1H, m, H-11β), 1.335 (1H, d, *J* = 6.3 Hz, H-29), 1.279 (1H, m, H-22), 1.174 (1H, m, H-12β), 1.172 (3H, s, H-18), 1.076 (1H, m, H-9), 0.963 (3H, s, H-19), 0.951 (1H, m, H-1α), 0.940 (1H, m, H-23), 0.839 (3H, d, *J* = 6.7 Hz, H-27), 0.819 (3H, d, *J* = 6.7 Hz, H-26), 0.723 (3H, d, *J* = 6.9 Hz, H-21); LRESIMS *m*/*z* 1128.1 [M + H]$^+$ (calcd for $C_{59}H_{72}F_9O_{11}$, 1128.2).

*Tris(R)-MTPA Ester of **13** (**13R**):* Pale white, amorphous solid; ^{1}H NMR (CD_3OD, 600 MHz) δ_H 7.20-7.70 (15H, m, MTPA-Ar), 5.271 (1H, m, H-28), 4.966 (1H, dd, *J* = 11.1, 8.9 Hz, H-6), 4.792 (1H, m, H-3), 4.571 (1H, dd, *J* = 10.5, 9.5 Hz, H-7), 3.565 (3H, s, MTPA-OMe), 3.507 (3H, s,

MTPA-OMe), 3.491 (3H, s, MTPA-OMe), 2.796 (1H, br s, H-14), 2.354 (1H, dd, *J* = 19.8, 10.5 Hz, H-16α), 2.228 (1H, br d, *J* = 19.8 Hz, H-16β), 1.899 (1H, m, H-4α), 1.895 (1H, m, H-20), 1.877 (1H, m, H-25), 1.758 (1H, m, H-1β), 1.772 (1H, m, H-8), 1.740 (1H, m, H-17), 1.735 (1H, m, H-22), 1.701 (1H, m, H-2α), 1.585 (1H, m, H-2β), 1.562 (1H, m, H-11α), 1.485 (1H, m, H-23), 1.446 (1H, m, H-5), 1.395 (1H, m, H-24), 1.377 (1H, m, H-22), 1.393 (1H, m, H-12α), 1.303 (1H, m, H-4β), 1.250 (1H, m, H-11β), 1.242 (3H, d, *J* = 6.3 Hz, H-29), 1.184 (1H, m, H-12β), 1.147 (3H, s, H-18), 1.102 (1H, m, H-23), 1.070 (1H, m, H-9), 1.047 (1H, m, H-1α), 0.943 (1H, s, H-19), 0.907 (3H, d, *J* = 6.4 Hz, H-27), 0.905 (3H, d, *J* = 6.4 Hz, H-26), 0.847 (3H, d, *J* = 6.9 Hz, H-21); LRESIMS *m*/*z* 1128.1 $[M + H]^+$ (calcd for $C_{59}H_{72}F_9O_{11}$, 1128.2).

Biological Assays. The cytotoxicity assays were performed in accordance with literature protocols.[16] Antimicrobial assays against pathogenic bacterial and fungal strains were performed according to the previously described method.[17] Isocitrate lyase, Na^+/K^+-ATPase and sortase A inhibition assays were performed according to previously described methods.[18] Measurement of glucose uptake level and differentiation of 3T3-L1 adipocytes were performed according to previously described method.[19]

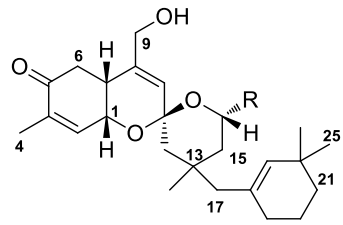

1 (R = OMe, 13*R)*
2 (R = OMe, 13*S)*
3 (R = OH, 13*R)*

Table 3. ^{13}C and ^{1}H NMR assignments for compounds **1**-**3** in MeOH-d_4.

	1		**2**		**3**	
position	δ_C	δ_H (*J* in Hz)	δ_C	δ_H (*J* in Hz)	δ_C	δ_H (*J* in Hz)
1	64.3	4.52, dd (5.4, 3.5)	69.5	4.65, br d (3.7)	64.1	4.52, dd (5.1, 3.2)
2	141.7	6.80, dq (5.4, 1.3)	145.5	6.79, br d (3.7)	141.8	6.75, dq (5.1, 1.2)
3	139.4		137.4		139.3	
4	15.9	1.81, s	15.6	1.75, br s	15.9	1.81, s
5	200.7		200.1		200.8	
6a	38.8	2.57, dd (16.0, 4.3)	39.7	2.71, dd (16.0, 7.7)	38.8	2.57, dd (16.1, 4.2)
6b		2.39, dd (16.0, 14.0)		2.63, dd (16.0, 5.1)		2.39, dd (16.1, 13.9)
7	34.4	2.58, ddd (14.0, 4.3, 3.5)	35.8	2.88, m	34.4	2.55, ddd (13.9, 4.2, 3.2)
8	143.7		140.8		143.5	
9a	63.7	4.06, s, 2H	63.6	4.07, dd, (13.8)	63.7	4.05, s, 2H
9b				3.99, d, (13.8)		
10	126.2	5.59, s	127.2	5.56, s	126.4	5.58, s
11	99.3		99.9		99.5	
12a	46.0	1.53, d (13.1)	45.1	1.82, d (14.2)	45.8	1.51, d (13.8)
12b		1.49, d (13.1)		1.28, d (14.2)		1.47, d (13.8)
13	35.2		34.7		35.4	
14	25.9	1.16, s	31.2	0.90, s	25.7	1.15, s
15a	43.3	1.56, dd (13.2, 2.1)	42.3	1.80, dd (13.4, 2.0)	45.1	1.57, dd (13.0, 2.1)
15b		1.30, dd (13.2, 10.0)		1.12, dd (13.4, 10.1)		1.30, dd (13.0, 10.0)
16	98.2	4.92, dd (10.0, 2.1)	98.2	5.05, dd (10.1, 2.1)	90.4	5.24, dd (10.0, 2.1)
17a	55.4	1.83, s, 2H	47.1	2.51, d (13.5)	55.5	1.82, s, 2H
17b				2.16, d (13.5)		
18	133.0		134.4		133.1	
19	138.2	5.12, s	138.0	5.18, s	138.2	5.12, s
20	32.9		32.9		32.9	
21	38.2	1.38, m, 2H	38.2	1.41, m, 2H	38.2	1.39, m, 2H
22a	21.3	1.61, m	21.4	1.61, m	21.4	1.61, m
22b		1.58, m		1.58, m		1.58, m
23	33.0	1.91, dd, 2H (11.9, 5.9)	33.1	1.97, dd, 2H (12.7, 6.3)	33.0	1.92, dd, 2H (11.6, 5.3)
24	30.7	0.95, s	30.8	0.96, s	30.9	0.96, s
25	30.6	0.94, s	30.7	0.95, s	30.7	0.95, s
26	56.6	3.47, s	56.6	3.44, s		

^{1}H and ^{13}C NMR were measured at 600 MHz and 150 MHz, respectively.

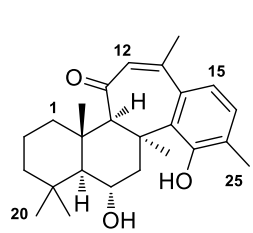

4

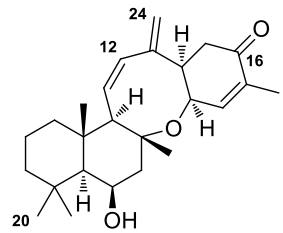

5

Table 4. ^{13}C-NMR and ^{1}H-NMR assignments for compounds **4-5**

	4[a]		**5**[a]		**5**[b]	
position	δ_C type	δ_H mult (*J* in Hz)	δ_C type	δ_H mult (*J* in Hz)	δ_C type	δ_H mult (*J* in Hz)
1	42.6, CH_2	1.95, ddd (13.1, 3.1, 3.1) 0.69, ddd (13.1, 13.1, 3.2)	44.6, CH_2	1.48, ddd (13.2, 3.3, 3.3) 0.89, ddd (13.2, 13.2, 3.1)	43.7, CH_2	1.48, ddd (13.2, 3.2, 3.2) 0.80, ddd (13.2, 13.2, 3.2)
2	19.4, CH_2	1.66, m 1.32, m	19.7, CH_2	1.73, m 1.36, m	18.9, CH_2	1.66, m 1.33, m
3	43.7, CH_2	1.33, m 1.10, ddd (13.7, 13.7, 3.4)	45.3, CH_2	1.33, m 1.19, ddd (13.5, 13.5, 4.5)	44.2, CH_2	1.61, m 1.11, ddd (12.7, 12.7, 3.2)
4	35.1, C		35.0, C		38.0, C	
5	59.9, CH	0.80, d (8.0)	57.9, CH	0.95, d (2.0)	57.0, CH	0.68, br d (1.2)
6	69.1, CH	4.14, ddd (8.0, 4.9, 3.1)	69.1, CH	4.57, br dd (5.7, 2.8)	68.8, CH	4.18, br dd (5.7, 3.3)
7	42.8, CH_2	3.48, dd (16.4, 3.1) 2.33, dd (16.4, 4.9)	44.7, CH_2	2.11, br d (13.6) 1.70, dd (13.6, 2.8)	44.3, CH_2	1.34, m 1.32, m
8	40.0, C		80.1, C		78.3, C	
9	69.9, CH	2.96, s	57.4, CH	2.58, d (9.3)	56.4, CH	2.29, d (9.3)
10	38.6, C		39.1, C		34.2, C	
11	203.2, C		130.1, CH	5.62, dd (11.2, 9.3)	128.7, CH	5.49, d (11.3, 9.3)
12	132.3, CH	6.15, s	133.6, CH	6.22, d (11.2)	132.7, CH	6.14, d (11.3)
13	151.4, C		149.2, C		148.0, C	
14	136.5, C		49.6, CH	3.42, m	48.6, CH	3.04, m
15	126.3, CH	7.31, d (8.0)	40.2, CH_2	2.79, dd (16.8, 8.5) 2.38, dd (16.8, 4.8)	39.5, CH_2	3.06, m 2.31, dd (17.8, 8.0)
16	128.8, CH	7.06, d (8.0)	202.3, C		198.2, C	
17	134.1, C		135.7, C		135.3, C	
18	152.6, C		147.5, CH	6.47, dq (8.5, 1.6)	143.9, CH	6.18, dq (5.0, 1.5)
19	142.8, C		67.5, CH	4.69, br dd (8.5, 4.6)	66.4, CH	4.04, br d (4.5)
20	34.4, CH_3	0.93, s	33.7, CH_3	0.99, s	33.4, CH_3	0.96, s
21	22.9, CH_3	0.99, s	24.1, CH_3	1.21, s	24.0, CH_3	1.26, s
22	25.9, CH_3	1.31, s	25.8, CH_3	1.30, s	25.5, CH_3	1.42, s
23	19.7, CH_3	1.33, s	17.1, CH_3	1.34, s	16.8, CH_3	1.34, s
24	29.3, CH_3	2.32, s	116.2, CH_2	4.90, br s 4.83, br s	115.7, CH_2	4.93, br s 4.80, br s
25	17.9, CH_3	2.23, s	15.5, CH_3	1.72, br d (1.6)	15.8, CH_3	1.81, s
O*H*						0.62, br s

[a] CD_3OD
[b] C_6D_6

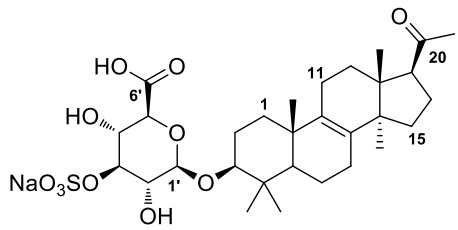

6

Table 5. ^{13}C-NMR and ^{1}H-NMR assignments for compound **6** in MeOH-d_4

	6	
position	δ_C, type	δ_H mult (*J* in Hz)
1	36.8, CH_2	1.73, m
		1.24, ddd (13.0, 13.0, 2.9)
2	27.4, CH_2	2.01, m
		1.67, m
3	90.6, CH	3.20, dd (11.5, 4.2)
4	40.3, C	
5	52.1, CH	1.09, dd (12.6, 2.0)
6	19.2, CH_2	1.72, m
		1.53, m
7	27.8, CH_2	2.10, m
		2.09, m
8	134.9, C	
9	136.3, C	
10	38.0, C	
11	22.1, CH_2	2.18, m
		2.12, m
12	31.3, CH_2	2.05, m
		1.77, ddd (11.6, 11.6, 3.7)
13	47.5, C	
14	51.4, C	
15	32.0, CH_2	1.71, m
		1.30, m
16	22.9, CH_2	2.25, m
		1.70, m
17	60.3, CH	2.98, dd (8.1, 8.1)
18	18.0, CH_3	0.61, s
19	19.7, CH_3	0.99, s
20	213.1, C	
21	31.5, CH_3	2.11, s
22	28.3, CH_3	1.06, s
23	16.8, CH_3	0.85, s
24	24.8, CH_3	1.00, s
1´	106.4, CH	4.42, d (7.8)
2´	74.5, CH	3.44, dd (9.5, 7.8)
3´	85.6, CH	4.24, dd (9.5, 9.5)
4´	72.2, CH	3.64, dd (9.5, 9.5)
5´	77.3, CH	3.62, d (9.5)
6´	176.3, C	

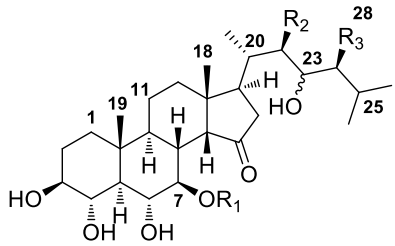

7 R_1 = H, R_2 = OH, 23*R*, R_3 = CH_3
8 R_1 = H, R_2 = OH, 23*R*, R_3 = H

Table 6. ^{13}C and ^{1}H NMR assignment for compounds **7** and **8** in MeOH-d_4

	7		**8**	
position	δ_C, type	δ_H mult (*J* in Hz)	δ_C, type	δ_H mult (*J* in Hz)
1	37.1, CH_2	1.03, ddd (13.5, 13.5, 3.6)	37.1, CH_2	1.03, ddd (13.5, 13.5, 3.4)
		1.70, ddd (13.5, 3.6, 3.6)		1.70, ddd (13.5, 3.4, 3.4)
2	29.2, CH_2	1.77, m	29.2, CH_2	1.77, m
		1.48, m		1.47, m
3	76.7, CH	3.33, ddd (10.8, 8.7, 5.3)	76.7, CH	3.34, ddd (11.7, 8.7, 5.3)
4	77.3, CH	3.73, dd (10.6, 8.7)	77.3, CH	3.73, dd (10.5, 8.7)
5	51.6, CH	1.15, dd (10.6, 10.6)	51.5, CH	1.15, dd (10.5, 10.5)
6	77.6, CH	3.62, dd (10.6, 8.8)	77.6, CH	3.62, dd (10.5, 8.9)
7	75.2, CH	4.41, dd (10.7, .8.8)	75.2, CH	4.41, dd (10.6, 8.9)
8	40.6, CH	1.66, m	40.6, CH	1.66, m
9	47.1, CH	1.00, m	47.1, CH	1.00, m
10	39.2, C		39.2, C	
11	22.3, CH_2	1.52, m	22.3, CH_2	1.51, m
		1.27, m		1.27, m
12	38.1, CH_2	1.28, m	38.3, CH_2	1.26, m
		1.38, ddd (10.0, 2.7, 2.7)		1.38, m
13	42.8, C		42.9, C	
14	52.8, CH	2.74, br s	52.7, CH	2.73, br s
15	223.0, C		223.0, C	
16	40.1, CH_2	2.33, dd (19.5, 9.8)	39.9, CH_2	2.32, dd (19.8, 10.0)
		2.85, br d (19.5)		2.87, br d (19.8)
17	49.6, CH	1.78, m	49.2, CH	1.76, m
18	19.5, CH_3	1.20, s	19.2, CH_3	1.19, s
19	15.2, CH_3	0.87, s	15.2, CH_3	0.87, s
20	35.0, CH	2.03, m	34.9, CH	2.10, m
21	13.9, CH_3	0.95, d (6.7)	13.7, CH_3	0.94, d (6.8)
22	74.7, CH	3.78, dd (7.6, 2.5)	77.5, CH	3.61, dd (7.6, 2.0)
23	75.4, CH	3.60, dd (7.5, 2.5)	73.0, CH	3.52, ddd (10.2, 7.4, 2.0)
24	42.0, CH	1.30, m	43.4, CH_2	1.32, ddd (14.1, 10.2, 3.8)
				1.23, ddd (14.1, 7.4, 2.5)
25	31.8, CH	1.65, m	25.4, CH	1.87, m
26	20.6, CH_3	0.92, d (6.5)	21.7, CH_3	0.92, d (6.4)
27	21.5, CH_3	0.97, d (6.5)	24.5, CH_3	0.95, d (6.4)
28	11.1, CH_3	0.88, d (6.8)		

[a-c]Data were measured at 150, 125, and 100 MHz for ^{13}C NMR, respectively.

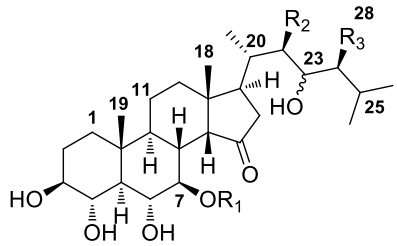

9 $R_1 = SO_3Na$, $R_2 = OH$, 23*R*, $R_3 = CH_3$
10 $R_1 = H$, $R_2 = H$, 23*S*, $R_3 = H$

Table 7. ^{13}C and ^{1}H NMR assignment for compounds **9** and **10** in MeOH-d_4

	9		**10**	
position	δ_C, type	δ_H mult (*J* in Hz)	δ_C, type	δ_H mult (*J* in Hz)
1	37.1, CH_2	1.10, ddd (13.4, 13.4, 3.5)	37.8, CH_2	1.03, ddd (13.5, 13.5, 3.4)
		1.69, ddd (13.4, 3.6, 3.6)		1.68, m
2	29.0, CH_2	1.77, m	30.0, CH_2	1.76, m
		1.47, m		1.48, m
3	76.8, CH	3.35, ddd (11.6, 8.3, 5.1)	77.5, CH	3.34, m
4	77.1, CH	3.74, dd (10.1, 8.6)	78.1, CH	3.72, dd (10.2, 8.9)
5	51.7, CH	1.19, dd (10.1, 10.1)	52.4, CH	1.15, dd (10.2, 10.2)
6	77.7, CH	3.89, dd (10.1, 8.6)	78.5, CH	3.60, dd (10.2, 8.9)
7	79.4, CH	5.04, dd (10.9, 8.6)	75.9, CH	4.34, dd (10.7, 8.9)
8	39.9, CH	1.76, m	41.1, CH	1.66, m
9	46.9, CH	1.09, m	47.8, CH	1.01, m
10	38.2, C		39.7, C	
11	22.6, CH_2	1.51, m	23.2, CH_2	1.50, m
		1.23, m		1.24, m
12	37.9, CH_2	1.24, m	39.7, CH_2	1.17, m
		1.36, m		1.39, m
13	42.6, C		43.4, C	
14	52.5, CH	2.89, br s	54.1, CH	2.77, br s
15	222.4, C		222.4, C	
16	39.8, CH_2	2.24, dd (19.6, 10.1)	39.1, CH_2	2.39, dd (19.8, 9.6)
		2.90, br d (19.6)		2.23, br d (19.8)
17	49.4, CH	1.75, m	50.5, CH	1.74, m
18	19.3, CH_3	1.21, s	20.1, CH_3	1.19, s
19	15.2, CH_3	0.87, s	15.9, CH_3	0.86, s
20	34.7, CH	2.03, m	33.0, CH	2.03, m
21	13.7, CH_3	0.93, d (6.7)	20.8, CH_3	0.95, d (6.9)
22	74.9, CH	3.87, dd (7.9, 2.0)	42.3, CH_2	1.57, m; 1.32, m
23	75.9, CH	3.60, dd (7.8, 2.0)	70.3, CH	3.69, m
24	41.6, CH	1.30, m	48.0, CH_2	1.31, m; 1.29, m
25	32.1, CH	1.65, m	26.3, CH	1.85, m
26	20.9, CH_3	0.94, d (6.7)	22.7, CH_3	0.91, d (6.7)
27	21.5, CH_3	0.97, d (6.7)	25.1, CH_3	0.93, d (6.7)
28	11.4, CH_3	0.90, d (6.8)		

[a-c]Data were measured at 150, 125, and 100 MHz for ^{13}C NMR, respectively.

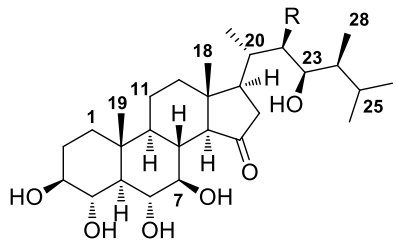

11 R = OH
12 R = H

Table 8. ^{13}C and ^{1}H NMR assignment for compounds **11** and **12** in MeOH-d_4

	11		**12**	
position	δ_C, type	δ_H mult (*J* in Hz)	δ_C, type	δ_H mult (*J* in Hz)
1	37.4, CH_2	1.10, m	37.4, CH_2	1.10, m
		1.70, m		1.70, ddd (13.0, 3.4, 3.4)
2	29.4, CH_2	1.80, m	29.5, CH_2	1.80 m
		1.49, m		1.52, m
3	76.5, CH	3.34, m	76.5, CH	3.33, m
4	77.0, CH	3.70, br d (10.5)	77.4, CH	3.70, dd (10.1, 8.8)
5	51.6, CH	1.17, dd (10.5, 10.5)	51.6, CH	1.17, dd (10.1, 10.1)
6	77.0, CH	3.78, dd (10.5, 8.3)	77.0, CH	3.78, dd (10.9, 8.8)
7	79.2, CH	3.30, m	79.3, CH	3.27, m
8	40.8, CH	1.78, m	40.8, CH	1.77, m
9	52.2, CH	0.95, m	52.2, CH	0.93, m
10	38.8, C		38.8, C	
11	22.0, CH_2	1.68, m	21.7, CH_2	1.65, m
		1.32, m		1.31, m
12	40.9, CH_2	1.48, m	40.6, CH_2	1.46, m
		2.14, m		2.17, m
13	44.6, C		44.8, C	
14	68.5, CH	2.26, d (9.7)	68.0, CH	2.30, d (9.8)
15	221.6, C		222.0, C	
16	42.2, CH_2	2.73, dd (19.0, 8.3)	42.6, CH_2	2.69, dd (19.6, 8.5)
		1.96, dd (19.0, 10.5)		1.96, dd (19.6, 10.8)
17	49.9, CH	2.11, m	53.5, CH	1.79, m
18	13.5, CH_3	0.84, s	13.5, CH_3	0.83, s
19	15.0, CH_3	0.90, s	15.0, CH_3	0.90, s
20	38.1, CH	1.63, m	34.7, CH	1.60, m
21	13.1, CH_3	0.98, d (6.4)	20.2, CH_3	1.07, d (6.5)
22	75.3, CH	3.40, dd (8.0, 1.1)	42.7, CH_2	1.57, m; 1.25, m
23	74.2, CH	3.69, dd (7.8, 1.1)	71.4, CH	3.82, ddd (6.6, 6.6, 3.0)
24	41.9, CH	1.17, m	44.6, CH	1.12, m
25	31.7, CH	1.64, m	31.3, CH	1.64, m
26	21.1, CH_3	0.91, d (6.6)	20.5, CH_3	0.91, d (6.8)
27	21.4, CH_3	0.95, d (6.6)	21.9, CH_3	0.95, d (6.8)
28	10.7, CH_3	0.83, d (6.7)	10.0, CH_3	0.84, d (6.6)

[a-c]Data were measured at 150, 125, and 100 MHz for ^{13}C NMR, respectively.

2. Steroids from the Sponge *Dictyonella* sp.

A new dictyoneolone (**14**), a secosteroid was isolated along with two known ergosterol peroxides (**15** and **16**) from a *Dictyonella* sp. sponge collected from Gageo-do, Korea. Based upon the results of combined spectroscopic analyses, the structure of this compound was determined to possess a highly unusual B/C fused ring. The configurations of **14** were determined by a combination of proton-proton couplings and NOESY analyses. Dictyoneolone exhibited weak cytotoxicity against the K562 and A549 cancer cell lines.

The specimens of *Dictyonella* sp. (Order Halichondriidae, Family Dictyonellidae) was collected from the offshore of Gageo-do, South Sea, Korea. Dictyoneolone (**14**), a white amorphous solid, was isolated by bioassay-guided solvent partitioning of crude extract followed by C_{18} vacuum flash chromatography and repeated HPLC.

2-1. Introduction

Marine sponges produce a wide variety of structurally unique and biologically active metabolites.[11] Among the novel sponge-derived compounds, steroids of unusual carbon frameworks and functionalities are

frequently encountered from diverse animals.[63] Thus, even in the early period of marine natural products research, sponges were highly regarded as the most prolific sources of novel steroids among marine invertebrates and the whole animal kingdom.[64-67] During the search of bioactive compounds from marine sponges, I encountered the red-colored clustering *Dictyonella* sp. sponge at Gageo-do, Korea, whose crude extract exhibited moderate cytotoxicity against the K562 cell-line (IC_{50} 272 μg/mL). Activity-guided fractionation of the extract, followed by vacuum flash chromatography and HPLC yielded three compounds. I reported the structure determination of one new secosteroid and two known ergosterol peroxides (**14-16**) by combined spectroscopic analyses.

Dictyoneolone (**14**) possessed a highly unusual B/C fused 10-membered ring bearing an 8,9-diketo group while ergosterol peroxides (**14-16**) had linked by peroxide groups. Compounds **15** and **16** were identified as liver X receptor (LXR) ligands with significantly more potency in the activation of LXRα than LXRβ.

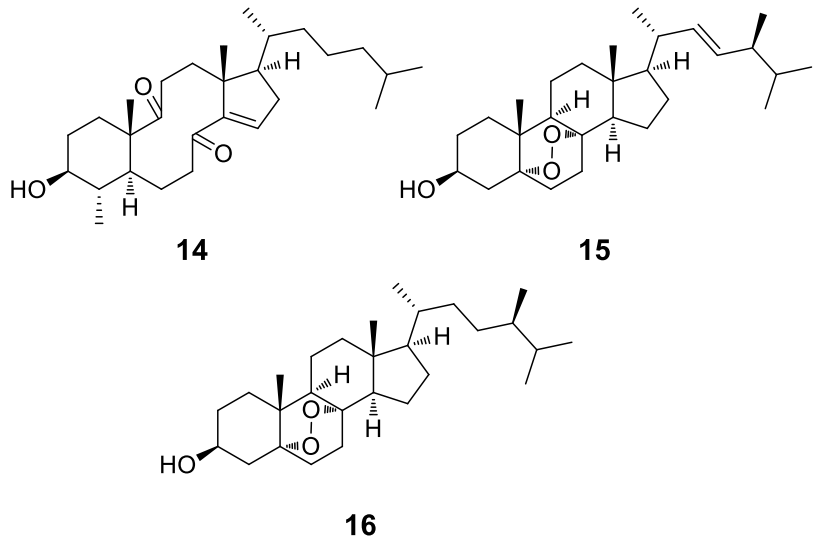

Figure 18. Chemical structures of isolated compounds **14-16**.

2-2. Results and discussion

Dictyoneolone (**14**) was isolated as a white, amorphous solid which analyzed for $C_{28}H_{46}O_3$ by HRFABMS analysis. The ^{13}C NMR spectrum of this compound showed conspicuous signals of two carbonyl carbons (δ_C 216.6 and 205.4), two olefinic carbons (δ_C 154.6 and 146.4), and an oxymethine carbon (δ_C 75.9), which matched with the strong IR absorption bands at 3442 and 1688 cm^{-1}. The remarkable shielding of a carbonyl carbon (δ_C 205.4), in conjunction with the deshielding of the olefinic carbons, strongly indicated the presence of a double bond-conjugated ketone group, which was supported by the UV absorption maximum at 242 nm. Additional signals in the ^{13}C NMR spectra were two unprotonated, five methine, ten methylene, and six methyl carbons in the shielded region (Table 9). Thus, **14** was thought to be a tricyclic compound based on the six

degree of unsaturation inherent in the mass data.

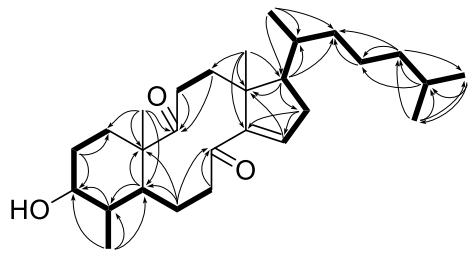

14

Figure 19. Key correlations of COSY (bold line) and HMBC (arrow) experiment for compound **14**.

Given this information, the planar structure of **14** was determined by a combination of ^{1}H COSY, HSQC, and HMBC experiments. First, all the protons and their attached carbons were matched by the HSQC data. Subsequently, the ^{1}H COSY data revealed the presence of a long spin system linearly consisted of protons attached at seven carbons (C-1-C-7). An oxymethine (δ_C 75.9, δ_H 3.17) was placed at C-3 by the proton-proton couplings of this methine with neighboring ones (Figure 18). Similarly, a methyl group (C-28, δ_C 16.3, δ_H 1.13) was found to be directly attached at the C-4 methine by the proton-proton coupling (J = 6.1 Hz) and the HMBC correlations of these methyl protons with C-3, C-4, and C-5. Then, the construction of a 1,3-dimethyl-cyclohexane moiety was accomplished by the HMBC data in which long-range correlations of an isolated methyl proton (H_3-19, δ_H 0.95) with the neighboring C-1 and C-5 carbons and an unprotonated carbon (C-10, δ_C 54.9).

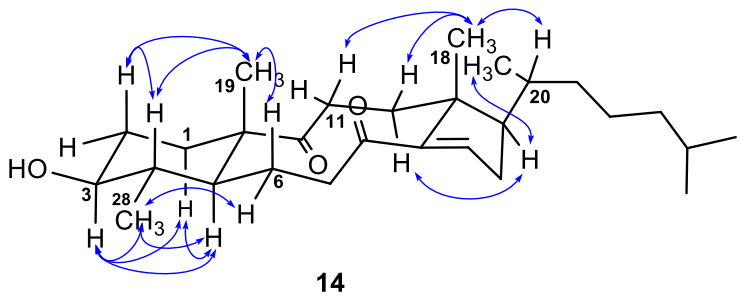

Figure 20. Key correlations of NOESY (arrow) experiment for compound **14**.

The H-19 methyl protons had an additional HMBC correlation with a carbonyl carbon (δ_C 216.6), placing this at the neighboring C-9 in the steroidal numbering system. Further extension of the carbon framework was accomplished by the additional correlations of this C-9 carbonyl carbon with the protons of an isolated spin system of dimethylene (H_2-11 and H_2-12). Similarly, the HMBC correlations of the H_2-6 and H_2-7 methylenes with another carbonyl carbon (δ_C 205.4) also placed this carbon at the neighboring C-8.

The ^{1}H COSY data revealed that most of the remaining protons, including the olefinic methine proton (δ_H 6.78), were connected by proton-proton couplings, forming a large proton assembly system (H-15-H-17 and H-20-H_3-27, Figure 18). The HMBC correlations of this olefinic methine (H-15) and its sequentially proton-proton coupled ones (H_2-16 and H-17) with neighboring carbons accommodated a cyclopentene moiety (C-13-C-17). Finally, the HMBC correlations of an isolated methyl proton (H_3-18, δ_H 1.20) with the ring carbons at C-13, C-14, and C-17, as well as the

previously assigned C-12, not only confirmed the five-membered D ring but also provided a direct connection between this and pre-described partial structure (C-1-C-12). Although the other connection of this moiety to the C-8 carbonyl carbon was not directly evidenced by the HMBC data, the characteristic shifts of C-8 (δ_C 205.4), C-14 (δ_C 154.6), C-15 (δ_C 146.4), and H-15 (δ_H 6.78), as well as the UV absorption at 242 nm possibly attributed from a conjugated ketone group, secured the connection between C-8 and C-14. Thus, the planar structure of **14** was determined to be a C-28 steroid possessing an 8,9-diketo group on an 8,9-seco carbon skeleton. A literature study revealed that this kind of B/C fused skeletons are very rare among steroids and related lanostane triterpenes. The skeletons are listed without proper description.[68] Although a number of synthetic derivatives from natural products have been reported,[69] to the best of my knowledge, dictyoneolone (**14**) is the first example of a natural product bearing this skeleton.

The relative configurations of dictyoneolone (**14**) were assigned by proton-proton couplings and NOESY analysis (Figure 19). The large couplings (ddd, J = 11.0, 11.0, 4.7 Hz) of H-3 with neighboring protons revealed its axial orientation to the A ring. The NOESY correlations of this proton with H-1α and H_3-28, in conjunction with that of the latter with H-5, placed all of these on one side of the ring system. In contrast, the NOESY correlations among H-2β, H-4, H-6β, and H_3-19 placed these protons on the

opposite side. Therefore, the A/B ring juncture had a *trans* configuration, and the 3-hydroxy and 28-methyl groups were placed β- and α-, respectively to the A ring. Similarly, the configurations at the C-17, C-18, and C-20 asymmetric centers were found to be the same as common steroids by the NOESY correlations of H_3-18 and H_3-21 with those at the adjacent positions. Thus, the structure of dictyoneolone (**14**) was determined to be a C-28 steroid possessing an 8,9-diketo-8,9-seco-4α-methylcholestane skeleton.

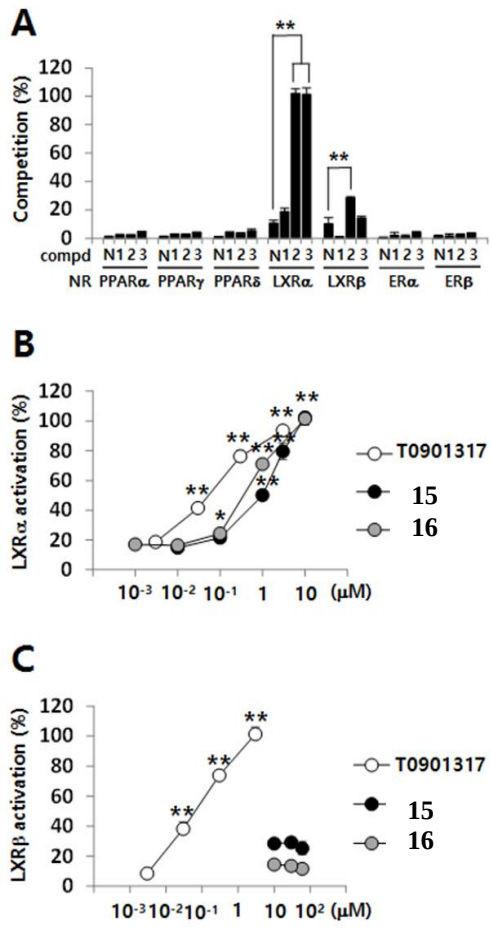

Figure 21. Competitive ligand receptor binding activity and coactivator recruitment activity of compounds **14-16**. (A) The TR-FRET-based receptor binding assays were performed with compounds **14-16**. DMSO (1 %) was used a negative control (N). The concentration response effects of compounds **15** and **16** were evaluated using TR-FRET-based LXRα coactivator assay (B) and the LXRβ assay (C). T0901317 was used as a positive control. Values represent the mean expression ± standard deviation (SD) (n = 3). *P ≤ 0.05 and **P ≤ 0.01.

.2-3. Experimental section

General Experimental Procedures. Optical rotations were measured on a JASCO P-1020 polarimeter using a 1-cm cell. UV spectra were recorded on a Hitachi U-3010 spectrophotometer. IR spectra were recorded on a JASCO 300E FT-IR spectrometer and Proton and carbon NMRs were measured on a JEOL, JNM-600 at 600 and 150 MHz (**15**) and on a Bruker, AVANCE 500 at 500 and 125 MHz (**14** and **16**), respectively. All compounds were measured by CD_3OD (3.31 ppm and 49.0 ppm). Mass spectrometric data were obtained at the Korea Basic Science Institute (Daegu, Korea) and were acquired using a JEOL JMS 700 mass spectrometer with *meta*-nitrobenzyl alcohol (NBA) as a matrix for the FABMS. Low-resolution ESIMS data were recorded on an Agilent Technologies 6130 quadrupole mass spectrometer with an Agilent Technologies 1200 series HPLC. HPLC was performed on a SpectraSystem p2000 equipped with a SpectraSystem RI-150 refractive index detector. All solvents were spectroscopic grade or distilled in a glass prior to use.

Animal Material. Specimens of *Dictyonella* sp. (Voucher number 13SH-13) were collected by hand using SCUBA equipment off the shore of Gageo-do, Korea, October 14, 2013. The sponge is cushion shaped with a 6 cm wide, 8 cm height. Color in life was red and changed to almost orange.

The consistency is slightly firm and the oscules are scattered on the sponge surface as 1 mm length. The surface is covered with a transparent membrane. Choanosomal skeleton is consisted of bundles of long styles and its size is up to 850-1,000 x 5-35 μm. The size of small acanthostyle is 200-250 x 10 μm at minimum. A voucher specimen (registry No. spo. 80) is deposited at the Natural History Museum, Hannam University, Daejeon, Korea.

Extraction and Isolation. The freshly collected specimens were immediately frozen and stored at −25 °C until use. The lyophilized specimens were macerated and repeatedly extracted with MeOH (2 L × 3) and CH_2Cl_2 (2 L × 3). The combined extracts (127.2 g) were successively partitioned between *n*–BuOH (36.0 g) and H_2O (84.1 g); the former fraction was repartitioned between H_2O-MeOH (15:85, 12.64 g) and *n*–hexane (19.74 g). The H_2O-MeOH layer was separated by C_{18} reversed–phase flash chromatography using a sequential mixture of H_2O and MeOH (six fractions in gradient, H_2O–MeOH, from 50:50 to 0:100), acetone, and finally EtOAc as the eluents.

Based on the results of ^{1}H NMR analyses, the less polar fraction eluted with MeOH (1.50 g) was separated by semi-preparative reversed-phase HPLC (YMC-ODS column, 10 mm × 250 mm; H_2O–MeOH, 10:90). Further purifications were then performed by reversed-phase HPLC (YMC-ODS column, 4.6 mm × 250 mm; H_2O–MeOH, 25:75) to yield compounds

1-**3** as amorphous solids. The finally isolated amounts were 1.8, 4.3 and 4.4 mg for **1**-**3**, respectively.

Dictyoneolone (14): white amorphous solid; $[\alpha]_D^{25}$ -26 (*c* 0.2, MeOH); UV (MeOH) λ_{max} (log ε) 242 (3.47) nm; IR (ZnSe) ν_{max} 3442, 2931, 2871, 1688 cm^{-1}; HRFABMS *m*/*z* 431.3516 $[M + H]^+$ (calcd for $C_{28}H_{47}O_3$, 431.3525).

Biological Assays. The cytotoxicity assays were performed in accordance with literature protocols.[62] Time-resolved fluorescence resonance energy transfer (TR-FRET) assays were performed to evaluate the ligand binding to nuclear receptors and coactivator recruitment as agonists. LanthaScreen™ TR-FRET peroxisome proliferator-activated receptor alpha (PPARα), gamma (γ), beta/delta (β/δ), and LanthaScreen™ estrogen receptor alpha (ERα), beta (β) competitive binding assays and Lanthascreen™ liver X receptor alpha (LXRα), beta (β) coactivator assays were conducted according to the manufacturer's instruction (Invitrogen, Waltham, Massachusetts, USA). Fluorescein-TRAP220/DRIP-2 peptide (Sequence: NTKNHPMLMNLLKDNPAQD) and fluorescein-D22 peptide (Sequence: LPYEGSLLLKLLRAPVEEV) were used for the LXRα and LXRβ coactivator assays, respectively.[66] All assays were measured by CLARIOstar (BMG LABTECH, Offenberg, Germany) with the instrument settings described in the TR-FRET manufacturer's instructions. TR-FRET

was detected with a 340 nm excitation filter and 495 and 520 nm emission filters after 3 h. The data was analyzed as the converted ratio of the 520 nm emission to the 495 nm emission versus the log scale of the ligand concentration. To determine the EC_{50} value, the data were fitted using the equation for sigmoidal dose response provided by MARS Data Analysis Software (BMG LABTECH, Offenberg, Germany).

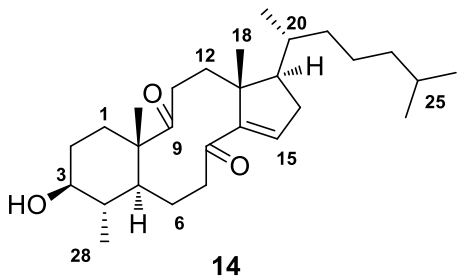

14

Table 9. ^{13}C and ^{1}H NMR assignment for compound **14** in MeOH-d_4

	14	
position	δ_C, type	δ_H, mult. (*J* in Hz)
1	33.0, CH_2	α: 1.98, m
		β: 1.34, ddd (13.5, 3.0, 3.0)
2	30.8, CH_2	α: 1.83, m
		β: 1.47, m
3	75.9, CH	3.17, ddd (11.0, 11.0, 4.7)
4	44.2, CH	1.27, m
5	46.4, CH	1.51, m
6	30.2, CH_2	α: 1.43, m
		β: 1.28, m
7	41.9, CH_2	α: 2.89, m
		β: 2.02, m
8	205.4, C	
9	216.6, C	
10	54.9, C	
11	32.8, CH_2	α: 2.88, m
		β: 1.90, m
12	29.7, CH_2	α: 1.73, br dd (12.8, 12.8)
		β: 2.42, br dd (12.8, 4.3)
13	53.8, C	
14	154.6, C	
15	146.4, CH	6.78, br s
16	37.0, CH_2	α: 2.66, ddd (18.0, 7.9, 3.2)
		β: 2.14, ddd (18.0, 10.7, 2.0)
17	51.3, CH	1.89, m
18	20.0, CH_3	1.20, s
19	14.8, CH_3	0.95, s
20	35.0, CH	1.62, m
21	19.6, CH_3	1.00, d (6.6)
22	37.1, CH_2	1.46, m; 1.10, m
23	25.2, CH_2	1.44, m; 1.24, m
24	40.6, CH_2	1.18, m; 1.16, m
25	29.2, CH	1.55, m
26	22.9, CH_3	0.89, d (6.5)
27	23.2, CH_3	0.90, d (6.5)
28	16.3, CH_3	1.13, d (6.1)

3. Polyene Diterpenes and Sesterterpenes from the Sponge *Phorbas* sp.

Three new diterpenes (**17** – **19**), which reminds of gagunin and linear diterpene bearing cyclohexane moiety, were isolated together with 5 known compounds (**20** – **24**) from the sponge *Phorbas* sp.

All of these new compounds have common points that it is originated from diterterpene skeleton. These are constructed as diverse type and number of rings. For instances, **17** and **24** are made by successively linked cyclic-penta, hexa, hepta moieties. Phorbaketals are rearranged sesterterpene as spiroketal in B/C ring. The structures of these new compounds (**17 - 19**), were determined by combined spectroscopic analyses.

The molecular formula of compound **17**, $C_{20}H_{28}O_5$, was determined by LRESIMS. This compound constitutes of 20 carbons (7 x C, 6 x CH, 2 x CH_2, and 5 x CH_3). There are clearly observed carbon signals, which are two carbonyl carbons (δ_C 170.5 and 162.8), 4 olefinic carbons (δ_C 159.3, 156.1, 132.9, and 122.0), 3 hydroxylated carbons (δ_C 84.4, 77.9, and 70.4), and 4 methyls (δ_C 29.5, 22.8, 22.3, 16.8). The planar structure of compound **17** was constructed by COSY and HMBC. The relative configuration was analyses by NOESY. New compounds **18** and **19** have same cyclohexane moiety and the difference between these is a linear chain. The relative and

absolute configurations of **18** are determined by NOESY and ECD calculations.

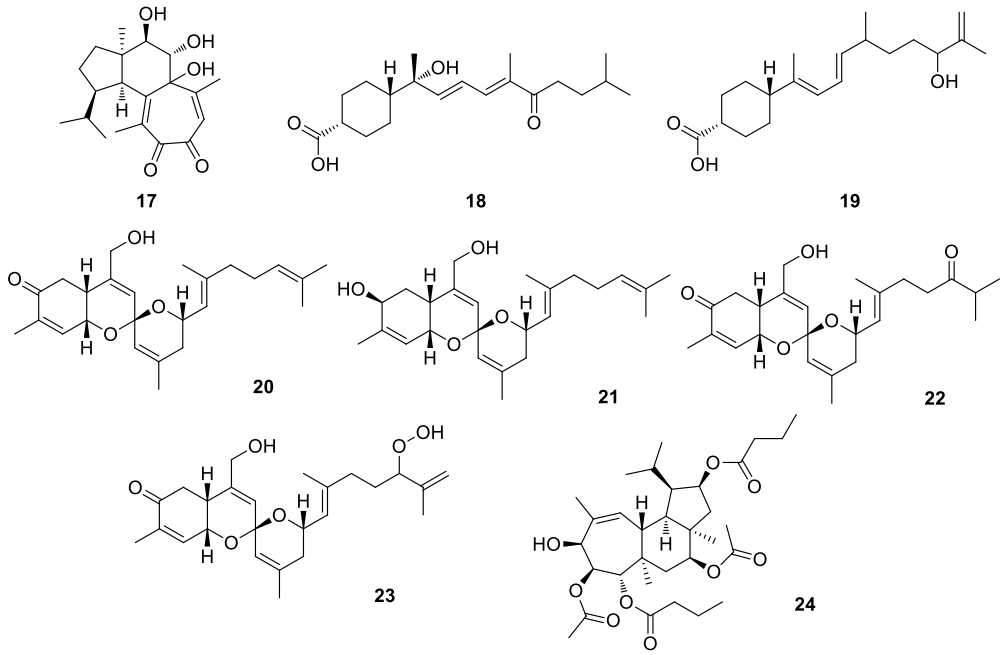

Figure 22. Chemical structures of isolated compounds **17-24**.

3-1. Introduction

New metabolites from the *Phorbas* sp. of marine sponge [Duchassaing and Michelotti (1864), order Poecilosclerida, family Anchinoidae] are found. Among several thousand unique marine sponges, I was curious to explore the chemistry of *Phorbas* species. I examined a *Phorbas* species collected from Gageo-do, Korea, which was found to contain three new diterpenes, four sesterterpenes and a diterpene.

In the sponge *Phorbas* sp., several secondary metabolites were

already reported having wide skeletal diversity and the significant bioactivity. During my search for bioactive compounds from Korean marine invertebrates, I decided to research a reddish *Phorbas* sp. sponge from Gageo-do, Korea. Combined analyses of LC-MS and ^{1}H NMR spectroscopy of an extract of the sponge revealed unusual constituents that motivated extensive investigations. Here, I report the structures of the diterpenes bearing tricyclic ring (**17**) and linear diterpene bearing a hexacyclic ring (**18** and **19**) along with four known sesterterpenes and a diterpene. Compound **17** is a tricyclic, reminiscent of gukulenin E. Compounds **18** and **19** are a well known skeletal class with phorbasin A.

3-2. Results and discussion

The molecular formula of a compound **17**, a yellowish amorphous solid, was deduced to be $C_{20}H_{28}O_5$ LRESIMS. In depth examination of the NMR data are needed that conspicuos 20 carbon signals were detected.

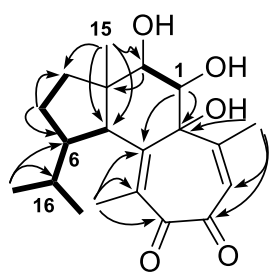

Figure 23. Key correlations of COSY (bold line) and HMBC (arrow) of **17**.

The chemical shifts of the protons and the carbons of the tricyclic moiety substituted with two carbonyls and three hydroxyl groups. Firstly, the tropolone was identified by 2-D data. A combination of COSY, HSQC, and HMBC analyses not only supported this interpretation but revealed parts of penta and hexa cyclic regions. However, configuration of C-14 was not assigned because I tried to run NMR with different solvents such as DMSO-d_6, CDCl3, there are no heteroatom-attached protons at all.

Configurational assignments of the asymmetric centers in **17** were decided based on coupling constant and NOESY analyses. The H-15 methyl proton at the ring and H-6/H-7. Together with the cross-peaks at H-2/H-7 and H-2/H-15, these data presented a cis ring junction between the six- and five-membered rings and α-orientations for H-2, H-6, H-7, and H-15. The β-orientations of H-1 and 21-OH were also confirmed by cross-peaks at H-1/H-4b.

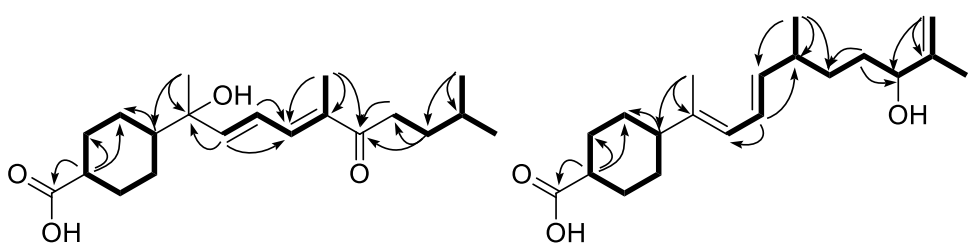

Figure 24. Key correlations of COSY (bold line) and HMBC (arrow) of **18** and **19**.

Diterpenes of **18** and **19**, a yellowish amorphous solid, was deduced to be $C_{20}H_{32}O_4$ and $C_{20}H_{32}O_3$ by LRESIMS respectively. Firstly,

two partial structures, which were a cyclic ring bearing a carboxylic acid and linear side chain were connected. The homonuclear 2D NMR COSY and HMBC data for **18** and **19** identified connectivity sequences indicative of two subunits

The absolute configuration of **17** was determined by comparing its CD spectrum and the ECD spectra of two possible enantiomers, which were calculated using time dependent density-functional theory (TD-DFT) at the B3LYP/def2-TZVPP//B3LYP/def-SV(P) level for all atoms. As shown in Fi gure 22, the ECD spectra of **17** was in accordance with the experimental CD spectra of **17**. The ECD spectra and the CD spectra of **17** displayed diagnostic negative and positive cotton effects at around 250 and 265 nm, respectively.

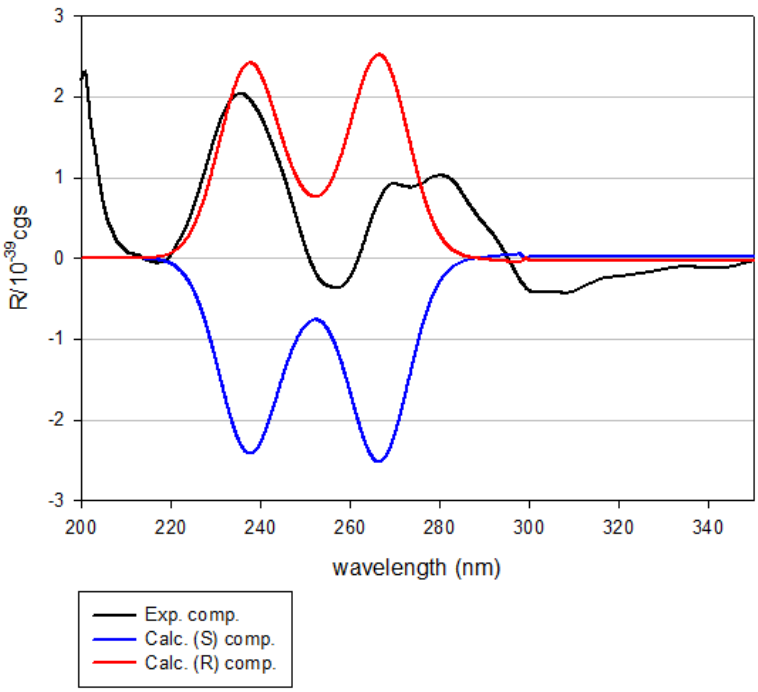

Figure 25. Experimental CD spectra of **18** (black), calculated ECD spectra of **18** (red), and *ent*-**18** (blue).

3-3. Experimental section

General Experimental Procedures. Optical rotations were measured using a JASCO P–1020 polarimeter with a 1-cm cell. UV spectra were acquired using a Hitachi U-3010 spectrophotometer. The ECD spectrum was recorded using an Applied Photophysics Chirascan-plus circular dichroism detector. IR spectra were recorded using a JASCO 300E FT–IR spectrometer with a ZnSe cell. NMR spectra were recorded in CD_3OD and $CDCl_3$ using Bruker Avance 600 and 500 spectrometers, with

internal standard solvent peaks at δ_H 3.30/δ_c 49.0 and δ_H 7.26/δ_c 77.0, respectively. Low-resolution electrospray ionization (ESI) mass spectrometry data were obtained at the National Instrumentation Center for Environmental Management (Seoul, Korea) on a Thermo-Finnigan LTQ-Orbitrap instrument equipped with a Dionex U-3000 HPLC system. HPLC was performed on a SpectraSYSTEM p2000 equipped with a refractive index detector (SpectraSYSTEM RI-150). All solvents used were of spectroscopic grade or were distilled prior to use.

Animal Material. Specimens of a *Phorbas* sp. (Voucher number 13SH-1) were collected by hand via SCUBA diving off the shore of Gageo-Do, Korea at a depth of 30 m on October 23 2013. The samples were dark red, and the gross morphological features were identical with those previously identified. The texture was very soft. The color of the living animal was dark red. In the skeleton, the megascleres took the form of tornotes (295−410 × 7−10 μm), small acanthostyles (145−185 × 8−10 μm), and large acanthostyles (300−420 × 9−11 μm), and the microscleres were isochelas (25−30 μm). The growth form of this specimen was a thick mass, while that from Naples was encrusting. The specimens were deposited (registry number Spo. 37) at the Natural History Museum, Hannam University, Korea, under the curatorship of C.J.S.

Extraction and Isolation. Freshly collected specimens were immediately frozen and stored at −25 ℃ until use. Lyophilized specimens

were macerated and repeatedly extracted with MeOH (3 x 3 L) and CH_2Cl_2 (2 x 3 L). The combined extracts (40.76 g) were successively partitioned between H_2O (58.36 g) and *n*-BuOH (25.64 g); the latter fraction was repartitioned between H_2O-MeOH (15:85, 13.35 g) and *n*-hexane (10.66 g). The aqueous MeOH layer was separated by C_{18} reversed-phase flash chromatography using sequential mixtures of MeOH and H_2O as eluents (six fractions in an H_2O-MeOH gradient, from 50:50 to 0:100), followed by acetone and then EtOAc.

Based on ^{1}H NMR and cytotoxicity analyses, the fraction that eluted with 30:70 H_2O-MeOH (56 mg) was separated by semi-preparative reversed-phase HPLC (YMC-ODS column, 10 mm × 250 mm; H_2O-MeOH, 20:80), yielding five peaks in order of elution. Further purification of the third peak by reversed-phase HPLC (YMC-ODS column, 4.6 mm × 250 mm; H_2O-MeOH, 45:55; t_R = 43 min) yielded 3.2 mg of compound **17**. The 10:90 H_2O-MeOH (986 mg) was separated by semi-preparative reversed-phase HPLC (YMC-ODS column, 10 mm × 250 mm; H_2O-MeOH, 65:35; t_R = 42 min), yielded 2.0 and 0.9 mg of compound **18** and **19**, respectively.

Diterpene (17): a yellowish amorphous solid; $[\alpha]_D^{25}$ -15 (*c* 0.5, MeOH); IR (ZnSe) ν_{max} 3349, 2955, 1735 cm^{-1}; ^{1}H and ^{13}C NMR data, Table 17; LRESIMS *m/z* 348.2 $[M]^+$ (calcd for $C_{20}H_{28}O_5$, 348.2.)

Diterpene (18): a yellowish amorphous solid; $[\alpha]_D^{25}$ +5 (*c* 0.5, MeOH); IR (ZnSe) ν_{max} 3450, 1683 cm^{-1}; LREIMS *m/z* 336.2 $[M]^+$ (calcd

for $C_{20}H_{32}O_4$, 336.2).

Diterpene (19): a yellowish amorphous solid; $[\alpha]_D^{25}$ +6 (*c* 0.5, MeOH); IR (ZnSe) ν_{max} 3455, 1689 cm^{-1}; LREIMS *m*/*z* 320.2 $[M]^+$ (calcd for $C_{20}H_{32}O_3$, 320.2).

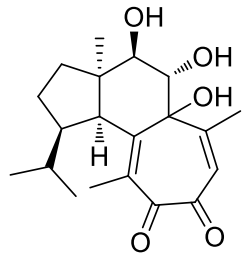

17

Table 10. ^{13}C and ^{1}H NMR assignment for compound **17** in MeOH-d_4

	17	
position	δ_C, type	δ_H, mult. (*J* in Hz)
1	77.9, CH	4.68, d (12.1)
2	70.4, CH	3.31, d (12.1)
3	55.1, C	
4	33.6, CH_2	2.58, dd (14.0, 7.0)
		1.35, ddd (14.0, 14.0, 7.2)
5	34.7, CH_2	2.03, m; 1.27, m
6	51.8, CH	2.09, m
7	54.5, CH	3.37, d (10.4)
8	159.3, C	
9	132.9, C	
10	170.5, C	
11	162.8, C	
12	122.0, CH	6.04, d (1.4)
13	156.1, C	
14	84.4, C	
15	29.5, CH_3	1.21, s
16	31.5, CH	1.19, dq (6.4,1.6)
17	22.3, CH_3	0.93, d (6.4)
18	22.8, CH_3	0.94, d (6.4)
19	10.2, CH_3	2.00, s
20	16.8, CH_3	1.88, d (1.4)

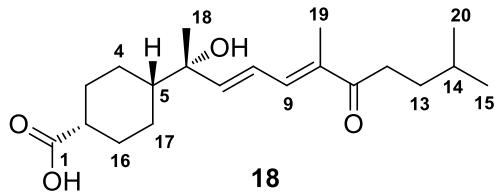

18

Table 11. ^{13}C and ^{1}H NMR assignment for compound **18** in MeOH-d_4

18		
position	δ_C, type	δ_H, mult. (*J* in Hz)
1	180.4, C	
2	41.0, CH	2.52, m
3	28.9, CH_2	2.22, m
		1.43, m
4	25.3, CH_2	1.67, m
		1.31, m
5	49.8, CH	1.40, m
6	76.1, C	
7	150.2, CH	6.27, d (15.2)
8	124.9, CH	6.66, dd (15.2, 11.1)
9	140.4, CH	7.19, d (11.1)
10	135.9, C	
11	204.9, C	
12	36.2, CH_2	2.74, m
		2.72, m
13	35.3, CH_2	1.47, m 2H
14	29.0, CH	1.56, m
15	22.8, CH_3	0.91, d (7.0)
16	25.0, CH_2	1.72, m
		1.22, m
17	29.1, CH_2	2.23, m
		1.43, m
18	25.4, CH_3	1.25, s
19	11.7, CH_3	1.86, d (1.24)
20	22.8, CH_3	0.91, d (7.0)

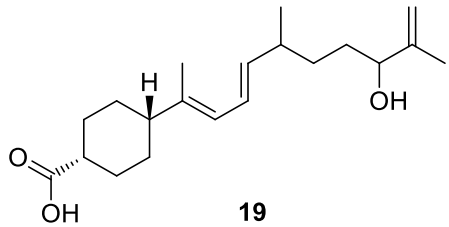

19

Table 12. ^{13}C and ^{1}H NMR assignment for compound **19** in MeOH-d_4

19		
position	δ_C, type	δ_H, mult. (*J* in Hz)
1	176.0, C	
2	38.4, CH	2.45, m
3	27.2, CH_2	2.09, m
		1.32, m
4	23.8, CH_2	1.54, m
		1.12, m
5	47.7, CH	1.25, m
6	140.7, C	
7	123.7, CH	5.75, d (9.2)
8	126.1, CH	6.23, dd (12.2, 9.2)
9	139.8, CH	5.77, d (12.2)
10	37.5, CH	2.08, m
11	32.2, CH_2	1.99, m 2H
12	32.3, CH_2	2.00, m 2H
13	76.5, CH	4.00, m
14	146.7, C	
15	17.1, CH_3	1.67, s
16	23.8, CH_2	1.54, m
		1.12, m
17	27.2, CH_2	2.09, m
		1.32, m
18	25.4, CH_3	1.25, s
19	15.5, CH_3	1.00, d (6.7)
20	20.8, CH_3	1.02, d (6.7)

4. Scalarane Sesterterpenes from the Sponge *Smenospongia* sp.

Three known scalaranes were isolated from the sponge *Smenospongia* sp. collected from Gageo-do, Korea. Based on the results of combined spectroscopic and chemical analyses, the known scalarane sesterterpenes differ from each other in hydroxyl or acetyl groups.

4-1. Introduction

Variable sesterterpenoids is one of the most conspicuous characteristics of sponge-derived terpenoids and distinguishes them from those of other marine organisms.[1,2] Among these sesterterpenoids, the tetracyclic scalarane and related carbon skeletons are the most abundant classes. Since the isolation of scarlarin from *Cacospongia* scalaris in early 1970s, numerous compounds of this skeletal class have been isolated from the order Dictyoceratida and continue to serve as chemical markers of these animals.[3-5] In general, members of this class of compounds exhibit antimicrobial,[6-8] cytotoxic,[9-28] and anti-inflammatory.[29-32] Previously, scalaranes were reported from my lab for the structures and bioactivity of five linear and scalarane-based sesterterpenoids obtained from *Smenospongia* sp.[24] These structures were already reported and researched as well. Therefore, results and discussion are replaced by references which

mentioned above.

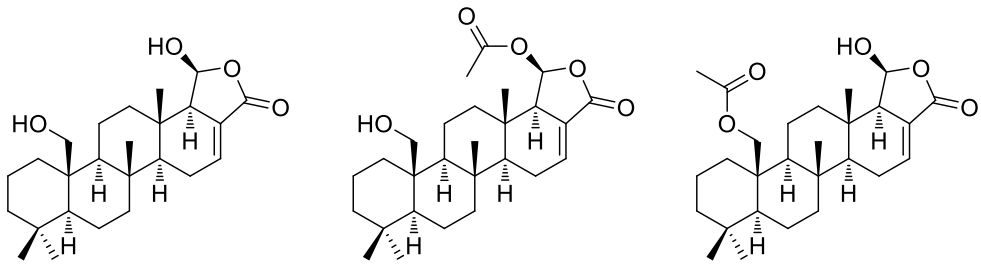

Figure 26. Chemical structures of isolated compounds (**25**-**27**).

4-2. Results and discussion

These compounds exhibited no cytotoxicity, antibacterial and Na+/K+-ATPase inhibitory activities. The molecular formula of scalarane (**25**) was deduced as $C_{25}H_{38}O_4$ by LRESIMS analysis. The ^{13}C and ^{1}H NMR data readily showed the three conspicuous signals: δ_C 170.3 (C), 138.1 (CH), 129.5 (C). Among those, two carbons are olefinic. Thus, in conjunction with the seven degree of unsaturation inherent in the mass data, **25** was determined to be a pentacyclic sesterterpene that was supported by the presence of four shielded methyl signals in the NMR data. Other compounds (**26** and **27**) also possess the same skeleton but differences are the substitutions of hydroxy to acetyl groups.

4-3. Experimental section

General Experimental Procedures. Optical rotations were measured on a JASCO P-1020 polarimeter using a 1 cm cell. UV spectra were recorded on a Hitachi U-3010 spectrophotometer. CD spectra were recorded using an Applied Photophysics Chirascan-plus circular dichroism detector. IR spectra were recorded on a JASCO 300E FT-IR spectrometer. Proton and carbon NMRs were measured at 500 and 125 MHz (**25** and **26**) and 400 and 100 MHz (**27**) in MeOH-d_4, respectively. Mass spectrometric data were obtained at the Korea Basic Science Institute (Daegu, Korea) and were acquired using a JEOL JMS 700 mass spectrometer with meta-nitrobenzyl alcohol (NBA) as a matrix for the FABMS. HPLC was performed on a SpectraSystem p2000 equipped with a SpectraSystem RI-150 refractive index detector. All solvents were spectroscopic grade or distilled in a glass prior to use.

Animal Material. Specimens of *Smenospongia* sp. (voucher number 13SH-4) were collected by hand using SCUBA equipment off the shore of Gageo-do, Korea, on October 13, 2013. The sponge is massive and 6 × 4 × 1.5 cm in diameters. Color in life was grey and changed to almost black. Skeletons were consisted of cored primary fibers and secondary fibers of 100-250 and 40-80 μm in a diameter, respectively. A voucher specimen (registry No. NIBRIV0000300312) is deposited at the Natural Institute of Biological Resources, Korea.

Extraction and Isolation. The freshly collected specimens were immediately frozen and stored at 25 ℃ until use. The lyophilized specimens were macerated and repeatedly extracted with MeOH (2 L × 3) and CH_2Cl_2 (2 L × 3). The combined extracts (36.33 g) were successively partitioned between *n*-BuOH (7.80 g) and H_2O (27.62 g); the former fraction was repartitioned between H_2O-MeOH (15:85) (2.60 g) and *n*-hexane (4.35 g). The aqueous MeOH layer was separated by C18 reversed phase flash chromatography using a sequential mixture of H_2O and MeOH (six fractions in gradient, H_2O-MeOH, from 50:50 to 0:100), acetone, and finally EtOAc as the eluents.

Based on the results of ^{1}H NMR and cytotoxicity analyses, the fraction eluted with 20:80 H_2O-MeOH (0.08 g), 10:90 H_2O-MeOH (0.24 g), and MeOH (0.59 g) fractions were chosen for separation. The 20:80 H_2O-MeOH fraction was separated by semi-preparative reversed-phase HPLC (YMC-ODS column, 10 mm × 250 mm; H_2O-MeOH, 30:70) yielding compound **27**. The 10:90 H_2O-MeOH fraction was separated by semi-preparative reversed-phase HPLC (H_2O-MeOH, 20:80), yielding, in order of elution, compounds **25** and **26** as amorphous solids. The finally isolated amount was 12.4, 15.6, and 13.5 mg for **25**-**27**, respectively.

III. Conclusion

The goal of these works is the investigation of new secondary metabolites from Korean charicteristic sponges. Furthermore, these works will serve good opportunities to discover Korean unique skeletal substances as well. Because new compounds from Korean sponges definitely contain interesting skeletons, which only could find in Korea and the thesis would be described with unique identity. Based on the chemical analysis and bioassay, novel substances from marine organisms have been isolated and demonstrated as new drug candidates.

Chemical investigation of chosed four sponges leads to isolation of 16 novel compounds and 11 known compounds. All these compounds had been structurally determined by combined spectroscopic and chemical analysis. Classifying these compounds, 13 compounds are the sesterterpenes, 11 steroids, 1 saponin, and 3 diterpenes classes.

Several bioactivity tests related to glucose uptake, LXR assay, anti-cancer, anti-microbial, and enzyme-inhibitory activities have been performed. Among those, gombaspiroketals, gombaside A, gombasterols showed potent bioactivities in anti-microbials and enzyme inhibition activities.

Although several metabolites gained few amounts and performed

limited bioactivity tests, overall, this study has successfully accomplished the biomedical potential of a marine organism. Diverse techniques were used when chemicals were needed to reveal chiral centers, physical properties, and to find pharmacophore.

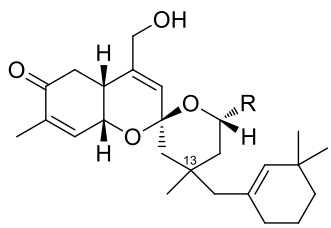

1 (R = OMe, 13*R*)
2 (R = OMe, 13*S*)
3 (R = OH, 13*R*)

gombaspiroketal A-C (**1**-**3**)

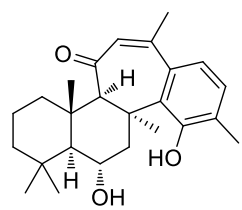

phorone B (**4**)

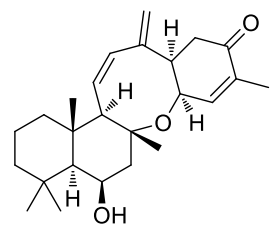

ansellone C (**5**)

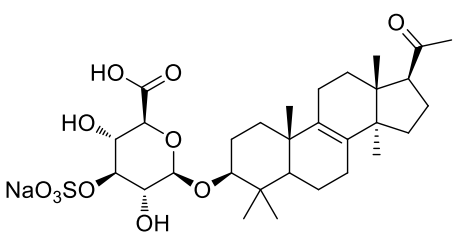

gombaside A (**6**)

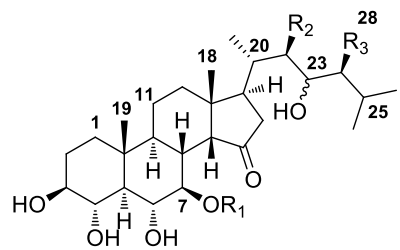

gombasterols A (**7**) R_1 = H, R_2 = OH, 23*R*, R_3 = CH_3
gombasterols B (**8**) R_1 = H, R_2 = OH, 23*R*, R_3 = H
gombasterols C (**9**) R_1 = SO_3Na, R_2 = OH, 23*R*, R_3 = CH_3
gombasterols D (**10**) R_1 = H, R_2 = H, 23*S*, R_3 = H

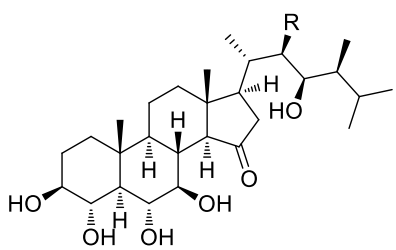

gombasterols E (**11**) R = OH
gombasterols F (**12**) R = H

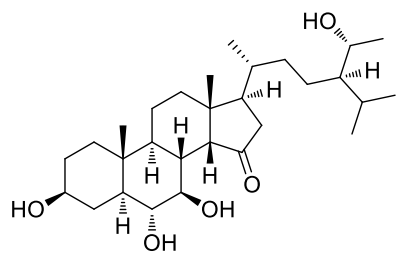

clathriol A (**13**)

Through these researches, there is a limited point that marine metabolites have a lot of obstacles to become a potential drug. First of all, it

is hard to gain substances from sponges even though metabolites exhibit strong bioactivies. There will be needed other techniques to obtain much quantities. However, endeavors to discover novel compounds, which does not identified in the world yet and tested them to show their bioactivity or cytotoxicity. Works finding new skeletal structures and relationship between structures and bioactivities were my pleasure for 6 years. There are already many examples being a drug from marine sponges by using variable techniques. Based upon my research, these works for chemicals would like to be used as valuable benefits for human beings in future.

Summary

During the four years of the Doctor of Philosophy studies, efforts are focused on the study of isolation and elucidation of secondary metabolites from tropical marine sponges.

To achieve visible outcomes from isolation and structure determination of novel substances from Korean marine sponges, four species collected from various locations of Korean sea were selected for chemical investigation. On the basis of combined data such as bioactivity tests and NMR analysis of the crude organic extracts, Among a number of Korean sponges, *Clathria gombawuiensis*, *Dictyonella* sp., *Phorbas* sp., *Smenospongia* sp. were chosen. From four selected sponges, 27 compounds have been isolated and 16 new ones among these have been structurally revealed by combined spectroscopic and chemical analysis. The structures of these 27 compounds belonged to several structural classes with variable biogenetic origins. Various bioassay tests regarding glucose uptake, LXR assay, anticancer, antimicrobial, and enzyme-inhibitory activities have been performed. Some of the isolated compounds showed potent bioactivities in anticancer, antimicrobials and enzyme inhibition activities.

1. Sesterterpenes, a Saponin, and Steroids from the Sponge *Clathria gombawuiensis*

Five new sesterterpenes, including gombaspiroketals A-C, phorone B, and ansellone C (**1**-**5**), gombaside A as a sponin (**6**), and steroids (**7**-**12**) together with a known steroid were isolated from the Sponge *Clathria gombawuiensis* collected from Korean waters. On the basis of the results of combined spectroscopic analyses, the structures of these compounds were determined to be highly rearranged sesterterpene spiroketal methoxyacetals (**1** and **2**) and a corresponding hemiacetal (**3**). The relative and absolute configurations were assigned by NOESY analysis and ECD calculations, respectively. These compounds exhibited moderate cytotoxicities and antibacterial activities.

The structures of phorone B (**4**) and ansellone C (**5**) were determined to be the sesterterpenes of the phorone and ansellone classes, respectively, whereas the saponin gombaside A (**6**) was a nortriterpene sodium *O*-sulfonato-glucuronide of the rare 4,4,14-trimethylpregnane class. The absolute configuration of the glucuronate of 6 was assigned by an application of the phenylglycine methyl ester (PGME) method. The new compounds exhibited moderate cytotoxicity against A549 and K562 cell lines, and compound **6** showed antibacterial activity. The cytotoxicity of **4** may be related to the presence of a free phenolic −OH group, as the

corresponding O-methoxy derivative of **4** is inactive. Six new polyoxygenated steroids (**7**-**12**) along with clathriol (**13**) were isolated from the Korean marine sponge *Clathria gombawuiensis* as well. Based upon the results of combined spectroscopic analyses,

The structures of gombasterols A-F (**7**-**12**) were elucidated to be those of highly oxygenated steroids possessing a 3β,4α,6α,7β-tetrahydroxy or equivalent (7β-sodium *O*-sulfonato for **9**) substitution pattern and a C-15 keto group as common structural motifs. The relative and absolute configurations of these steroids, including the rare 14β configuration of **7**-**10**, were determined by a combination of NOESY, *J*-based analyses, the 2-methoxy-2-(trifluoromethyl)phenylacetic acid (MTPA) method, and X-ray crystallographic analysis. The absolute configuration of **11** was also assigned by these methods. These compounds moderately enhanced 2-deoxy-2-[(7-nitro-2,1,3-benzoxadiazol-4-yl)amino]-D-glucose (2-NBDG) uptake in differentiated 3T3-L1 adipocytes and phosphorylation of AMP-activated protein kinase (AMPK) and acetyl-CoA carboxylase (ACC) in differentiated mouse C2C12 skeletal myoblasts.

2. Steroids from the Sponge *Dictyonella* sp.

A new dictyoneolone (**14**), a secosteroid was isolated along with two known ergosterol peroxides (**15** and **16**) from a *Dictyonella* sp. sponge collected from Gageo-do, Korea. Based upon the results of combined

spectroscopic analyses, the structure of this compound was determined to possess a highly unusual B/C fused ring. The configurations of **14** were determined by a combination of proton-proton couplings and NOESY analyses. Dictyoneolone exhibited weak cytotoxicity against the K562 and A549 cancer cell lines.

The specimens of *Dictyonella* sp. (Order Halichondriidae, Family Dictyonellidae) was collected from the offshore of Gageo-do, South Sea, Korea. Dictyoneolone (**14**), a white amorphous solid, was isolated by bioassay-guided solvent partitioning of crude extract followed by C_{18} vacuum flash chromatography and repeated HPLC.

3. Polyene Diterpenes and Sesterterpenes from the Sponge *Phorbas* sp.

Three new diterpenes (**17** – **19**), which reminds of gagunin and linear diterpene bearing cyclohexane moiety, were isolated together with 5 known compounds (**20** – **24**) from the sponge *Phorbas* sp.

All of these new compounds have common points that it is originated from diterterpene skeleton. These are constructed as diverse type and number of rings. For instances, **17** and **24** are made by successively linked cyclic-penta, hexa, hepta moieties. Phorbaketals are rearranged sesterterpene as spiroketal in B/C ring. The structures of these new compounds (**17** - **19**), were determined by combined spectroscopic analyses.

4. Scalarane Sesterterpenes from the Sponge *Smenospongia* sp.

Three known scalarane sesterterpenes were isolated from the sponge *Smenospongia* sp. collected from Gageo-do, Korea. Based on the results of combined spectroscopic and chemical analyses, the known scalarane sesterterpenes differ from each other in hydroxyl or acetyl groups.

Sponge-derived sesterterpenes often exhibit diverse and potent bioactivities. In our measurement, however, the scalarane compounds **25**-**27** exhibited no cytotoxicity against A549 and K562 cancer cell-lines with the inhibition levels of several compounds often comparable to those of doxorubicin.

References

1. Montaser, R.; Luesch, H. *Future Med. Chem.* **2011**, *3*, 1475-1489.
2. Molinski, T. F.; Dalisay, D. S.; Lievens, S. L.; Saludes, J. P. *Nat. Rev. Drug. Discov.* **2009**, *8*, 69-85.
3. Newman, D. J.; Cragg, G. M.; Sander, K. M. *Nat*. *Prod*. *Rep*. **2000**, *17*, 215-234.
4. Ebada, S. S.; Edrada, R. A.; Lin, W.; Proksch, P. *Nat*. *Protoc*. **2008**, *3*, 1820-1831.
5. Hu, Y.; Chen, J.; Hu, G.; Yu, J.; Zhu, X.; Lin, Y.; Chen, S.; Yuan, J. *Mar. Drugs* **2015**, *13*, 202-221.
6. Mehbub, M. F.; Lei, J.; Franco, C.; Zhang, W. *Mar. Drugs* **2014**, *12*, 4539-4577.
7. Spikema, D.; Franssen, M. C. R.; Osinga, R.; Tramper, J.; Wijffels, R. H. *Mar. Biotechnol.* **2005**, *7*, 142-162.
8. Donia, M.; Hamann, M. T. *The Lancet* **2003**, *3*, 338-348.
9. Hu, G.-P.; Yuan, J.; Sun, L.; She, Z.-G.; Wu, J.-H.; Lan, X.-J.; Zhu, X.; Lin, Y.-C.; Chen, S.-P. *Mar*. *Drugs* **2011**, *9*, 514-525.
10. Perdicaris, S.; Vlachogianni, T.; Valavanidis, A. *Nat. Prod. Chem. Res.* **2013**, *1*, 1-8.
11. Blunt, J. W.; Copp, B. R.; Keyzers, R. A.; Munro, M. H. G.; Prinsep, M. R. *Nat*. *Prod*. *Rep*. **2017**, *34*, 235–294, and earlier reports in the series.

12. Kernan, M. R.; Faulkner, D. J. *J. Org. Chem.* **1988**, *53*, 4574–4578.

13. Stephenson, L. M.; Smith, D. E.; Current, S. P. *J. Org. Chem.* **1982**, *47*, 4171−4173.

14. Manes, L. V.; Naylor, S.; Crews, P.; Bakus, G. J. *J. Org. Chem.* **1985**, *40*, 284−286.–258.

15. Woo, J.-K.; Jeon, J.-e.; Kim, C.-K.; Sim, C. J.; Oh, D.-C.; Oh, K.-B.; Shin, J. *J. Nat. Prod.* **2013**, *76*, 1380−1383.

16. Rho, J.-R.; Hwang, B. S.; Sim, C. J.; Joung, S.; Lee, H.-Y.; Kim, H.-J. *Org. Lett.* **2009**, *11*, 5590−5593.

17. Wang, W.; Mun, B.; Lee, Y.; Reddy, M. V.; Park, Y.; Lee, J.; Kim, H.; Hahn, D.; Chin, J.; Ekins, M.; Nam, S.-J.; Kang, H. *J. Nat. Prod.* **2013**, *76*, 170−177.

18. Forestieri, R.; Merchant, C. E.; de Voogd, N. J.; Matainaho, T.; Kieffer, T. J.; Andersen, R. J. *Org. Lett.* **2009**, *11*, 5166−5169.

19. Daoust, J.; Fontana, A.; Merchant, C. E.; de Voogd, N. J.; Patrick, B. O.; Kieffer, T. J.; Andersen, R. J. *Org. Lett.* **2010**, *12*, 3208−3211.

20. Crews, P.; Bescansa, P. *J. Nat. Prod.* **1986**, *49*, 1041−1052.

21. Kim, H. J.; Sim, C. J. *Integr. Biosci.* **2006**, *10*, 109−114.

22. (a) Go´mez, P. *Zootaxa* **2014**, *3790*, 51−85. (b) Zea, S.; Rodríguez, A.; Martínez, A. M. *Zootaxa* **2014**, *3835*, 401−436.

23. (a) Tanaka, Y.; Katayama, T. *Nippon Suisan Gakkaishi* **1976**, *42*, 801−805. (b) Tanaka, Y.; Fujita, Y.; Katayama, T. *Nippon Suisan*

Gakkaishi **1977**, *43*, 767−772. (c) Tanaka, Y.; Soejima, T.; Katayama, T. *Nippon Suisan Gakkaishi* **1978**, *44*, 1283−1285.

24. Sun, X.; Sun, S.; Ference, C.; Zhu, W.; Zhou, N.; Zhang, Y.; Zhou, K. *Bioorg*. *Med*. *Chem*. *Lett*. **2015**, *25*, 67−69.

25. (a) Sperry, S.; Crews, P. *Tetrahedron Lett*. **1996**, *37*, 2389−2390. (b) Capon, R. J.; Miller, M.; Rooney, F. *J*. *Nat*. *Prod*. **2001**, *64*, 643−644. (c) Zuleta, I. A.; Vitelli, M. L.; Baggio, R.; Garland, M. T.; Seldes, A. M.; Palermo, J. A. *Tetrahedron* **2002**, *58*, 4481−4486. (d) Laville, R.; Thomas, O. P.; Berrue´, F.; Marquez, D.; Vacelet, J.; Amade, P. *J*. *Nat*. *Prod*. **2009**, *72*, 1589−1594. (e) El-Naggar, M.; Conte, M.; Capon, R. J. *Org*. *Biomol*. *Chem*. **2010**, *8*, 407−412. (f) Wei, X.; Henriksen, N. M.; Skalicky, J. J.; Harper, M. K.; Cheatham, T. E., III; Ireland, C. M.; Van Wagoner, R. M. *J*. *Org*. *Chem*. **2011**, *76*, 5515−5523.

26. (a) Ohta, S.; Okada, H.; Kobayashi, H.; Oclarit, J. M.; Ikegami, S. *Tetrahedron Lett*. **1993**, *34*, 5935−5938. (b) Davis, R. A.; Mangalindan, G. C.; Bojo, Z. P.; Antemano, R. R.; Rodriguez, N. O.; Concepcion, G. P.; Samson, S. C.; de Guzman, D.; Cruz, L. J.; Tasdemir, D.; Harper, M. K.; Feng, X.; Carter, G. T.; Ireland, C. M. *J*. *Org*. *Chem*. **2004**, *69*, 4170−4176. (c) Ravichandran, S.; Wahidullah, S.; D'Souza, L.; Anbuchenzhian, R. M. Russ. *J*. *Org*. *Chem*. **2011**, *37*, 428−435.

27. (a) Keyzers, R. A.; Northcote, P. T.; Webb, V. *J. Nat. Prod*. **2002**, *65*, 598−600. (b) Keyzers, R. A.; Northcote, P. T.; Berridge, M. V. *Aust. J. Chem*. **2003**, *56*, 279−282.

28. Woo, J.-K.; Jeon, J.-e.; Kim, C.-K.; Sim, C. J.; Oh, D.-C.; Oh, K.-B.; Shin, J. *J. Nat. Prod*. **2013**, *76*, 1380−1383.

29. Wang, W.; Lee, Y.; Lee, T. G.; Mun, B.; Giri, A. G.; Lee, J.; Kim, H.; Hahn, D.; Yang, I.; Chin, J.; Choi, H.; Nam, S.-J.; Kang, H. *Org. Lett*. **2012**, *14*, 4486−4489.

30. Daoust, J.; Chen, M.; Wang, M.; Williams, D. E.; Chavez, M. A. G.; Wang, Y. A.; Merchant, C. E.; Fontana, A.; Kieffer, T. J.; Andersen, R. J. *J. Org. Chem*. **2013**, *78*, 8267−8273.

31. Ohtani, I.; Kusumi, T.; Kashman, Y.; Kakisawa, H. *J. Am. Chem. Soc*. **1991**, *113*, 4092−4096.

32. The numbering system of **5** is different from ansellone B for the comparison of NMR data with **4**.

33. Daoust, J.; Fontana, A.; Merchant, C. E.; de Voogd, N. J.; Patrick, B. O.; Kieffer, T. J.; Andersen, R. J. *Org. Lett*. **2010**, *12*, 3208−3211.

34. Rho, J.-R.; Hwang, B.-S.; Joung, S.; Byun, M. R.; Hong, J.-H.; Lee, H.-Y. *Org. Lett*. **2011**, *13*, 884−887.

35. Hosny, M.; Rosazza, J. P. N. *J. Nat. Prod*. **1999**, *62*, 853−858.

36. Crublet, M.-L.; Pouny, I.; Delaude, C.; Lavaud, C. *J. Nat. Prod*. **2002**,

65, 1560−1567.

37. Avilov, S. A.; Silchenko, A. S.; Antonov, A. S.; Kalinin, V. I.; Kalinovsky, A. I.; Smirnov, A. V.; Dmitrenok, P. S.; Evtushenko, E. V.; Fedorov, S. N.; Savina, A. S.; Shubina, L. K.; Stonik, V. A. *J. Nat. Prod*. **2008**, *71*, 525−531.

38. Yabuuchi, T.; Kusumi, T. *J. Org. Chem*. **2000**, *65*, 397−404.

39. Epstein, W. W.; Van Lear, G. *J. Org. Chem*. **1966**, *31*, 3434−3435.

40. Anderson, C. G.; Epstein, W. W.; Van Lear, G. *Phytochemistry* **1972**, *11*, 2847−2852.

41. Gonza´lez, A. G.; Leo´n, F.; Rivera, A.; Padro´n, J. I.; Gonza´lez-Plata, J.; Zuluaga, J. C.; Quintana, J.; Este´vez, F.; Bermejo, J. *J. Nat. Prod*. **2002**, *65*, 417−421.

42. Mosmann, T. J. *Immunol. Methods* **1983**, *65*, 55−63.

43. Oh, K.-B.; Lee, J. H.; Chung, S.-C.; Shin, J.; Shin, H. J.; Kim, H.-K.; Lee, H.-S. *Bioorg. Med. Chem. Lett*. **2008**, *18*, 104−108.

44. Aiello, A.; Fattorusso, E.; Menna, M. *Steroids* **1999**, *64*, 687-714.

45. (a) Catalan, C. A. N.; Thompson, J. E.; Kokke, W. C. M. C.; Djerassi, C. *Tetrahedron* **1985**, *41*, 1073-1084. (b) Djerassi, C.; Silva, C. J. *Acc. Chem. Res*. **1991**, *24*, 371-378. (c) Giner, J.-L. *Chem. Rev.* **1993**, *93*, 1735-1752.

46. (a) Sheikh, Y. M.; Djerassi, C. *Tetrahedron* **1974**, *30*, 4095-4103. (b)

D′Auria, M. V.; Minale, L.; Riccio, R. *Chem. Rev.* **1993**, *93*, 1839-1896. (c) Stonik, V. A. *Russ. Chem. Rev.* **2001**, *70*, 673-715.

47. (a) Fiorucci, S.; Distrutti, E.; Bifulco, G.; D′auria, M. V.; Zampella, A. *Trends Pharmacol. Sci.* **2012**, *33*, 591-601. (b) Sica, D.; Musumeci, D. *Steroids* **2004**, *69*, 743-756. (c) Ivanchina, N. V.; Kicha, A. A.; Stonik, V. A. *Steroids* **2011**, *76*, 425-454.

48. (a) Burgoyne, D. L.; Andersen, R. J.; Allen, T. M. *J. Org. Chem.* **1992**, *57*, 525-528. (b) Yang, L.; Andersen, R. J. *J. Nat. Prod.* **2002**, *65*, 1924-1926.

49. (a) Keyzers, R. A.; Northcote, P. T.; Webb, V. *J. Nat. Prod.* **2002**, *65*, 598-600. (b) Keyzers, R. A.; Northcote, P. T.; Berridge, M. V. *Aust. J. Chem.* **2003**, *56*, 279-282.

50. Sperry, S.; Crews, P. *J. Nat. Prod.* **1997**, *60*, 29-32.

51. Kobayashi, J.; Shinonaga, H.; Shigemori, H.; Umeyama, A.; Shoji, N.; Arihara, S. *J. Nat. Prod.* **1995**, *58*, 312-318.

52. Shoji, N.; Umeyama, A.; Shin, K.; Takeda, K.; Arihara, S.; Kobayashi, J.; Takei, M. *J. Org. Chem.* **1992**, *57*, 2996-2997.

53. Fu, X.; Ferreira, M. L. G.; Schmitz, F. J.; Kelly, M. *J. Org. Chem.* **1999**, *64*, 6706-6709.

54. (a) Cachet, N.; Regalado, E. L.; Genta-Jouve, G.; Mehiri, M.; Amade, P.; Thomas, O. P. *Steroids* **2009**, *74*, 746-750. (b) Regalado, E. L.; Tasdemir, D.; Kaiser, M.; Cachet, N.; Amade, P.; Thomas, O. P. *J. Nat. Prod.* **2010**, *73*, 1404-1410. (c) Regalado, E. L.; Turk, T.; Tasdemir,

D.; Gorjanc, M.; Kaiser, M.; Thomas, O. P.; Fernández, R.; Amade, P. *Steroids* **2011**, *76*, 1389-1396.

55. (a) Gonzalez, A. G.; Barreira, R. F.; Francisco, C. G.; Rocio, J. A.; Lopez, E. S. *Ann. Quimica* **1974**, *70*, 250-253. (b) Lucker, M. *Secondary Metabolism in Microorganisms, Plants, and Animals*; Springer-Verlag: Berlin, Heidelberg, New York, Tokyo, 1984; pp 230-249. (c) Miyamoto, T.; Higuchi, R.; Komori, T.; Fujioka, T.; Mihashi, K. *Tetrahedron Lett.* **1986**, *27*, 1153-1156. (d) Deepak, D.; Grove, J. F.; Haslam, E.; Khare, A.; Khare, N. K.; Srivastava, S. *Progress in the Chemistry of Organic Natural Products*; Springer-Verlag: New York, 1996; Vol. 69, pp 71-156. (e) Yadava, R.; Rathore, K. *Asian J. Chem.* **1999**, *11*, 699-702. (f) Hsiao, P.-Y.; Lee, S.-J.; Chen, I.-S.; Hsu, H.-Y.; Chang, H.-S. *Phytochemistry* **2016**, *130*, 282-290

56. (a) Woo, J.-K.; Kim, C.-K.; Kim, S.-H.; Kim, H.; Oh, D.-C.; Oh, K.-B.; Shin, J. *Org. Lett.* **2014**, *16*, 2826-2829. (b) Woo, J.-K.; Kim, C.-K.; Ahn, C.-H.; Oh, D.-C.; Oh, K.-B.; Shin, J. *J. Nat. Prod.* **2015**, *78*, 218-224.

57. Kim, H. J.; Sim, C. J. *Korean J. Syst. Zool.* **2005**, *21*, 111-122.

58. Ulukaya, E.; Ozdikicioglu, F.; Oral, A. Y.; Demirci, M. *Toxicol. in Vitro* **2008**, *22*, 232–239.

59. Kim, C.-K.; Woo, J.-K.; Kim, S.-H.; Cho, E.; Lee, Y.-J.; Lee, H.-S.; Sim, C. J.; Oh, D.-C.; Oh, K.-B.; Shin, J. *J. Nat. Prod.* **2015**, *78*, 2814-2821.

60. (a) Johansson, M.; Karlsson, L.; Wennergren, M.; Jansson, T.; Powell, T. L. *J. Clin. Endocrinol. Metab.* **2003**, *88*, 2831–2837. (b) Oh, K.-B.; Lee, J. H.; Chung, S.-C.; Shin, J.; Shin, H. J.; Kim, H.-K.; Lee, H.-S. *Bioorg. Med. Chem. Lett.* **2008**, *18*, 104−108. (c) Oh, K.-B.; Kim, S.-H.; Lee, J.; Cho, W.-J.; Lee, T.; Kim, S. *J. Med. Chem.* **2004**, *47*, 2418-2421.

61. (a) Kim, W. H.; Lee, J.; Jung, D. W.; Williams, D. R. *Sensors (Basel)* **2012**, *12*, 5005-5027. (b) Nguyen, P. H.; Yang, J. L.; Uddin, M. N.; Park, S. L.; Lim, S. I.; Jung, D. W.; Williams, D. R.; Oh, W. K. *J. Nat. Prod.* **2013**, *76*, 2080-2087. (c) Lee, J.; Jung, D.-W.; Kim, W.-H.; Um, J.-I.; Yim, S.-H.; Oh, W.-K.; Williams, D. R. *ACS Chem. Biol.* **2013**, *8*, 1803-1814.

62. (a) Huang, S.; Czech, M. P. *Cell Metab.* **2007**, *5*, 237-252. (b) Carling, D. *Trends. Biochem. Sci.* **2004**, *29*, 18-24. (c) Hardie, D. G. *Annu. Rev. Pharmacol. Toxicol.* **2007**, *47*, 185-210. (d) Nguyen, P. H.; Choi, H. S.; Ha, T. K. Q.; Seo, J. Y.; Yang, J. L.; Jung, D. W.; Williams, D. R.; Oh, W. K. *Bioorg. Med. Chem. Lett.* **2017**, *27*, 40-44. (e) Zhang, B.; Salituro, G.; Szalkowski, D.; Li, Z.; Zhang, Y.; Royo, I.; Vilella, D.; Díez, M. T.; Pelaez, F.; Ruby, C.; Kendall, R. L. *Science.* **1999**, *284*, 974-977.

63. Aiello, A.; Fattorusso, E.; Menna, M. *Steroids* **1999**, *64*, 687-714.

64. (a) Sheikh, Y. M.; Djerassi, C. *Tetrahedron* **1974**, *30*, 4095-4103. (b) Djerassi, C.; Silva, C. J. *Acc. Chem. Res.* **1991**, *24*, 371-378.

65. Giner, J.-L. *Chem. Rev.* **1993**, *93*, 1735-1752.

66. D′Auria, M.V.; Minale, L. Riccio, R. *Chem. Rev.* **1993**, *93*, 1839-1895.

67. Stonik, V. A. *Russ*. *Chem*. *Rev*. **2001**, *70*, 673-715.

68. (a) CA 27765-65-7; (b) CA 34660-19-0; (C) CA 37697-47-5; (d) CA 39204-63-2; (e) CA 72853-97-5; (f) CA 137366-04-2.

69. (a) Snatzke, G.; Fehlhaber, H.-W. *Liebigs Ann. Chem*. **1963**, *663*, 123-135. (b) Snatzke, G.; Nisar, A. *Liebigs Ann*. *Chem*. **1965**, *683*, 159-174. (c) Aoyama, S.; Sasaki, K. *Chem. Pharm. Bull.* **1970**, *18*, 481-489. (d) Aoyama, S. *Chem. Pharm. Bull.* **1971**, *19*, 896-905. (e) Rodewald, W. J.; Jagodziński, J. J.; *Pol. J. Chem.* **1981**, *55*, 1751-1757. (f) Lorenc, L.; Bondarenko, L.; Pavlović, V.; Fuhrer. H.; Rihs, G.; Kalova, J.; Mihailović, M. L. *Helv*. *Chim*. *Acta* **1989**, *72*, 608-623. (g) Castellano, E. E.; Zukerman-Schpector, J.; Rehder, V. L. G.; Marsaioli, A. J. *Acta Cryst*. **1989**, *C45*, 966-970. (h) Rehder, V. L. G.; Fujiwara, F. Y.; Marsaioli, A. J. *Quim. Nova* **1990**, *13*, 266-272. (i) Tinant, B.; Declercq, J. P.; Dabovic, M.; Kristic, N.; Lorenc, L.; Mihailović, M. L. *Bull*. *Soc*. *Chim*. *Belg*. **1993**, *102*, 539-544.

APPENDIX A:

^{1}H and ^{13}C NMR Spectroscopic Data of Isolated Compounds

List of Figures

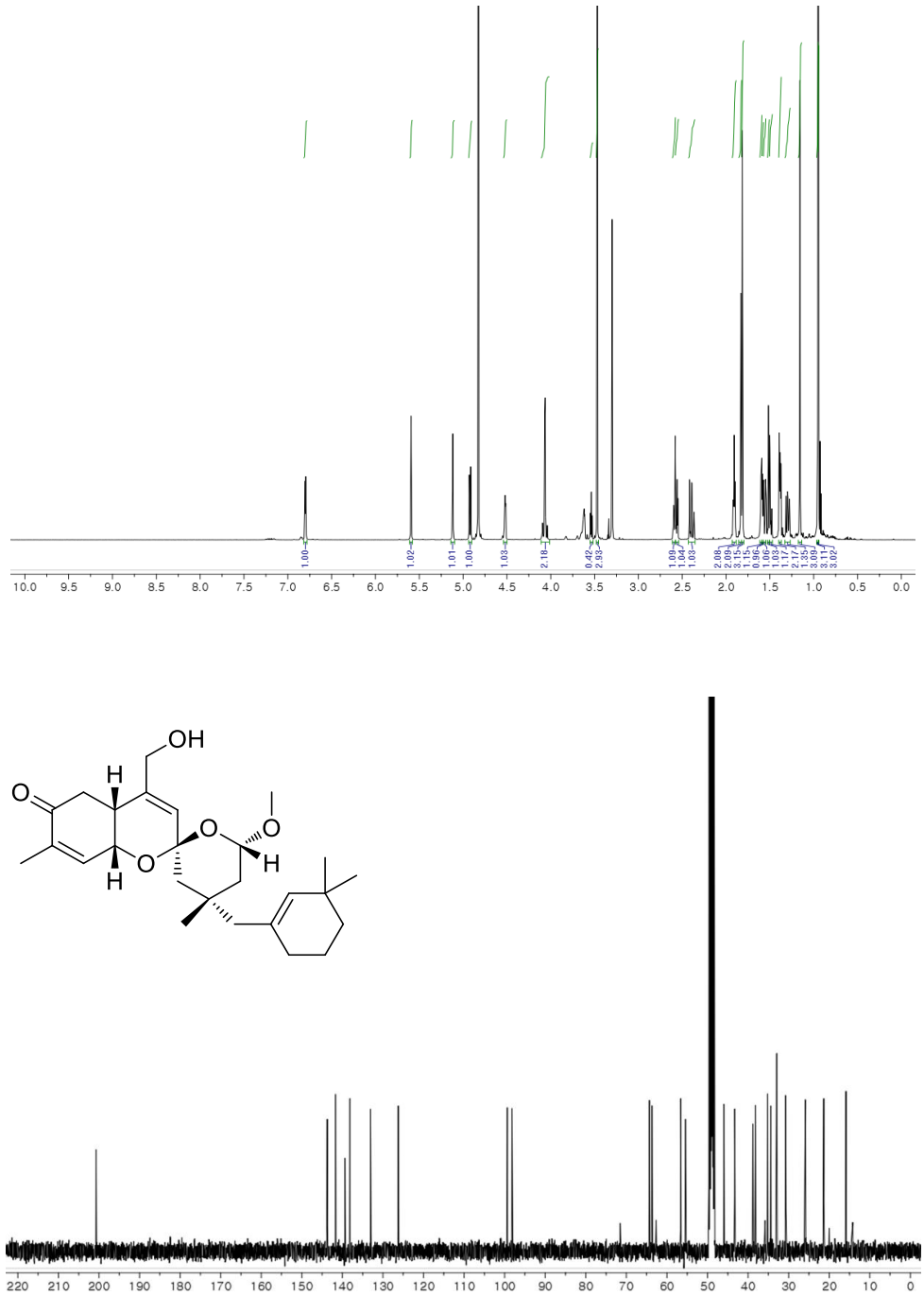

Figure A1. ^{1}H (600 MHz) and ^{13}C (150 MHz) NMR spectra of compound **1** (MeOH-d_4)

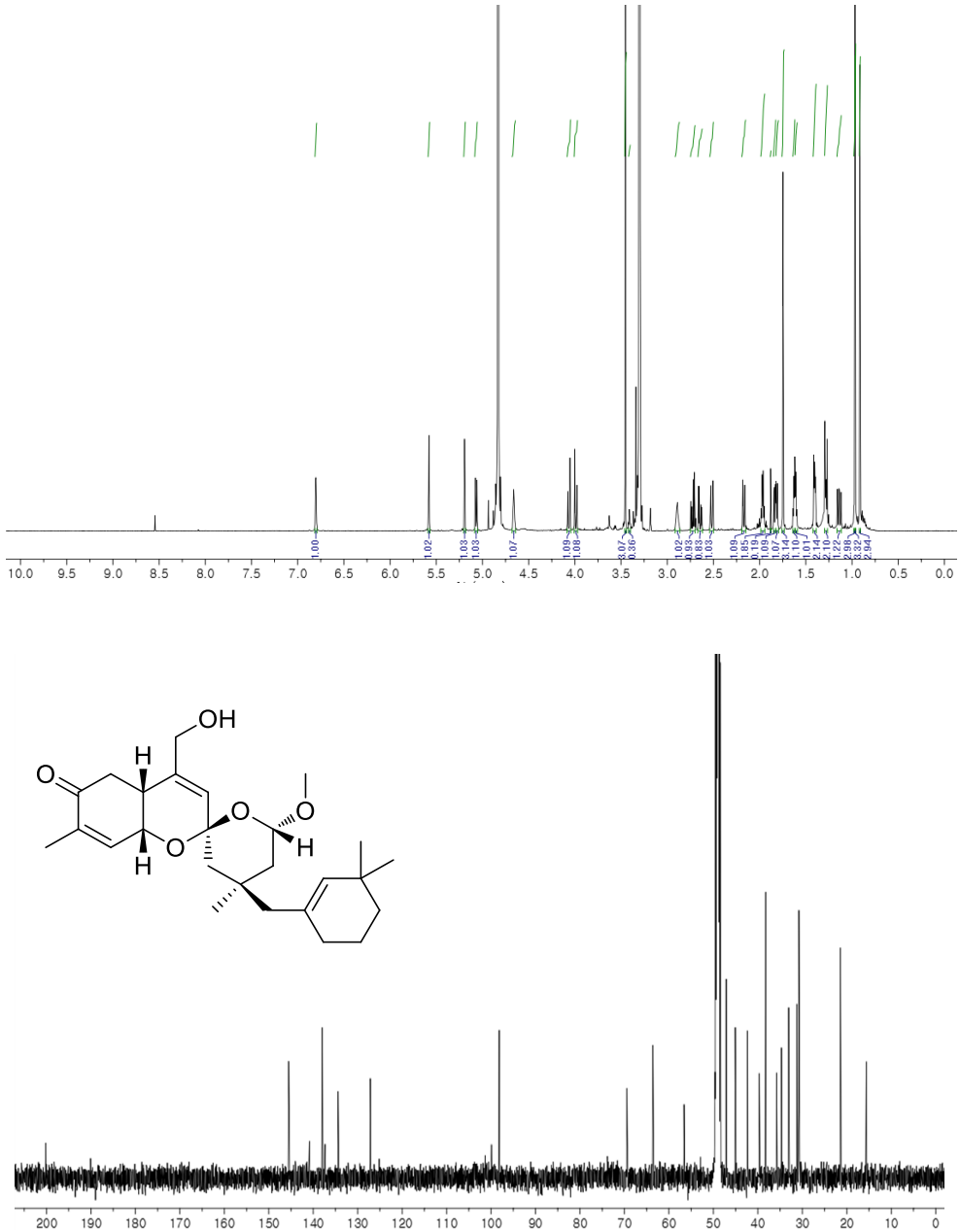

Figure A2. ^{1}H (600 MHz) and ^{13}C (150 MHz) NMR spectra of compound **2** (MeOH-d_4)

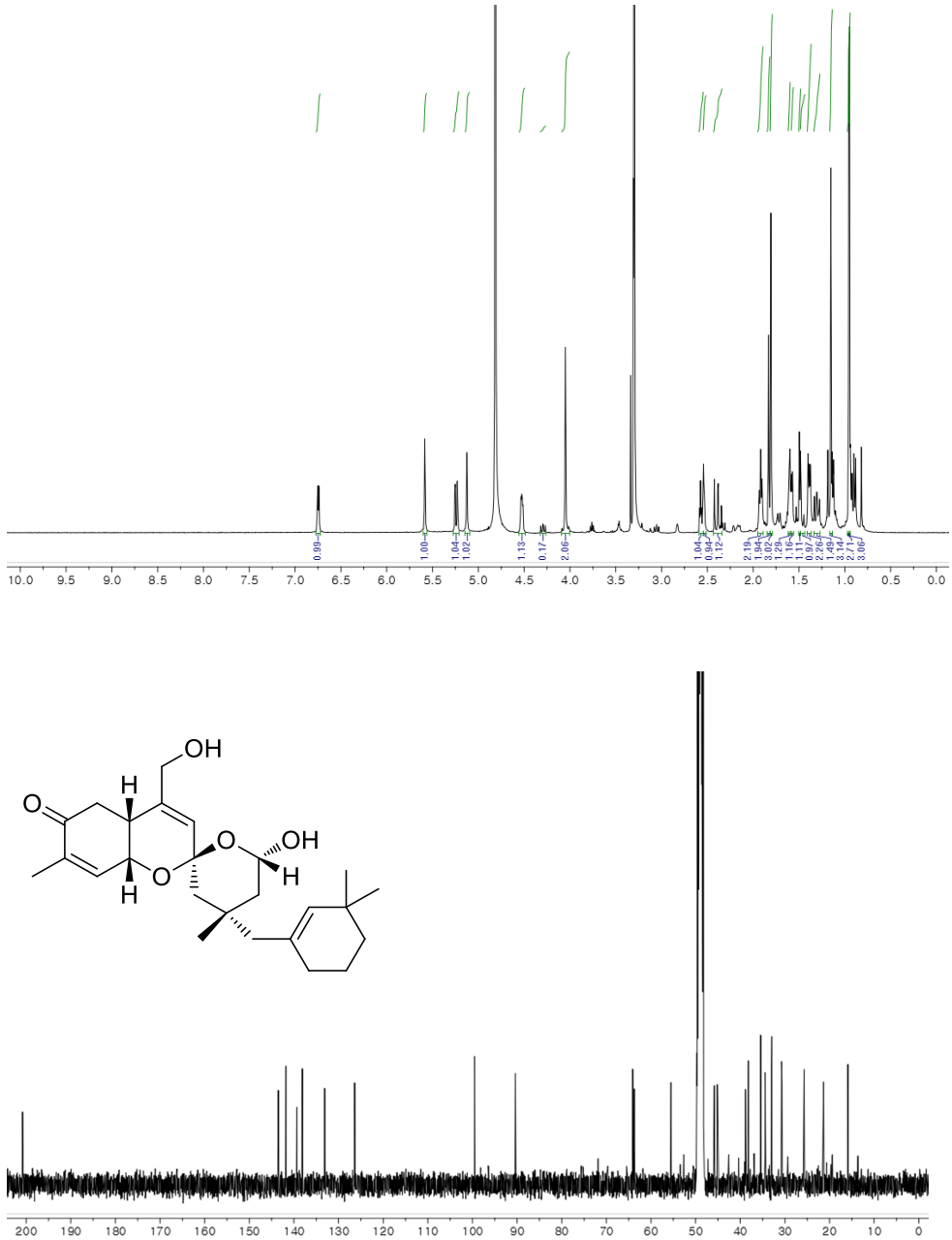

Figure A3. ^{1}H (600 MHz) and ^{13}C (150 MHz) NMR spectra of compound **3** (MeOH-d_4)

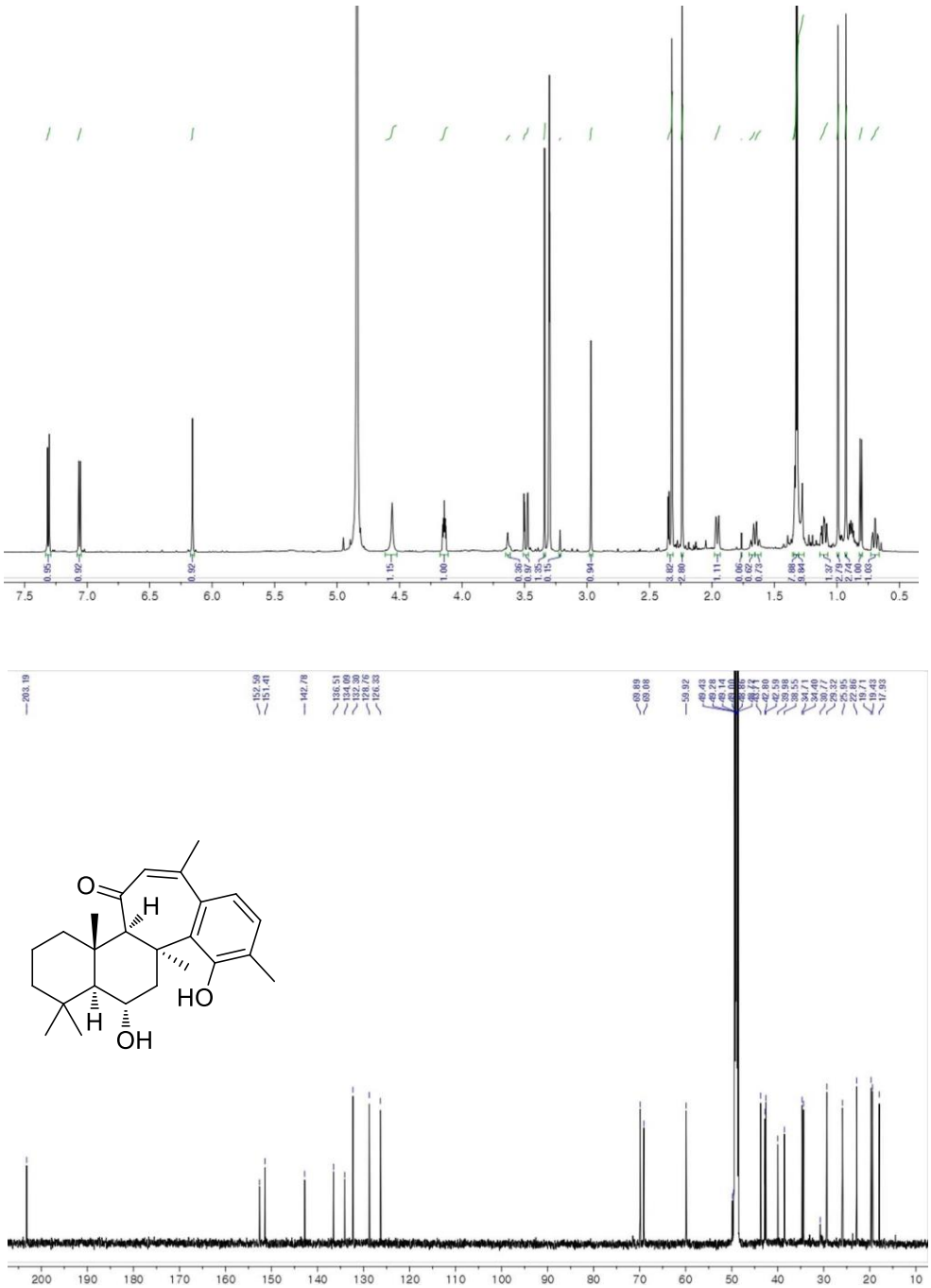

Figure A4. ^{1}H (500 MHz) and ^{13}C (125 MHz) NMR spectra of compound **4** (MeOH-d_4)

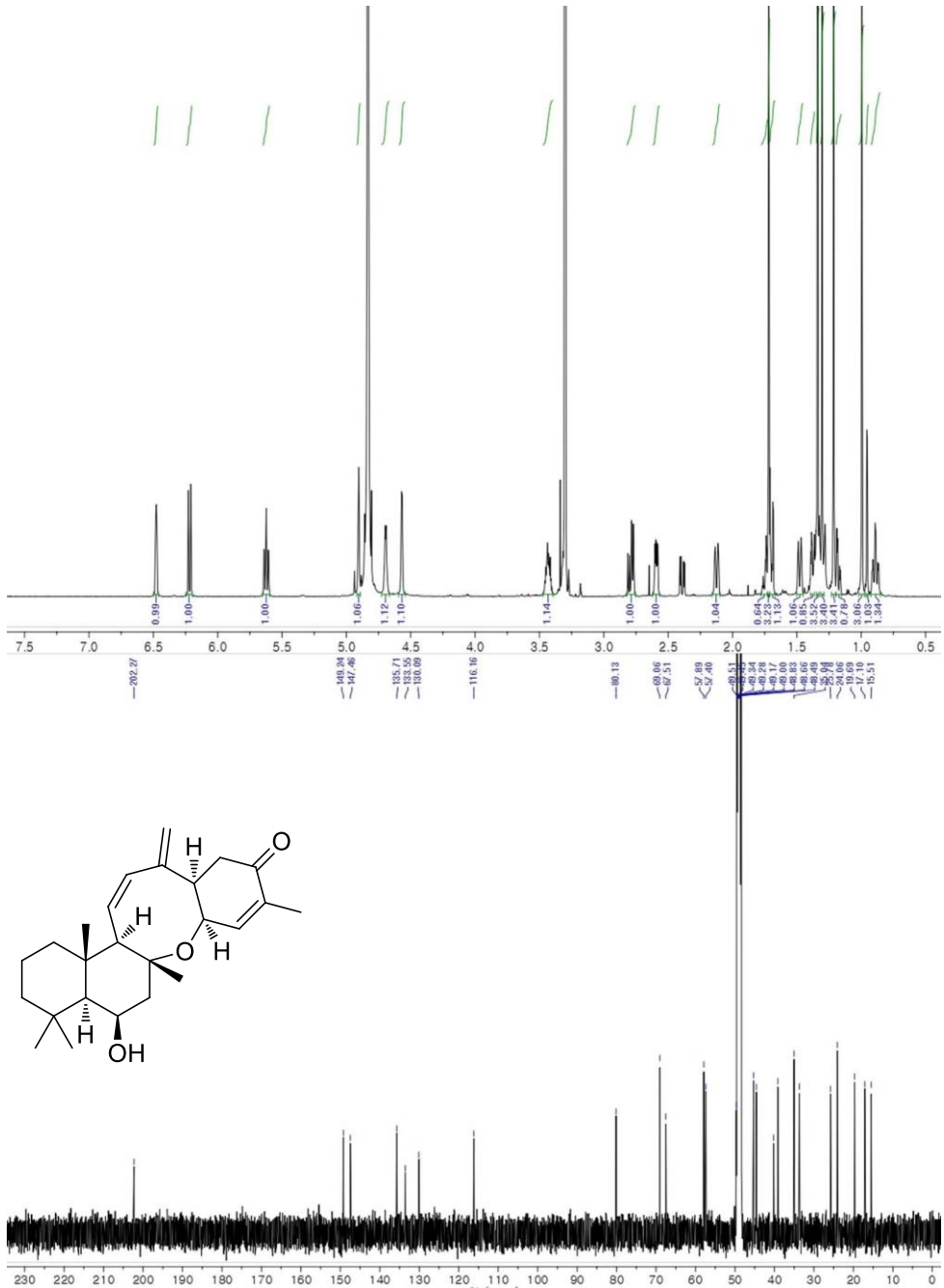

Figure A5. ^{1}H (500 MHz) and ^{13}C (125 MHz) NMR spectra of compound **5** (MeOH-d_4)

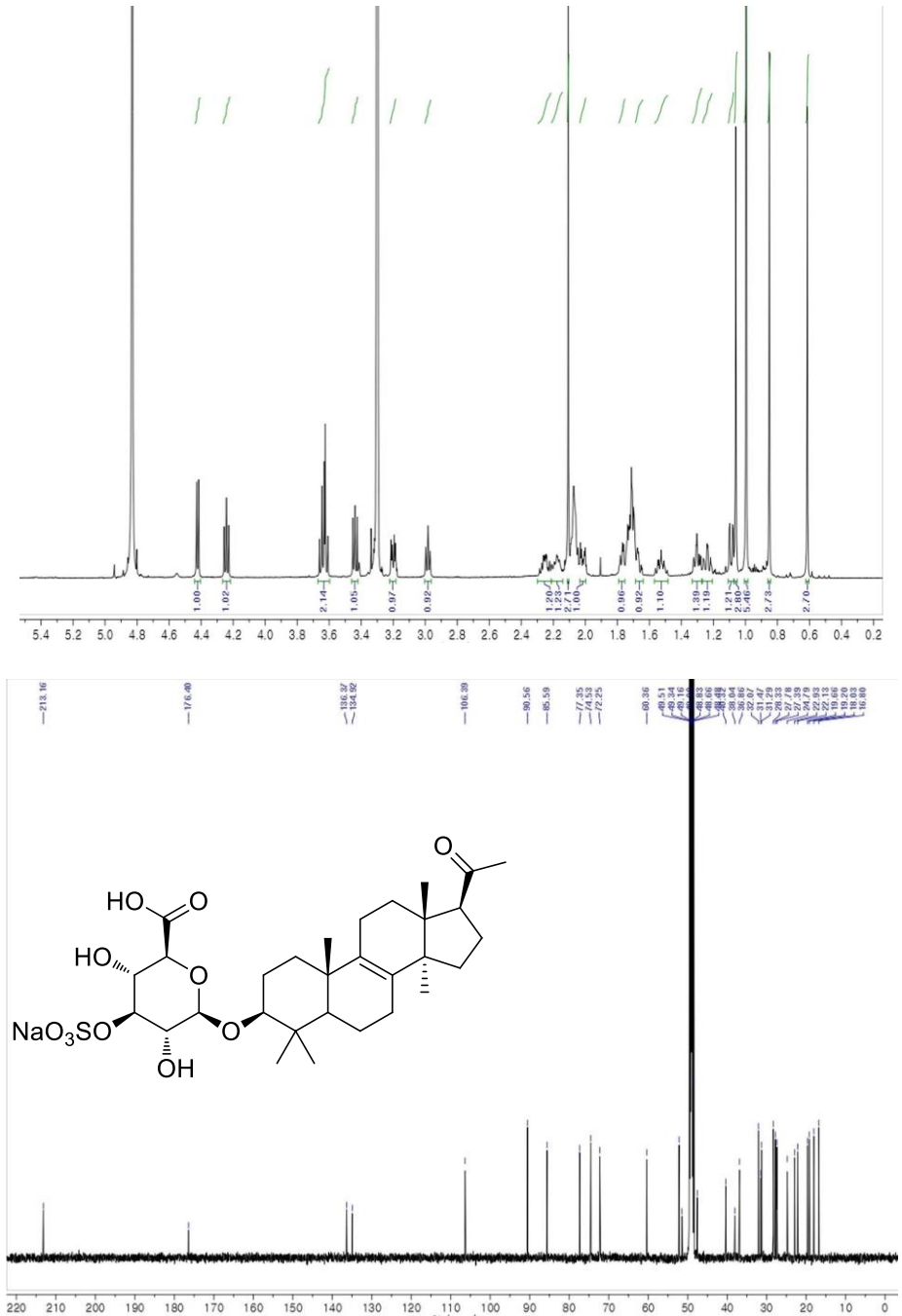

Figure A6. ^{1}H (600 MHz) and ^{13}C (150 MHz) NMR spectra of compound **6** (MeOH-d_4)

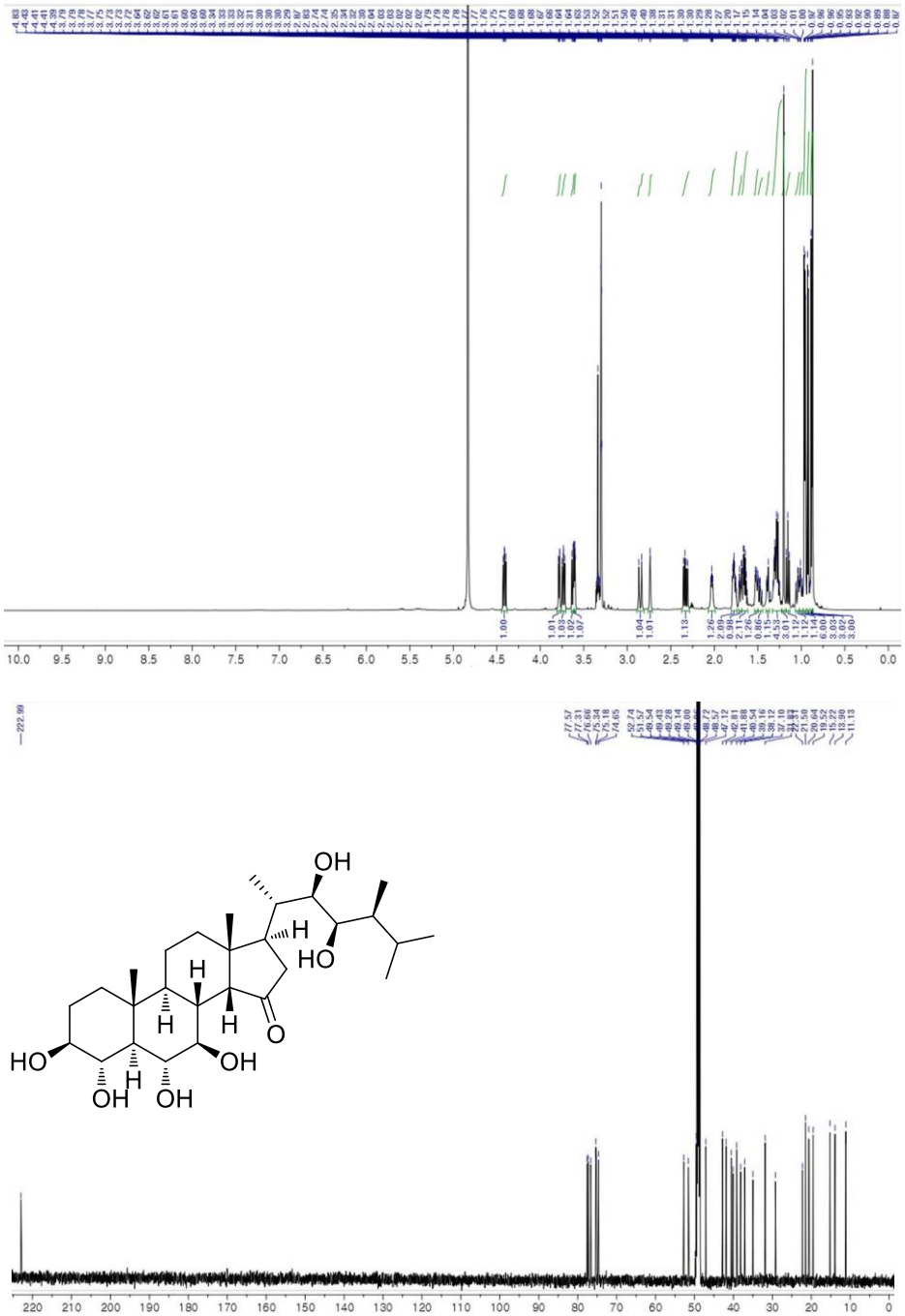

Figure A7. ^{1}H (600 MHz) and ^{13}C (150 MHz) NMR spectra of compound **7** (MeOH-d_4)

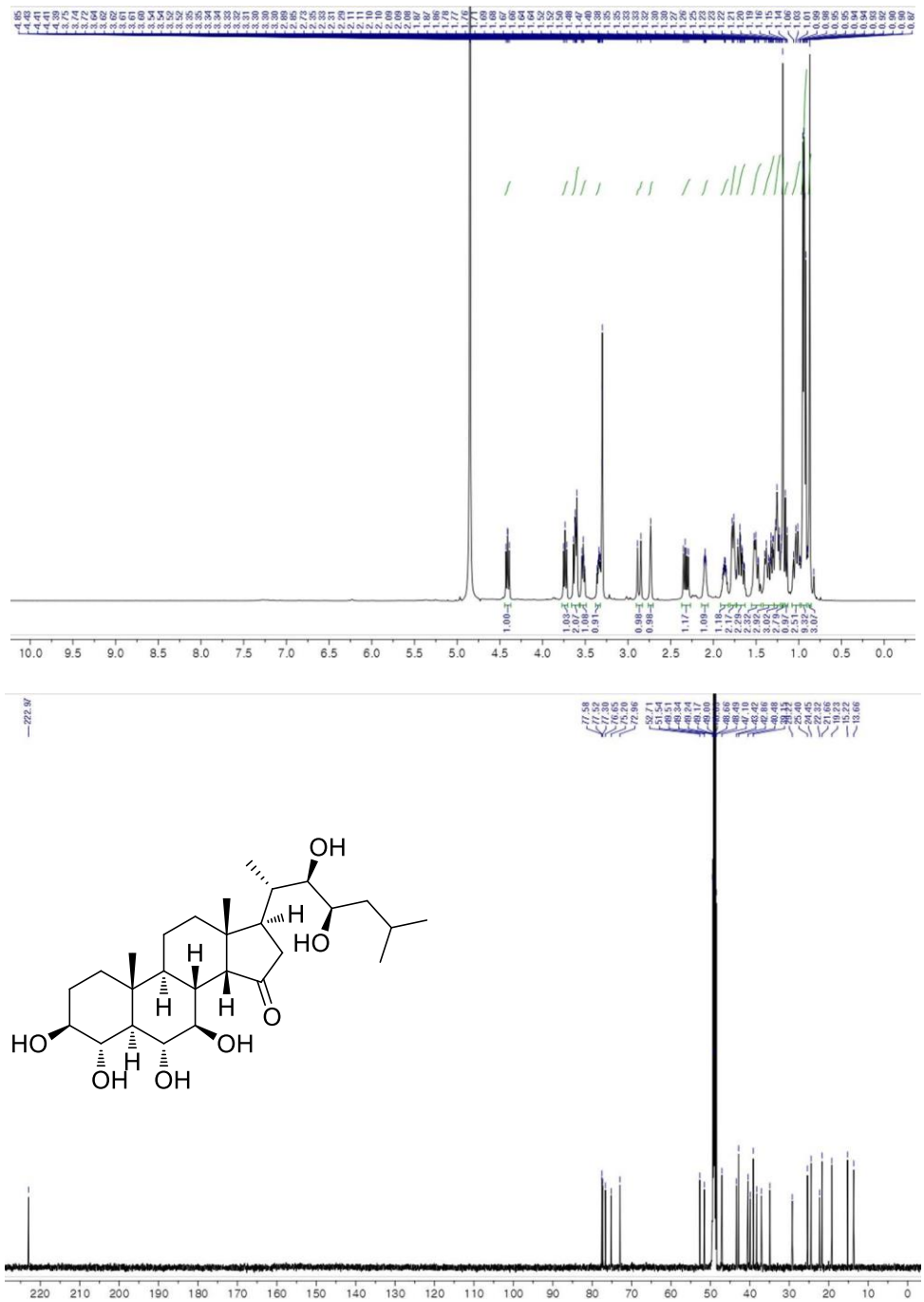

Figure A8. ^{1}H (400 MHz) and ^{13}C (100 MHz) NMR spectra of compound **8** (MeOH-d_4)

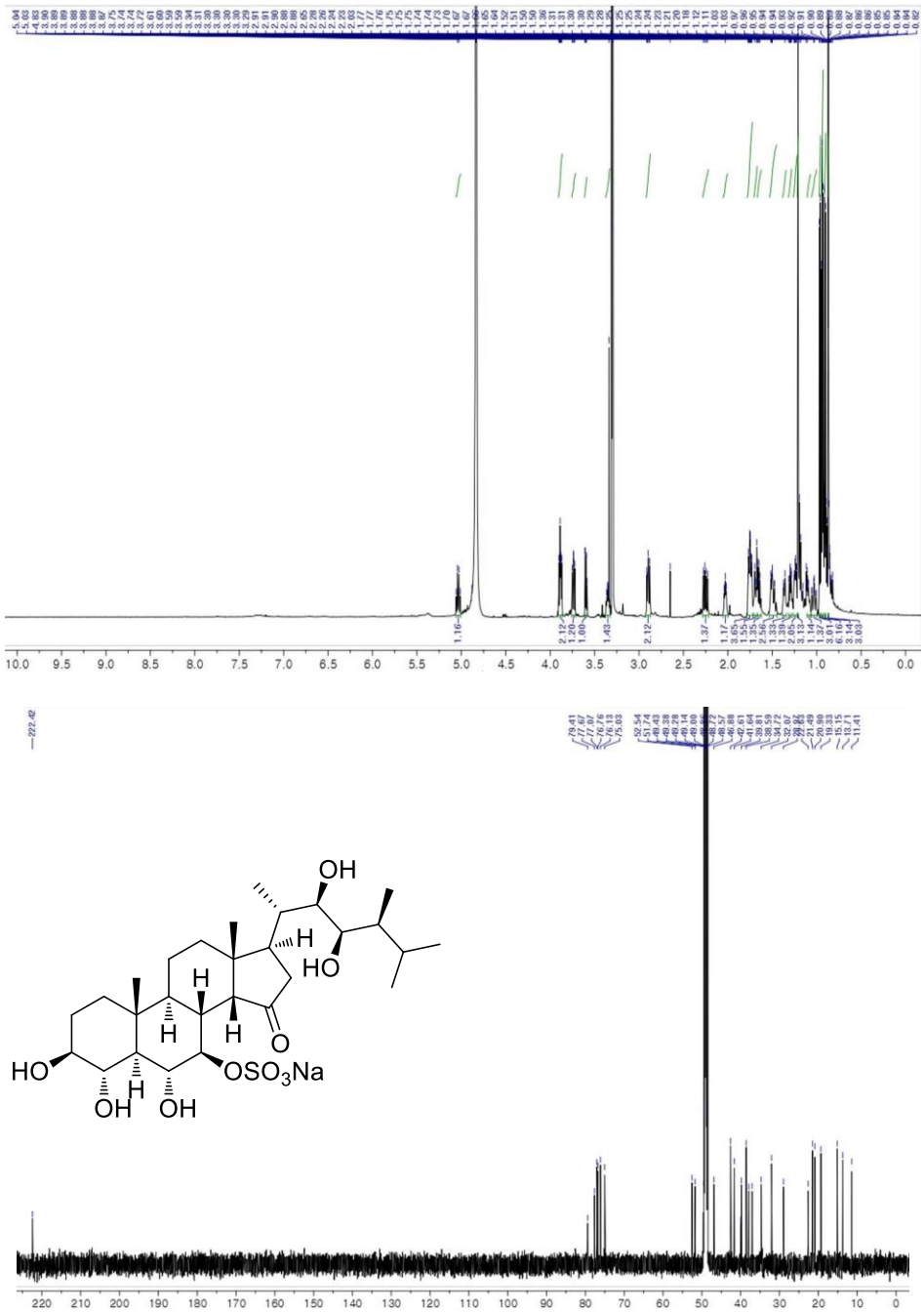

Figure A9. ^{1}H (500 MHz) and ^{13}C (125 MHz) NMR spectra of compound **9** (MeOH-d_4)

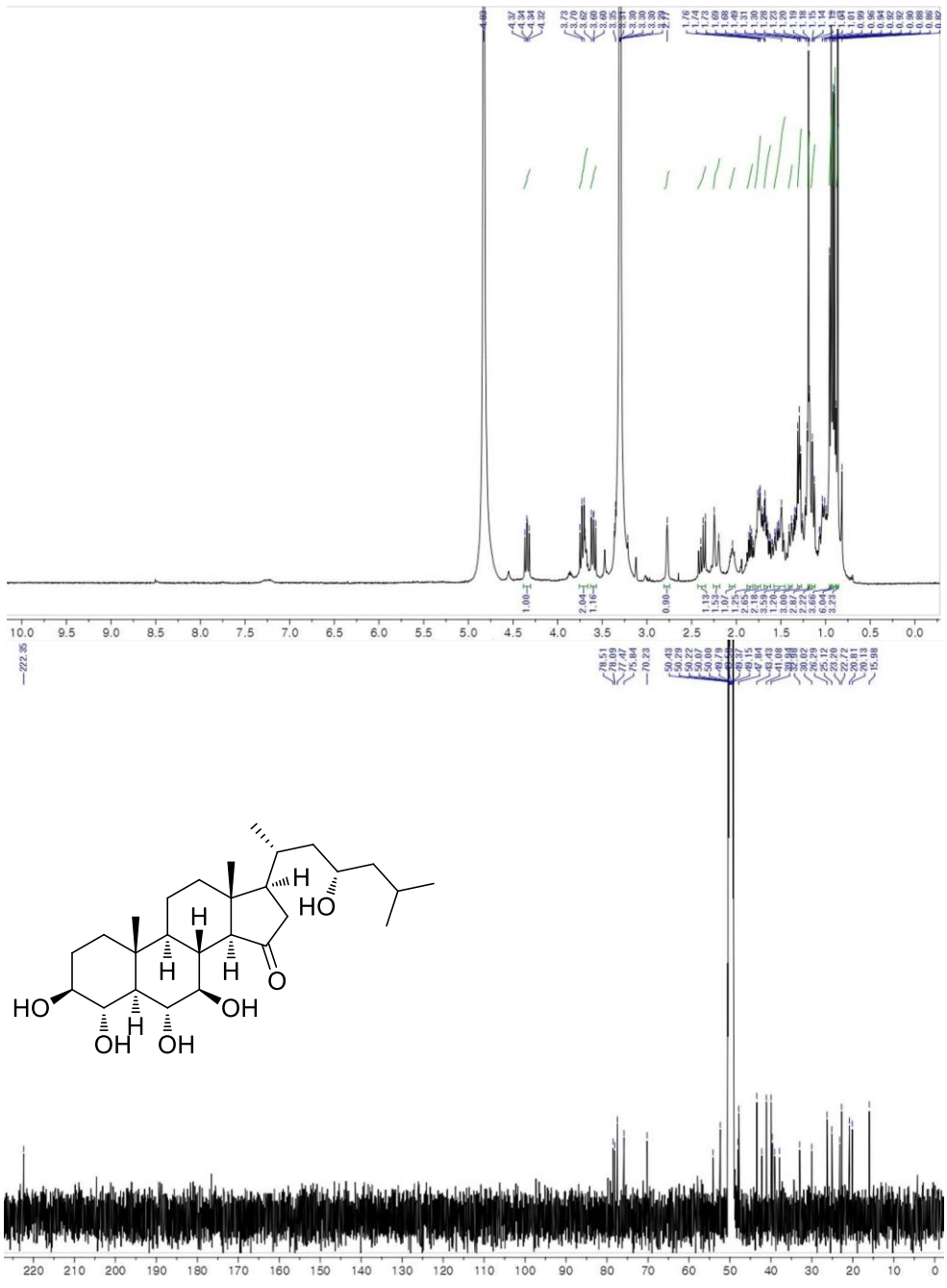

Figure A10. ^{1}H (500 MHz) and ^{13}C (125 MHz) NMR spectra of compound **10** (MeOH-d_4)

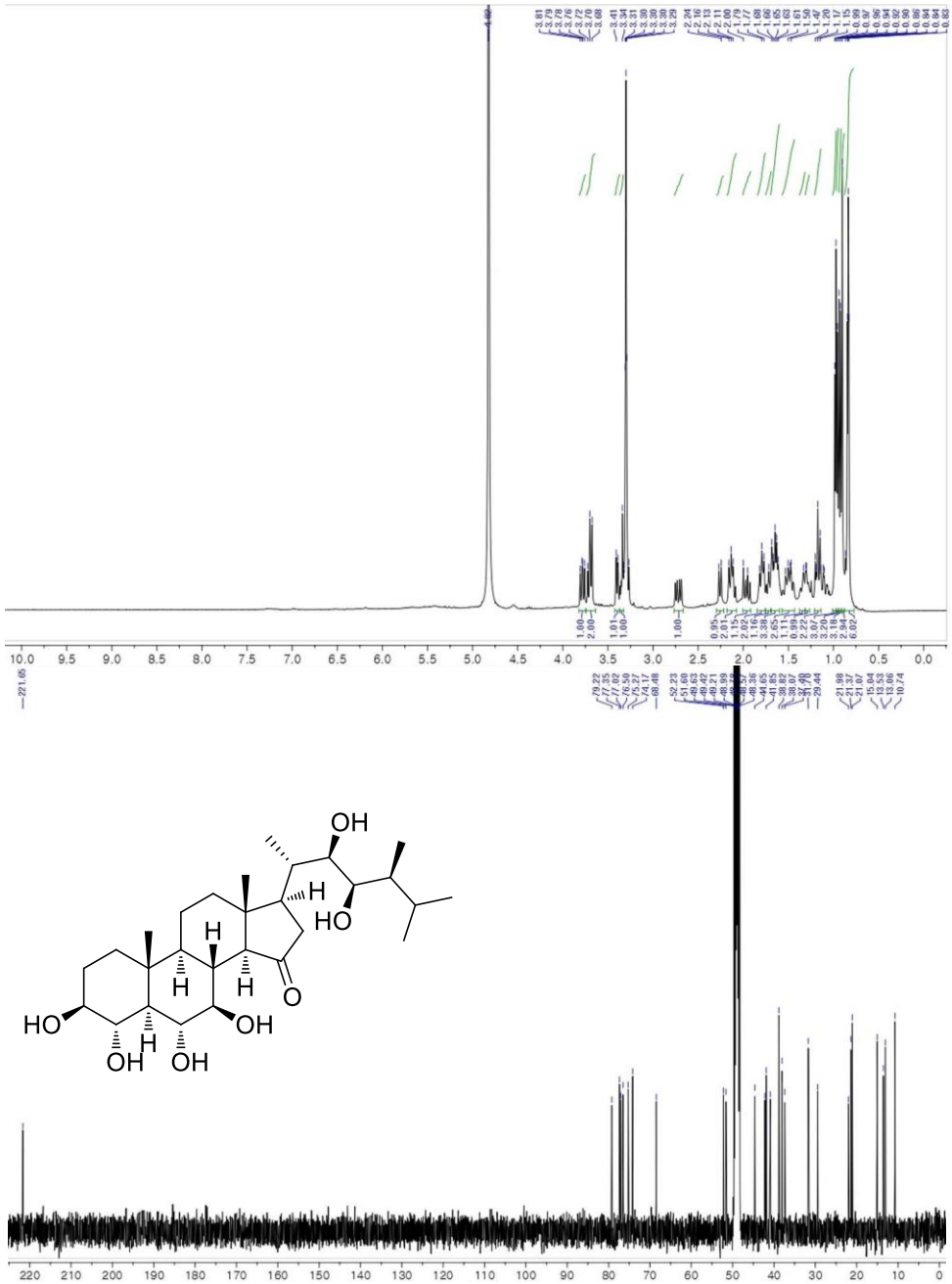

Figure A11. ^{1}H (400 MHz) and ^{13}C (100 MHz) NMR spectra of compound **11** (DMSO-d_6)

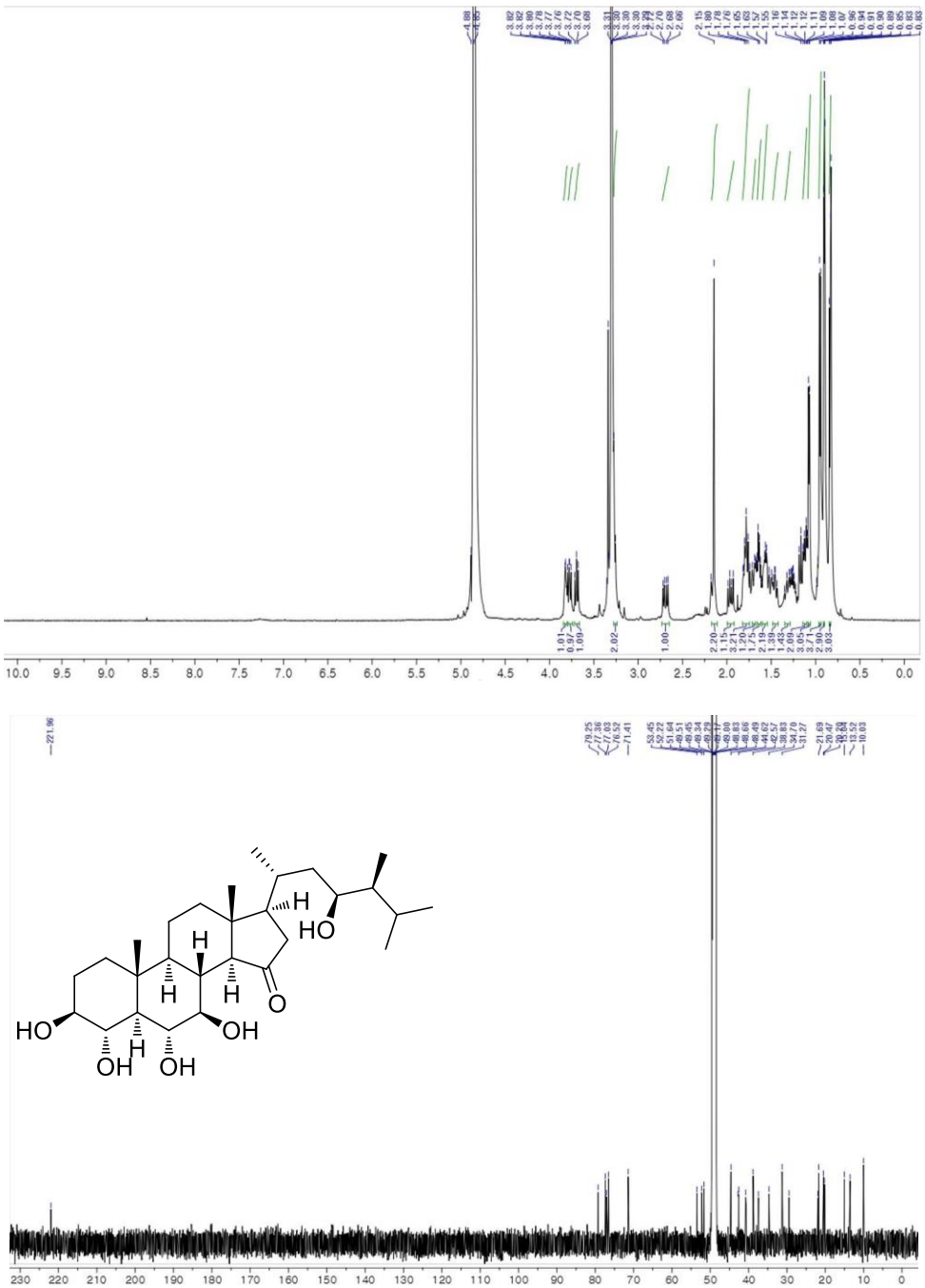

Figure A12. ^{1}H (500 MHz) and ^{13}C (125 MHz) NMR spectra of compound **12** (MeOH-d_4)

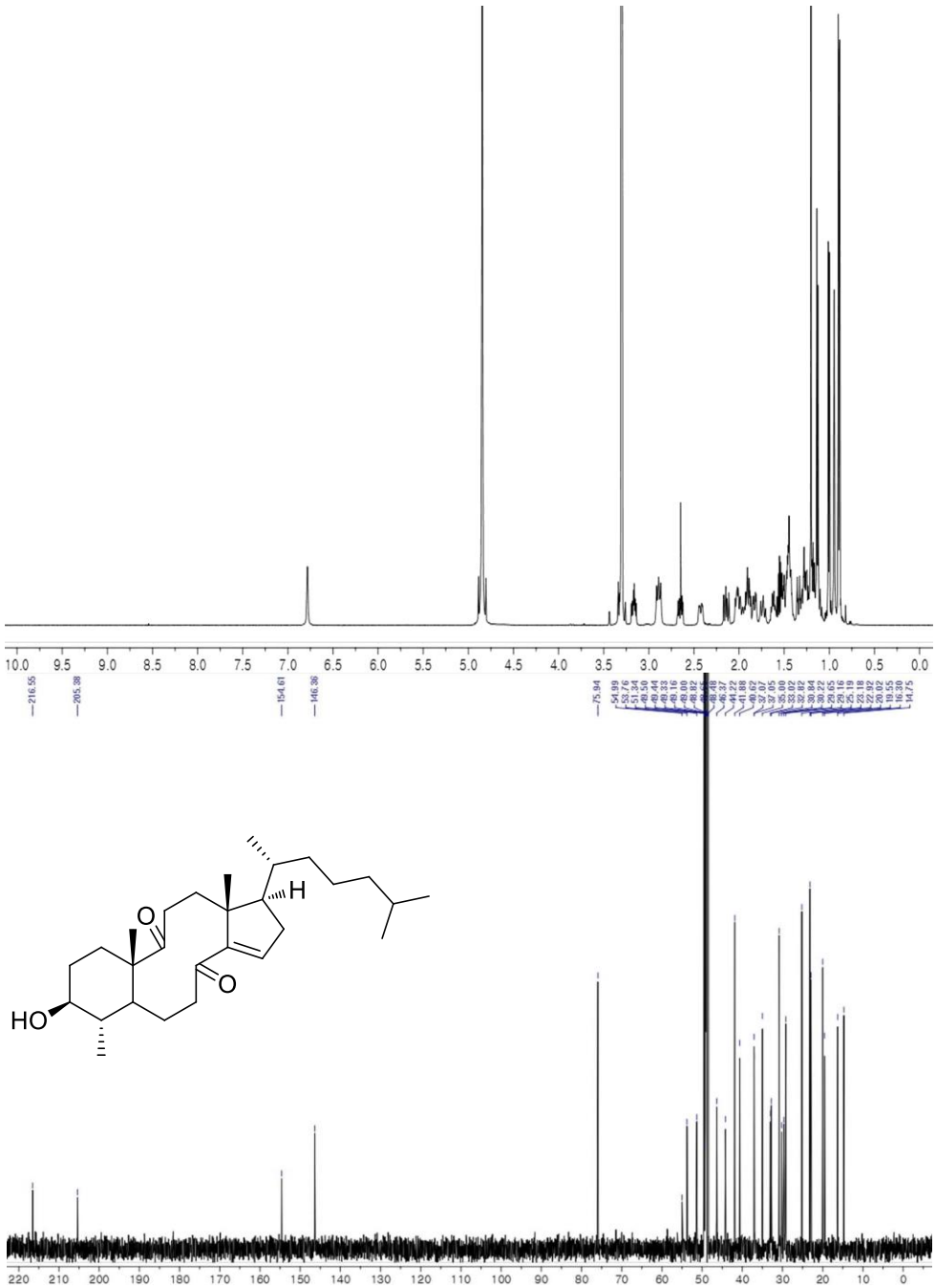

Figure A13. ^{1}H (600 MHz) and ^{13}C (150 MHz) NMR spectra of compound **14** (MeOH-d_4)

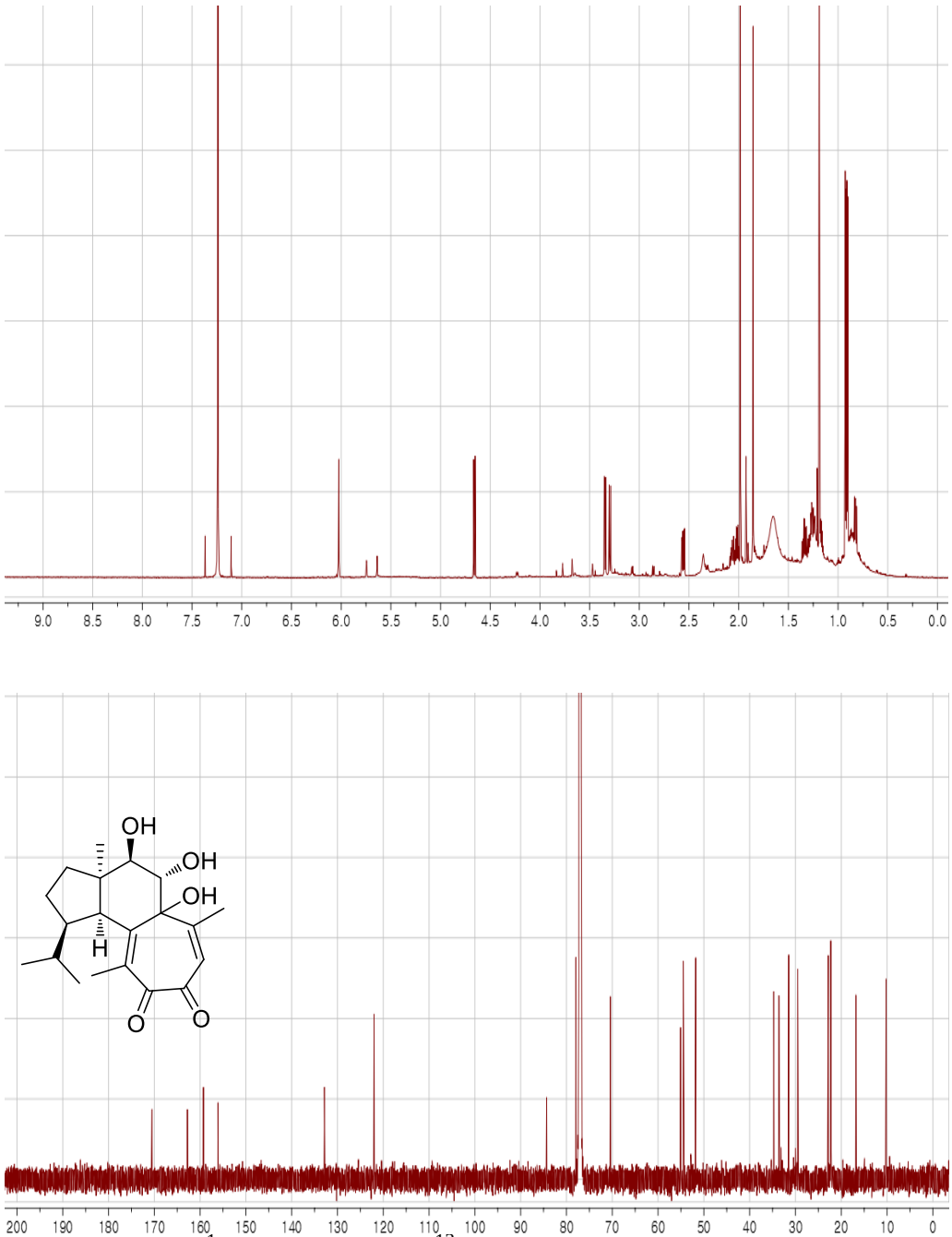

Figure A14. ^{1}H (500 MHz) and ^{13}C (125 MHz) NMR spectra of compound **17** (MeOH-d_4)

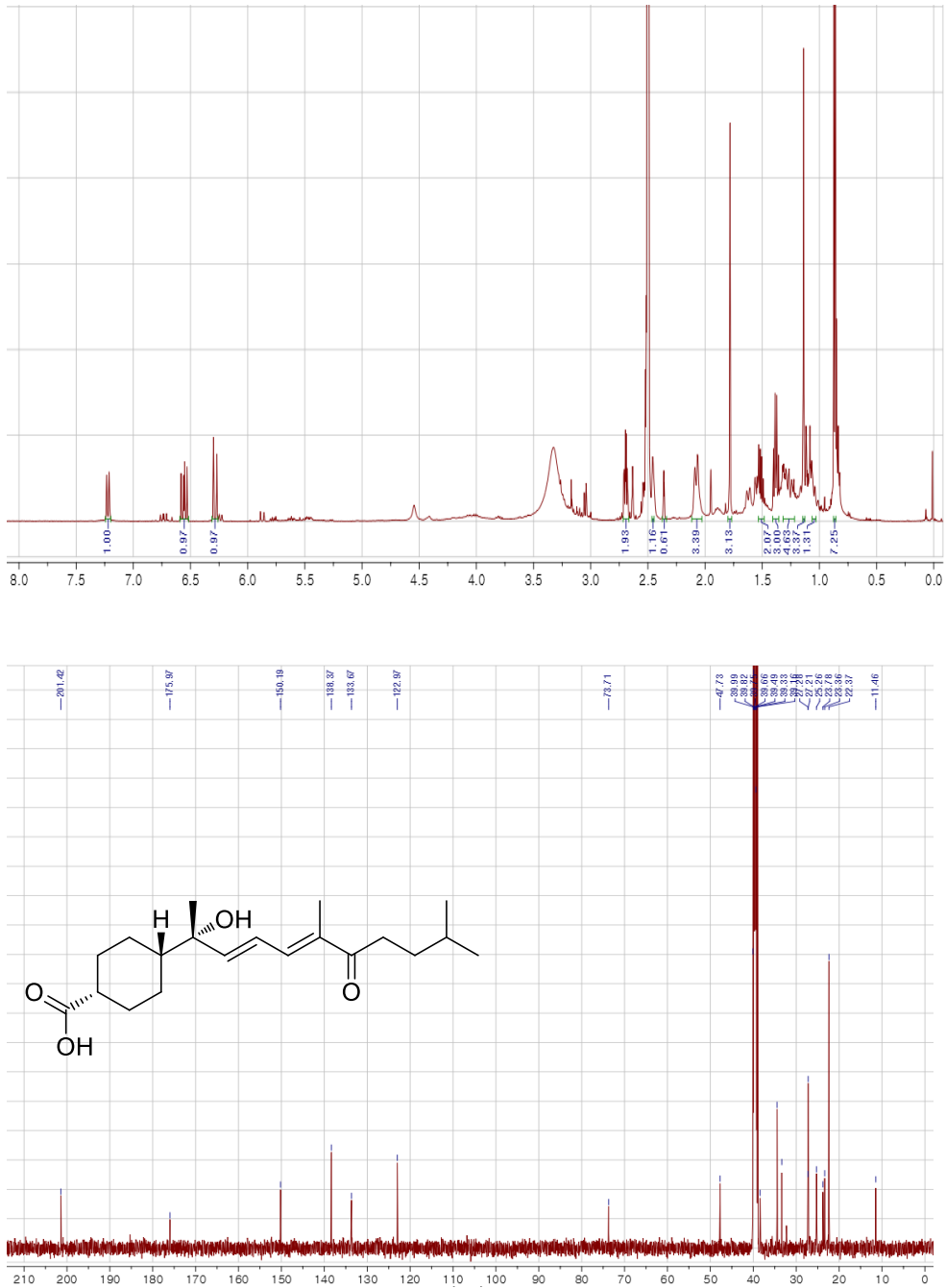

Figure A15. ^{1}H (600 MHz) and ^{13}C (150 MHz) NMR spectra of compound **18** (MeOH-d_4)

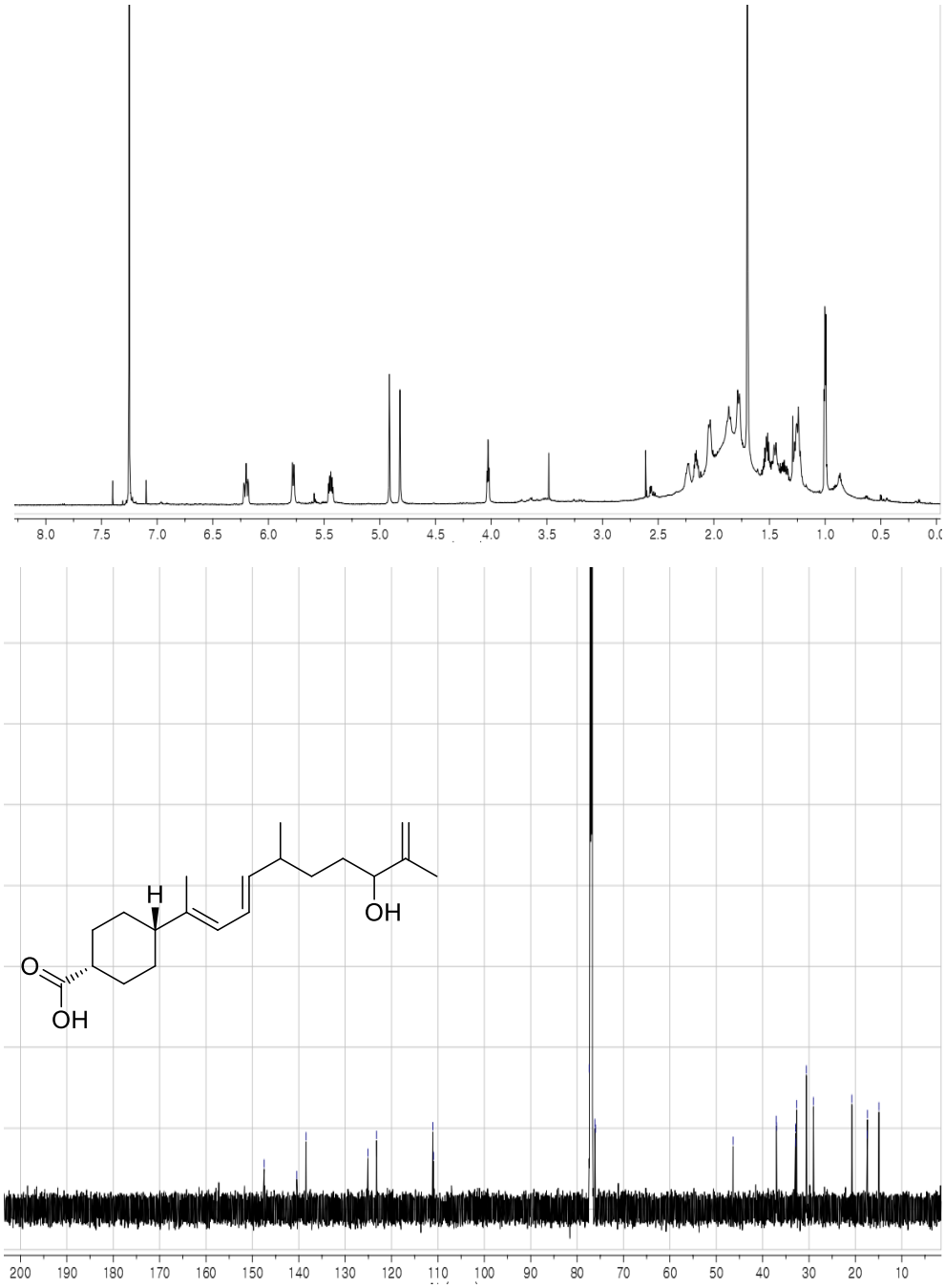

Figure A16. ^{1}H (400 MHz) and ^{13}C (100 MHz) NMR spectra of compound **19** (MeOH-d_4)

APPENDIX B:

Supporting Information

List of Contents

B1. Biological Assays Methods

Cytotoxicity assays, antimicrobial assays, and isocitrate lyase, sortase A, and Na^+/K^+-ATPase inhibition assays were performed as described previously.[44, 45a-c, 46] For the cytotoxicity test, an MTT viability assay was performed as previously described with slight modifications.[65] MTT was first prepared as a stock solution of 5 mg/mL in phosphate buffered saline (PBS, pH 7.2) and was filtered. At the end of the treatment period (24 h, 48 h, and 72 h), with three different test drug concentrations in triplicate, MTT solution (20 μL) was added to each well and then incubated for 4 h at 37 °C; then solubilizing buffer (10% sodium dodecyl sulfate dissolved in 0.01 N HCl, 100 μL) was added to each well. After overnight incubation, the 96-well plate was read by an enzyme-linked immunosorbent assay (ELISA) reader at 570 nm for absorbance to determine the cell (A549 cell line and/or K562) viability. The viable cells produced a dark blue formazan product, whereas no such staining was formed by dead cells. The LC_{50} value was defined as the concentration that resulted in a 50% decrease in cell viability compared to that of control reactions in the absence of an inhibitor. The values (mean ± SD) were calculated from the dose–response curves of three concentrations of each test sample in three independent experiments (n = 3).

B2. Energy minimized conformation of compound 16

Computational analysis. The ground-state geometries were optimized with density functional theory (DFT) calculations, using Turbomole 6.5 at the basis set def-SV(P) for all atoms and functional B3LYP/DFT level, the ground states were further confirmed by the harmonic frequency calculation. The calculated ECD data corresponding to the optimized structures were obtained with TDDFT at the functional B3LYP/DFT level at the basis set def2-TZVPP for all atoms. The CD spectra were simulated by overlapping for each transition, where σ is the width of the band at 1/e height. ΔEi and Ri are the excitation energies and rotatory strengths for transition i, respectively. In the current work a value of σ was 0.10 eV.

$$\Delta\epsilon(E) = \frac{1}{2.297 \times 10^{-39}} \frac{1}{\sqrt{2\pi\sigma}} \sum_{i}^{A} \Delta E_i R_i e^{[-(E-\Delta E_i)^2/(2\sigma)^2]}$$

Parameters of Level DFT
DFT settings (Functional B3-LYP / Gridsize M3)
Geometry optimization options (Energy 10^{-6} Hartree, Gradient norm $\left|\mathrm{dE}/\mathrm{dxyz}\right| = 10^{-3}$ Hartree/Bohr)

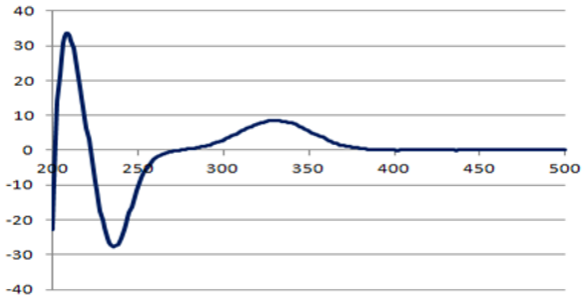

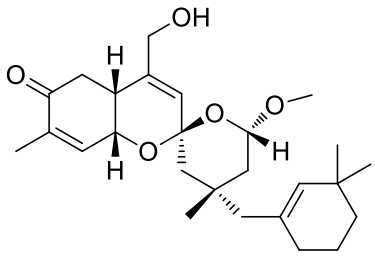

Gombaspiroketal A

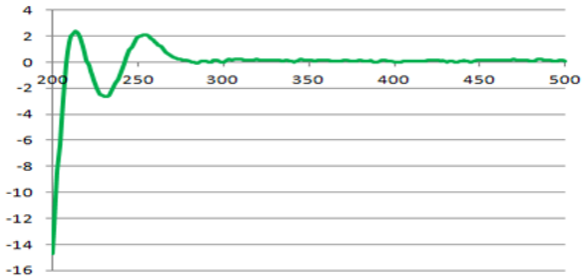

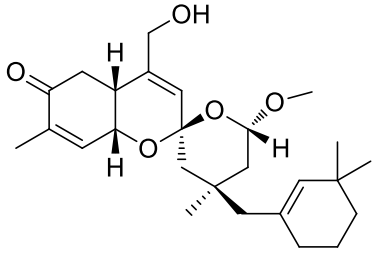

Gombaspiroketal B

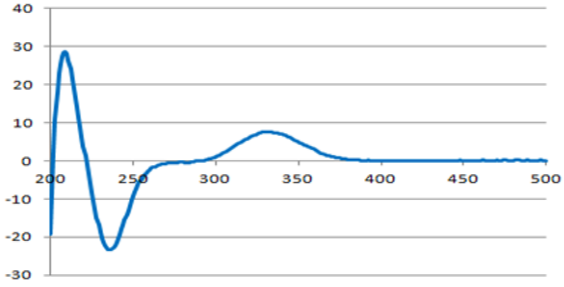

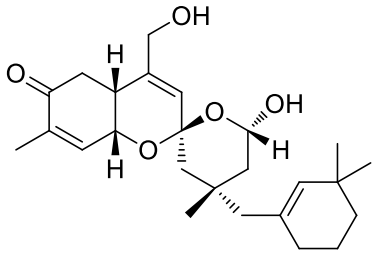

Gombaspiroketal C

국문초록

한국 해면동물로부터 분리한 이차대사산물에 대한 구조결정

서울대학교 대학원
약학과
천연물과학 전공
우 정 균

추출물의 생리 활성 측정으로 선별한 4 종의 한국 해면 (*Clathria gombawuiensis*, *Dictyonella* sp., *Phorbas* sp., *Smenospongia* sp.) 에서 한국에서만 얻을 수 있는 고유의 신규 물질을 발견하는데 주력하였다. 미지의 이차대사산물을 순수하게 획득하기 위해 여러 추출법을 시도하였고, 이 추출물을 다양한 조건의 chromatography 기법을 사용해 분리를 완료했다. 이렇게 얻어진 순수한 물질들을 NMR, IR, CD, UV, MS 등 다양한 분광학적 분석기기를 사용하여 각 화합물의 특성을 분석했다.

각각의 분광 자료에 의하여 총 28 개의 순수한 물질들을 얻었는데 이중 16 종의 신규 물질들을 구조 결정하였으며, 11 종의 기지 물질들을 동정하였다. 입체구조 결정을 위하여 spectroscopic analyses, computational methods 그리고 chemical reactions 등 다양한 방법이 시도되었으며, 분리된 물질들은 여러 계열의 화합물 (13 종의 sesterterpene 계열;

gombaspiroketals A-C, ansellone C, phorone B, scalaranes 3 종, phorbaketals 4 종, gagunin L, 1 종의 saponin 계열; gombaside A, 10 종의 steroid 계열; gombasterols A-G, dictyoneolone, 1 종, clathriol A, ergosterol peroxides 2 종, 3 종의 diterpene 계열) 을 포함하는 것으로 밝혀졌다.

분리된 물질들은 세포 독성 검사 (K562 human erythroleukemia cell, A549 lung carcinoma cell), 항미생물검사 (그람양성박테리아, 그람음성 박테리아, 병원성진균), 효소저해검사 (Na^+/K^+-ATPase, isocitrate lyase, sortase A) 등이 실시되었고, 스테로이드 (gombasterols A-F 와 clathriol) 일곱 물질은 3T3-L1 adipocytes를 가지고서 2-deoxy-2-[(7-nitro-2,1,3-benzoxadiazol-4-yl)amino]-D-glucose (2-NBDG) uptake 활성을 하였고 C2C12 skeletal myoblasts에서 phosphorylation of AMP-activated protein kinase (AMPK) and acetyl-CoA carboxylase (ACC) 를 측정하여 뛰어난 활성을 나타냈다. 더불어 gombaspiroketal A, gombaside A, 물질들은 cytotoxicity에 주목할 만한 활성이 있는 것으로 나타났다.

주요어 : 한국 해면, 이차대사산물, 구조 결정, 생리 활성
학번 : 2014-30571

Publication List

1. "Gombamide A, a Cyclic Thiopeptide from the Sponge *Clathria gombawuiensis*" J.-K. Woo, J.-e. Jeon, C.-K. Kim, C. J. Sim, D.-C. Oh, K.-B. Oh, J. Shin *J. Nat. Prod*. **2013**, *76*, 1380-1383.

2. "Gombaspiroketals A–C, Sesterterpenes from the Sponge *Clathria gombawuiensis*" J.-K. Woo, C.-K. Kim, S.-H. Kim, H. Kim, D.-C. Oh, K.-B. Oh, J. Shin, *Org. Lett*. **2014**, *16*, 2826-2829.

3. "Additional Sesterterpenes and a Nortriterpene Saponin from the Sponge *Clathria gombawuiensis*" J.-K. Woo, C.-K. Kim, C.-H. Ahn, D.-C. Oh, K.-B. Oh, J. Shin *J. Nat. Prod*. **2015**, *78*, 218-224.

4. "A New Sesterterpene from the Korean *Sarcotragus* sp. Sponge" J.-K. Woo, Ju-eun Jeon, B. Kim, C. J. Sim, D.-C. Oh, K.-B. Oh, J. Shin, *Nat. Prod. Sci.* **2015**, *21*, 237-239.

5. "Meroterpenoids from a Tropical *Dysidea* sp. Sponge" C.-K. Kim, J.-K. Woo, S.-H. Kim, E. Cho, Y.-J. Lee, H.-S. Lee, C. J. Sim, D.-C. Oh, K.-B. Oh, J. Shin *J. Nat. Prod*. **2015**, *78*, 2814-2821.

6. "Callyazepin and (3*R*)-Methylazacyclodecane, Nitrogenous Macrocycles from a *Callyspongia* sp. Sponge" C.-K. Kim, J.-K. Woo, Y.-J. Lee, H.-

S. Lee, C. J. Sim, D.-C. Oh, K.-B. Oh, J. Shin *J. Nat. Prod.* **2016**, *79*, 1179-1183.

7. "*nonG*, a Constituent of the Nonactin Biosynthetic Gene Cluster, Regulates Nocardamine Synthesis in *Streptomyces albus* J1074" W. Park, J.-K. Woo, J. Shin, K.-B. Oh *Biochem. Biophys. Res. Comm.* **2017**, *490*, 664-669.

8. "Polyoxygenated Steroids from the Sponge *Clathria gombawuiensis*" J.-K. Woo, T. K. Q. Ha, D.-C. Oh, W.-K. Oh, K.-B. Oh, J. Shin *J. Nat. Prod.* **2018**, *in press.*